INFORMATION TO USERS

This manuscript has been reproduced from the microfilm master. UMI films the text directly from the original or copy submitted. Thus, some thesis and dissertation copies are in typewriter face, while others may be from any type of computer printer.

The quality of this reproduction is dependent upon the quality of the copy submitted. Broken or indistinct print, colored or poor quality illustrations and photographs, print bleedthrough, substandard margins, and improper alignment can adversely affect reproduction.

In the unlikely event that the author did not send UMI a complete manuscript and there are missing pages, these will be noted. Also, if unauthorized copyright material had to be removed, a note will indicate the deletion.

Oversize materials (e.g., maps, drawings, charts) are reproduced by sectioning the original, beginning at the upper left-hand corner and continuing from left to right in equal sections with small overlaps. Each original is also photographed in one exposure and is included in reduced form at the back of the book.

Photographs included in the original manuscript have been reproduced xerographically in this copy. Higher quality 6" x 9" black and white photographic prints are available for any photographs or illustrations appearing in this copy for an additional charge. Contact UMI directly to order.

UMI

A Bell & Howell Information Company
300 North Zeeb Road, Ann Arbor MI 48106-1346 USA
313/761-4700 800/521-0600

UNIVERSITÉ D'OTTAWA
UNIVERSITY OF OTTAWA

ISOLATION OF THE SPINAL MUSCULAR ATROPHY CANDIDATE GENE: THE NEURONAL APOPTOSIS INHIBITOR PROTEIN

A thesis submitted to the School of Graduate Studies University of Ottawa in partial fulfilment of the requirements for the degree of Doctor of Philosophy, Department of Biochemistry, Faculty of Medicine.

By Natalie Roy

ABSTRACT

The childhood spinal muscular atrophies (SMA) are neurodegenerative disorders characterised by progressive spinal cord motor neuron depletion and are among the most common autosomal recessive disorders. Type I SMA is the most frequent monogenic cause of death in infancy. The loss of motor neurons in SMA, has led to suggestions that an inappropriate continuation or reactivation of normally occurring motor neuron apoptosis may underlie the disorder. The gene resonsible for the SMA's was mapped to a region of 5q13 flanked proximally by the marker CMS-1 and distally by the marker D5S557. We present a 3 Megabase yeast artificial chromosome (YAC) contig constructed from three libraries encompassing the D5S435/D5S629/CMS-1-SMA-D5S557/D5S112 interval. The D5S629/CMS-1-SMA-D5S557 interval is unusual insofar as chromosome 5 specific repetitive sequences are present and many of the simple tandem repeats (STR) are located at multiple loci which are unstable in our YAC clones. A long range restriction map which demonstrates the SMA containing interval to be 550 kb is presented. Moreover, a 210 kb cosmid array from both a YAC specific and a chromosome 5 specific cosmid library in addition to a 500 kb PAC array has been assembled. These arrays encompass the region containing the markers shown to be in strong linkage disequilibrium with Type I SMA, indicating that the SMA gene is located in close proximity to or within thses arrays.

In keeping with the hypothesis that a mechanism of apoptosis may underlie the disorder, we have isolated a gene encoding the neuronal apoptosis inhibitor protein (NAIP), which is homologous to baculoviral inhibitor of apoptosis proteins (IAP) and is partially deleted in individuals with Type I SMA . Concurrently, a second candidate gene encoding survival motor neuron (SMN), which is contiguous with the NAIP locus on 5q13.1 was also reported (Levebre et al. 1995. Cell 80, 155). SMN is deleted in a significant majority of SMA individuals, leaving unclear the precise role of the two genes in SMA causation. In an effort to delineate the role of NAIP in SMA pathogenesis, we have studied the effect of NAIP on cell death induced by different apoptotic triggers and determined the cellular distribution of the protein in human spinal cord. We report that overexpression of NAIP in Rat-1, HeLa and CHO cells suppresses apoptosis induced by menadione, tumor necrosis factor alpha (TNF-α) and serum withdrawal. Immunocytochemistry employing polyclonal antiserum raised against human NAIP demonstrates immunoreactivity in motor neurons. NAIP mediated inhibition of cell death and the immunolocalization of the protein to motor neurons are consistent with a role for NAIP both in the naturally occurring programmed motor neuron death, and , when defective, in the pathogenesis of SMA. Moreover, NAIP appears to be the first member of a novel family of human genes with anti-apoptotic activity. Three novel human IAPs have subsequently been identified and shown to suppress apoptosis (Liston et al. 1996. Nature 379, 349). Two of these were also identified based on their ability to associate with the tumor necrosis factor receptor II (TNFRII) via a TNF receptor associated factor

1 and 2 (TRAF1-TRAF2) heterocomplex (Rothe et al. 1995. Cell 83, 1243) These data provide evidence for a central role of NAIP and IAPs not only in apoptosis but as regulators in these signalling pathways.

ACKNOWLEDGEMENTS

I thank Dr. Alex E. MacKenzie for his support, guidance and friendship during these studies. I am also grateful to Dr. R.G. Korneluk for his expertise and advice. I would especially like to thank my collegues for their help, support and friendship. In particular I would like to thank J.B., M.N. and J.W.

DEDICATION

To my parents, Philomena and Leger, and M.G.T.

TABLE OF CONTENTS

Abstract	ii
Acknowledgements	v
Dedication	vi
Table of Contents	vii
List of Figures	x
List of Tables	xiv
List of Abbreviations	xv

CHAPTER I:
GENERAL INTRODUCTION

1. Clinical features of SMA	1
2. Morphology of motor neuron and muscle in SMA	3
3. Apoptosis	5
a. neuronal apoptosis	7
b. Bcl-2 and its family members	9
c. Viral apoptosis	11
d. ICE proteases	14
e. The TNF family of receptors	18
4. The three forms of SMA map to chromosome 5q11.2 - q13.3.	23
5. Positional cloning: an overview	24
6. Summary of work	31

CHAPTER II:
PHYSICAL MAP OF THE SMA REGION AT 5Q13 BASED ON YAC, PAC AND COSMID CONTIGUOUS ARRAYS

1. Introduction 36

2. Materials and Methods 37

a. YAC libraries and screening 37
b. Cosmid and YAC DNA preperation 38
c. YAC end isolation and inter-*Alu* PCR 38
d. Pulsed field gel electrophoresis 39
e. PCR analysis and hybridisation 40
f. Chromosome 5 cosmid library screening 40
g. Construction of cosmid library from YAC 76C1 and screening 41
h. Assembly of PAC contig 42

3. Results 43

a. Construction of YAC contig 43
b. Long range restriction map and estimates of long range physical distance 51
c. Cosmid contig assembly from the chromosome 5 library 54
d. Cosmid contig assembly of YAC 76C1 cosmids 58
e. Assembly of PAC contig 62
f. Duplications/ Deletions 65

4. Discussion 71

CHAPTER III:
ISOLATION OF THE SMA CANDIDATE GENE: THE NEURONAL APOPTOSIS INHIBITOR PROTEIN (NAIP)

1. Introduction 76

2. Materials and Methods 78

a. Exon trapping 78
b. PCR analysis and hybridization 80
c. RT-PCR 82

3. Results 82

a. Exon trapping and identification of *naip* 82
b. *Naip* gene structure 85
c. Deleted and truncated forms of *Naip* at 5q13 90
d. *Naip* gene mutational analysis 97
e. RT-PCR analysis 100
f. Mapping of *smn* 102

4. Discussion 106

CHAPTER IV:
NAIP INHIBITS CELL DEATH AND IS EXPRESSED IN MOTOR NEURONS OF THE SPINAL CORD

1. Introduction 115

2. Materials and Methods 116

a. Antibody production 116
b. Immunoblotting 116
c. Immunohistochemistry 117
d. Adenovirus construction, purification and titre 117
e. Cell death assays 119

3. Results 120

a. Assesment of NAIP antibody 120
b. Cell death assays 121
c. Immunohistochemistry / Immunoblotting 133

4. Discussion 137

CHAPTER V:
CONCLUSION 148

REFERENCES 158

LIST OF FIGURES

CHAPTER I:

INTRODUCTION

Figure 1-1: Morphological stages during cellular apoptosis 6

Figure 1-2: ICE protease activation and cleavage 16

Figure 1-3: Apoptotic signal transduction of the TNF receptor superfamily 21

Figure 1-4: Schematic of the apoptotic cascade 22

Figure 1-5: Sequential steps to identify a disease gene 25

Figure 1-6: Localisation of SMA to 5q11.2-13.3 32

CHAPTER II:

PHYSICAL MAP OF THE SPINAL MUSCULAR ATROPHY GENE REGION AT 5Q13 BASED ON YAC, PAC AND COSMID CONTIGUOUS ARRAYS

Figure 2-1: Pulsed field gel electrophoresis and stability of YAC clones 46

Figure 2-2: Generation of YAC end STS 47

Figure 2-3: YAC contig of the SMA gene region 49

Figure 2-4: Partial YAC digestion map construction 52

Figure 2-5: Long range restriction map of the SMA region. 53

Figure 2-6: Representative cosmid walking step 56

Figure 2-7: Amplification of the CATT-1 locus 57

Figure 2-8: A representative subset of mapped cosmids from our contiguous array 60

Figure 2-9: *Alu* fingerprinting of cosmids to determine overlap 61

Figure 2-10: PAC contig of SMA locus 63

Figure 2-11: Linkage disequlibrium and physical mapping of SMA locus at 5q13. 64

Figure 2-12: Sequence duplication in the SMA region identified by p151.2 69

Figure 2-13: Sequence duplication detected in our PAC array 70

CHAPTER III:

ISOLATION OF THE SMA CANDIDATE GENE THE NEURONAL APOPTOSIS INHIBITOR PROTEIN (NAIP)

Figure 3-1: Exon trapping protocol. 83

Figure 3-2: Physical mapping of the NAIP region at 5q13 86

Figure 3-3: cDNA sequence and predicted amino acid sequence of NAIP. 87

Figure 3-4: Domain structure of NAIP and viral IAPs. 88

Figure 3-5: Schematic of NAIP deleted and truncated loci found in YAC and PAC clones 91

Figure 3-6: Exon probings of Southern blots containing PAC clones 92

Figure 3-7: Structure of intact and internally deleted and truncated NAIP loci at 5q13 93

Figure 3-8: Hybridization of PACs and genomic DNA to elucidate genomic architecture 94

Figure 3-9: PCR analysis of the 6 kb, exon 5-6 deletion. 95

Figure 3-10: Schematic of PCR mutational analysis performed across NAIP 98

Figure 3-11: Multiplex PCR analysis of exon 5 and exon 12 in a Type III family 99

Figure 3-12: RT-PCR amplification of RNA on tissues from SMA and non-SMA individuals 101

Figure 3-13: *Smn* analysis of PACs and genomic DNA 104

Figure 3-14:. Location of SMN in our PAC contiguous array 105

CHAPTER IV:

NAIP INHIBITS CELL DEATH AND IS EXPRESSED IN MOTOR NEURONS OF THE SPINAL CORD.

Figure 4-1: Immunofluorescence of Cos-1 cells transfected with a myc-tagged NAIP expression construct. 122

Figure 4-2: Western blot analysis of NAIP expression detected by the anti-human NAIP (E1.0) antibody. 123

Figure 4-3: Expression of NAIP in Rat-1, CHO and HeLa pooled stable lines and adenovirus infected cells analysed by Western blotting 124

Figure 4-4: Expression of adenovirus expressing β-galactosidase and anti-sense NAIP. 125

Figure 4-5: Effect of NAIP on cell death induced by serum deprivation in CHO cells. 127

Figure 4-6: Effect of NAIP on cell death induced by treatment with menadione (20 μM) in CHO cells 128

Figure 4-7: Effect of NAIP on cell death induced by treatment with menadione (10 μM) in Rat-1 cells 130

Figure 4-8: Effect of NAIP on cell death induced by treatment with menadione (5 μM) in Rat-1 cells. 131

Figure 4-9: Effect of NAIP on cell death induced by treatment with TNF-α and cyclohexamide in HeLa cells. 132

Figure 4-10: Immunofluorescence analysis of human spinal cord tissue. 134

Figure 4-11: Western blot analysis of tissue protein extracts with anti-human NAIP antibody 135

Figure 4-12: Domain structure of the IAP family 138

LIST OF TABLES

CHAPTER II:

PHYSICAL MAP OF THE SPINAL MUSCULAR ATROPHY GENE REGION AT 5Q13 BASED ON YAC, PAC AND COSMID CONTIGUOUS ARRAYS

TABLE 1-1: Origin and size of YAC clones 45

TABLE 1-2: Markers and STS's utilised in this study 50

LIST OF ABBREVIATIONS

BAC	bacterial artificial chromosome
BAD	Bcl-2/Bcl-x associated death promoter homolog
BAG-1	Bcl-2 associated athanogene
BAK	Bcl-2 homologous antagonist killer
BAX	Bcl-2 associated X protein
BCL-2	B-cell lymphoma 2
BIR	baculovirus iap repeat
bp	base pair
BSA	bovine serum albumin
cDNA	complementary DNA
CED	cell death defective
CEPH	Centre d'Etudes de polymorphisme humaines
CHO	Chinese hamster ovary cells
CrmA	cytokine response modifier
DIAP	*Drosophila* IAP
DMEM	Dulbecco's Modified Eagle Medium
DTT	dithiothreitol
EBV	Epstein-Barr virus
EDTA	ethylenediamenetetraacetic acid disodium salt
EMG	electromyography
FADD	Fas associated death domain

GST	glutathione-s-tranferase
HIAP	human iap
hr	hour
IAP	inhibitor of apoptosis protein
ICE	interleukin-1β converting enzyme
ICH	ICE and CED-3 homolog
ICRF	Imperial Cancer Reasearch Foundation
IPTG	isopropyl-1-thio-beta-D-galactoside
kb	kilobase
kD	kilo Daltons
LB	Luria-Bertani medium
LMP-1	latent membrane protein
Mb	megabase
ml	mililitre
mM	millimolar
MSR	microsattelite repeat
NAIP	Neuronal apoptosis inhibitor protein
NCE	National Centres of Excellance
NF-κB	nuclear factor kappa B
ng	nanaogram
NGF	nerve growth factor

PAC	P1 artificial chromosome
PARP	poly-ADP-ribose polymerase
PBS	phosphate buffered saline
PCR	polymerase chain reaction
PEG	polyethylene glycol
PFGE	pulsed field gel electrophoresis
pfu	plaque forming units
PNI	protease nexin-1
RIP	receptor interacting protein
SDS	sodium dodecyl sulphate
SMA	Spinal muscular atrophy
SMN	survival motor neuron
STS	sequence tagged site
SSC	standard saline citrate buffer
TBE	Tris-borate, EDTA buffer
TNF	tumour necrosis factor
TNFR	TNF receptor
TRADD	TNF receptor death domain
TRAF	TNF receptor associated factor
Tris	tris(hydroxymethyl)aminomethane
µl	microliter
µg	microgram

μmol	micromole
XIAP	X linked iap
YAC	yeast artificial chromosome

CHAPTER I:

INTRODUCTION

The childhood spinal muscular atrophies (SMA) are a group of autosomal recessive, neurodegenerative disorders characterised primarily by the depletion of spinal motor neurons manifesting as weakness and wasting of proximal voluntary muscles. The SMAs have been classified into three types (Type I, II and III) based upon the age of onset, clinical picture and progression of the disorder (Dubowitz, 1978; 1991; Pearn, 1980). Together the childhood onset SMAs affect 1 in 10000 live births world-wide with estimated carrier frequencies of 1 in 80 for type I and 1 in 100 for Types II and III. Type I SMA is one of the most common monogenic cause of death in infancy and together the childhood SMAs are the among the most common autosomal recessive disorders (Emery, 1991).

Clinical features of SMA

Type I SMA (Werdnig-Hoffmann disease, acute infantile SMA) is the most severe form with onset *in utero* or within the first few months of life (Gamstrop, 1967; reviewed in Hausmanowa-Petrusiwicz and Fidzianska-Dolot, 1984). Characteristic features include muscle wasting and floppiness or generalised hypotonia. Weakness occurs primarily in the axial and proximal muscles and is most prominently detected in the pelvic girdle. These

children are unable to raise their heads, roll over or sit unsupported and are never able to walk. There is however no facial or extraocular involvement and cardiac muscle is not affected. Bulbar weakness is common, observed as difficulty in sucking and swallowing. Due to the severe weakness of the intercostal muscles, breathing is almost entirely diaphragmatic and the chest has a bell shaped appearance. These infants are prone to recurrent chest infections and as a result suffer from respiratory insufficiency, rarely surviving the first few years of life.

Clinical features of Type II SMA, the intermediate form, appear between the ages of 2 and 6 (Fried and Emery, 1977). Motor development is delayed in these children and atrophy is observed principally in the proximal muscles in the lower extremities (Moosa and Dubowitz, 1973). As a result, these children are able to sit but unable to stand or walk unaided. The prognosis is quite variable with survival into adolescence or early adulthood. The intercostal muscles are usually not as severely affected upon onset as those children with Type I SMA however, it develops later and these children die due to respiratory complications.

The mildest form of SMA first described by Kugelberg and Welander, Type III, manifests a mildly progressive course with children maintaining independent ambulation at a normal age or somewhat later (Garvie and Woolf, 1966). Weakness usually develops between the ages of 3 and 17 and is mainly confined to the muscles of the pelvic girdle,

leading to difficulty in climbing stairs or getting up from the floor. No respiratory insufficiency is initially observed with these individuals and they may survive well into adulthood.

Morphology of Motor neuron and muscle

The fundamental lesion of SMA is the degeneration and consequent loss of the anterior horn cells at all levels of the spinal cord (reviewed in Fidzanska-Dolot and Hausmanova-Petrusewicz, 1984). Predominantly there is a dramatic loss of these neurons at the cervical and lumbar levels. The neurons which remain appear shrunken and angulated however occasionally swelling and chromatolysis is also observed (Greenfield and Stern, 1927; Chou and Faraday, 1971). Some reports document changes in the motor nuclei of the Vth to XII cranial nerves. The presence of immature neurons, characterised by the deficiency of Nissl substance and its localisation at the periphery of neurons as a delicate ring, has been observed in children with Werdnig-Hoffmann (Hausmanova et al, 1980; Fidzianska and Rafalowska, 1983). The microglial and astrocytic proliferation that is occasionally observed are believed to be a consequence rather than the cause of neuronal damage. Electromyogram results are characteristic of denervation with individual motor unit potentials that are either normal or of large amplitude or long duration (Buchthal and Olsen, 1970). The large amplitude indicate reinnervation by surviving neurones with consequent increase in the territory of the motor neuron. This is

in contrast to disorders which directly affect the muscle and would characteristically have an EMG profile of low amplitude and short duration. Motor nerve conduction velocities are said to be normal although they can be slower in children that are the most severely affected (Moosa and Dubowitz, 1976).

Two populations of muscle fibers are detected in muscle biopsies of individuals with SMA; shrunken, denervated muscle fibers and normal or hypertropied fibers (reviewed in Fidzanska-Dolot and Hausmanova-Petrusewicz, 1984; Sarnat, 1984). The atrophic fibers, as in the normal, are a mixture of Type I and Type II fibers. The hypertrophied fibers are characteristically type I fibers and are ballooned probably as a result of increased neural stimulation which results possibly as an attempt to compensate for the weakness of the small fibers which make up the majority of fibers. Individuals with Type I SMA typically have muscle fibers with single distributed nuclei, a reduction of diameter, well preserved architecture and normal structure of myofibrils in addition to small muscle cells which resemble myotubes. These features are characteristic of fetal muscle and indicate a lack of development due to a defect affecting fusion as opposed to atrophy of mature muscle fibers (Hausmanova-Petrusewicz et al, 1980). The observation of immature motor neurons and muscle cells in individuals with Type I SMA suggest that the signal for cell death occurs early in development. Afferent input is important for continued maturation of the neuron and disruption of this trophic support may further contribute to the death of neurons. The cellular pathology of SMA has led to suggestions

that uncontrolled apoptosis of motor neurons resulting from defective genetic regulation underlies the disorder (Oppenheim et al, 1991; Sarnat et al, 1984).

Apoptosis

Apoptosis or programmed cell death is a normal physiological cell suicide program first described by Kerr et al (1972). Different cell types undergoing apoptosis all display the same morphological characteristics (Figure 1-1). The nucleus and cytoplasm condense. DNA is degraded by endonucleases, plasma membrane integrity is maintained and cells fragment into apoptotic bodies which are phagocytosed by neighbouring cells. These dying cells are eliminated without an inflammatory response. This process differs from necrotic death that results from physical trauma or chemical injury and is accompanied by an inflammatory response (Kerr et al, 1972). The regulated process of cell suicide or apoptosis plays a crucial role during embryogenesis, tissue maintenance and remodelling, and serves to remove cells such as self reactive lymphocytes, tumour cells, those infected by a virus or others with irreparable damage. The control of cell number is now seen as a balance between cell proliferation, differentiation and apoptosis. The inhibition of apoptosis may contribute to the pathogenesis of cancer, autoimmune disorders and viral infection while the uncontrolled continuation of apoptosis results in cell loss and degenerative disorders (Thompson, 1995). The apoptotic response is genetically

Figure 1-1: Morphological stages during cellular apoptosis

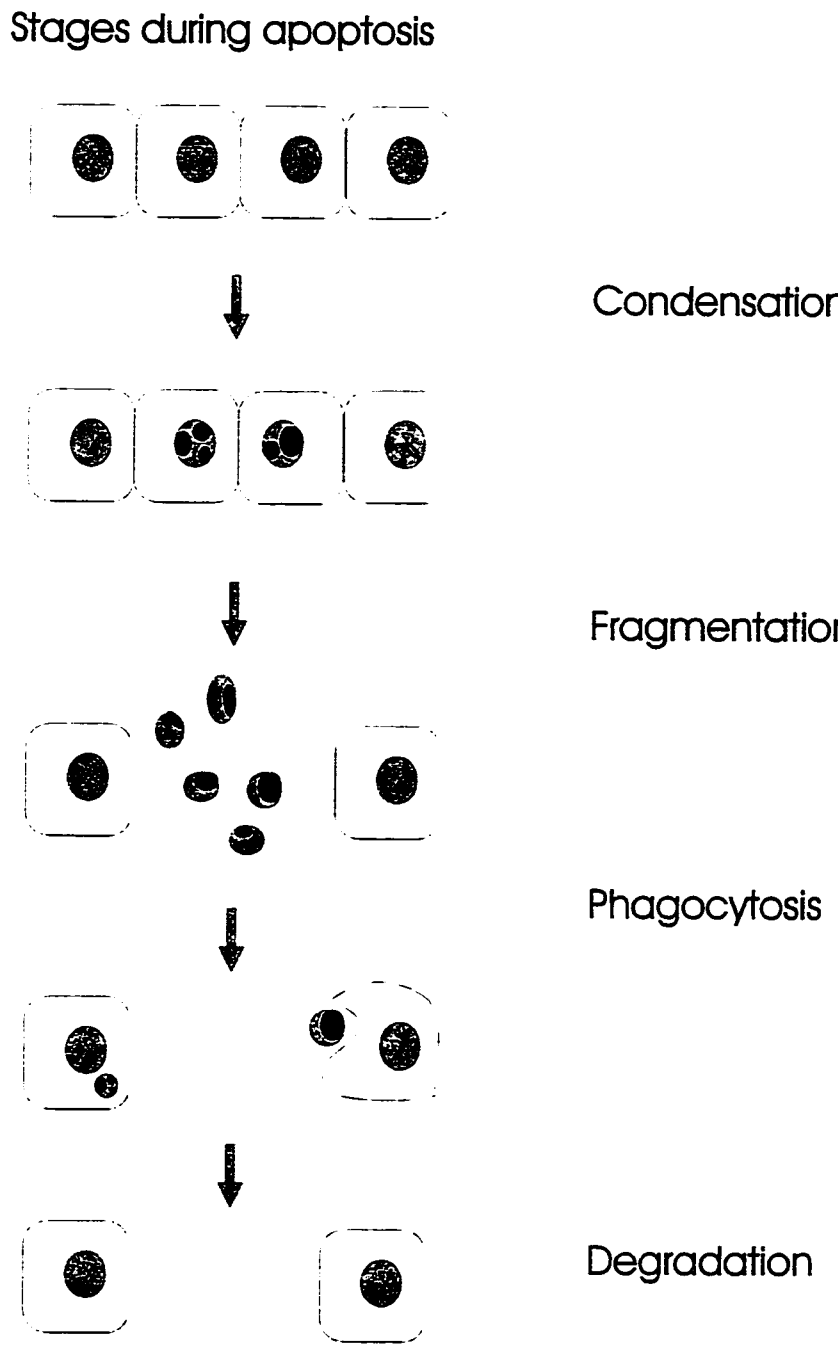
Stages during apoptosis
Condensation
Fragmentation
Phagocytosis
Degradation

controlled and many of the gene products involved in both the induction and inhibition of apoptosis are now being defined.

Neuronal apoptosis

Restricted periods of naturally occurring cell death ensue during development of the nervous system (Cunningham 1982; Cowan et al, 1984; Oppenheim, 1991). In the period when postmitotic lumbosacral motoneurons are forming synaptic connections with their target muscle (synaptogenesis), approximately 50% of these motoneurons undergo programmed cell death (Hamburger and Oppenheim, 1982; Oppenheim, 1978). Neurons compete for sufficient amounts of trophic factor from target tissues and those which do not receive adequate trophic support activate a cell death program. Experiments which recapitulate this process in vitro by growth factor withdrawal of cultured neurons have revealed that these neurons die by apoptosis (Arends and Wyllie, 1991). Not only is apoptosis a fundamental process during nervous system maturation but increasing evidence suggests that the cell loss which is observed during neurodegenerative disorders occurs by apoptosis. Cultured neurons in vitro can be induced to undergo apoptosis in the presence of β-amyloid protein or a synthetic prion peptide implying activation of the apoptotic pathway in both Alzheimer's and Creutzfeldt-Jacob disease (Loo et al, 1993; Forloni et al, 1993). Moreover the characteristic DNA fragmentation that occurs during apoptosis is observed in the temporal cortex and striatum of patients with Alzheimer's

and Huntington's disease respectively (Dragunow et al, 1995). Furthermore, cultured cortical neurons of Down's syndrome patients undergo apoptosis which is accompanied by an increase in reactive oxygen species (Busciglio and Yanker, 1995). In addition to neurodegenerative disorders, insults such as ischemia which cause subpopulations of neurons to die, do so by initiating the apoptotic cascade (MacManus et al, 1993; 1994; Linnik et al, 1993). Hence not only may apoptosis be fundamental in the development of the nervous system but as well in its maintenance and degeneration.

Genetic studies in the nematode *Caenorhabditis elegans* were the first to identify regulatory genes of the cell death pathway. The lineage and fate of the 1090 cells in the nematode are known, of these the 131 which die have been shown to be under the same genetic control (Sulston et al, 1983; Ellis and Horvitz, 1986). *Ced-3* and *ced-4* (cell death defective) control the execution of cell death which is inhibited by *ced-9*. Evidence that *ced-3* and *ced-4* are instrumental in programmed cell death has been demonstrated by loss of function mutations in either of these genes. This phenotype resembles that observed in *ced-9* gain of function mutations and it is well established that *ced-9* is required actively and continually to prevent all cell deaths within the animal (Hengartner et al, 1992). Interestingly, *ced-3* shows sequence similarity to the mammalian interleukin converting enzyme (ICE), a cysteine protease (Yuan et al, 1993), first implicating a potential role of proteases in the apoptotic cascade. *Ced-9* is homologous to the first mammalian negative regulator of cell death identified, bcl-2.

Bcl-2 and its family members

The proto-oncogene bcl-2 was originally isolated at the translocation breakpoint between chromosomes 14 and 18 found in many human B-cell lymphomas (Bakhshi et al, 1985). The translocation results in overexpression of bcl-2 mRNA as it is put under the control of the immunoglobulin heavy chain locus (Seto et al., 1988). Mice which carry a bcl-2-immunoglobulin minigene (transgene), creating high levels of bcl-2 expression in the immune system, show extended survival of B cells and produce lymphomas (McDonnell et al, 1989; Sentman et al, 1991). Although an oncogene, bcl-2 neither induced cell proliferation or cell cycle progression.

It has since been demonstrated however that bcl-2 protects a variety of mammalian cell types from apoptosis induced by numerous triggers (Vaux et al, 1988; Hockenberry et al, 1991; Nunez et al, 1990; Garcia et al, 1992; Allsop et al, 1993; Batistatou et al, 1993; Mah et al, 1993). The ability to suppress apoptosis in such a wide variety of systems suggested that bcl-2 might act at a control point in the apoptotic pathway. In neurons, bcl-2 can inhibit growth factor withdrawal-induced cell death in phaeochromocytoma (PC12) cells (Batistateu et al, 1993; Mah et al, 1993), sympathetic neurons (Garcia et al, 1992) and in sensory neurons (Allsop et al, 1993). However, bcl-2 is inefficacious in protecting ciliary neurons from apoptosis when deprived of ciliary nerve growth factor

(CNTF) suggesting divergence in components of the cell death pathway (Allsopp et al, 1993). In agreement with these findings, bcl-2 knockout mice progress normally through development implicating the presence of other bcl-2 family members and functional redundancy (Veis et al, 1993; Kamada et al, 1995). These mice do, however, develop polycystic kidneys and suffer postnatal immune function failure due to a dramatic loss of mature B and T cells by apoptosis. Subsequently a number of bcl-2 family members have been cloned which share homology at three highly conserved regions known as Bcl-2 homology -1, 2 and 3 (BH1, BH2 and BH3) domains demonstrated to be important for protein-protein interaction. These include: bcl-x (Boise et al, 1993); bax (Oltvai et al, 1993); bak (Chittenden et al, 1995; Farrow et al, 1995) and bad (Yang et al, 1995).

The bcl-2 family member, bcl-x, is the first example of a gene, which depending on splicing, plays either a positive or a negative regulatory role in cell death (Boise et al, 1993). Bcl-xl (long) contains the BH1 and BH2 domains with homology to bcl-2 and is capable of protecting cells from apoptosis. The spliced form bcl-xs (short), lacks these domains and inhibits the action of bcl-2 and bcl-xl resulting in cell death. Bax, isolated based on its ability to bind bcl-2, inhibits the ability of bcl-2 and bcl-xl to suppress apoptosis (Oltvai et al, 1993). Bax is capable of forming homodimers as well as heterodimers with bcl-2 or bcl-xl and when Bax is produced in excess it will promote apoptosis. A point mutation in bcl-2 which prevents its dimerization with bax abolishes its ability to suppress death suggesting that the ratio of bcl-2 to bax and the ratio of

heterodimers versus homodimers determines the cells susceptibility to an apoptotic signal (Yin et al, 1994). In support of this model, the population of neurons which are susceptible to cell death induced by transient global ischemia express high levels of bax and concurrently low levels of bcl-2 implying that the levels of these two proteins determine the sensitivity of these neurons to an apoptotic insult (Krajewski et al, 1995). The ability of bcl-2, bcl-xl and the adenovirus protein EIB (19K) to suppress cell death may be inhibited by another family member, bak (Chittenden et al, 1995; Farrow et al, 1995). The ability of bcl-xl to interact with bak or bax and form heterodimers does not appear to affect its ability to confer apoptotic resistance suggesting that the mechanism of bcl-x suppression of apoptosis may differ from that of bcl-2 (Cheng et al, 1996). Bax can be displaced from bcl-xl by Bad, which itself can interact with bcl-x inhibiting its ability to suppress cell death. However, bad does not interact with bax allowing bax to form homodimers. Again it appears to be the ratio of these homodimers to heterodimers which determines the cells fate. Taken together these data would argue that proteins that cause apoptosis are the key modulators in the pathway and that those which suppress apoptosis do so by sequestration or inhibition of components promoting death.

Viral apoptosis

Viral infection can result in cellular apoptosis in the host as a defence mechanism to protect against viral propagation. In response, many viruses have developed

mechanisms to inhibit this apoptosis allowing themselves to replicate to a high titre. Suppression of apoptosis may promote viral latency as is observed in the case of the Epstein Barr virus (EBV) protein, latent membrane protein (LMP-1), which induces an increase in the level of endogenous bcl-2 expression (Henderson et al 1991). An EBV homolog of bcl-2, BHRF1, has been identified that protects B cells from apoptosis, extending their survival and thereby maximizing viral production (Henderson et al, 1993). Adenoviruses sustain proliferation by expression of E1B (19 kDa), suppressing cell death directly (Rao et al, 1992; White et al, 1992). Additionally transformation of cells has been demonstrated to occur through the co-operation of both E1A, which induces apoptosis mediated by p53 and E1B which by inhibiting p53, suppresses apoptosis (Debbas and White, 1993). Bcl-2 can replace E1B to complement E1A transformation (Rao et al, 1992).

The p35 protein encoded by *Autographica california* nuclear polyhedrosis virus (AcMNRV), blocks apoptosis induced by viral infection in *Spodopteria frugipoda* (SF21) cells (Clem et al, 1991; Clem and Miller, 1993). Normally this virus replicates in host cells and forms polyhedral occlusion bodies filled with noninfectious virus particles. A mutant virus (vAcAnh or annihalator) was identified based on its inability to produce occluded virus despite containing the polyhedron gene (Clem et al, 1991). Infection of Spodoptera frugiperda (SF-21) cells with vAcAnh results in premature lysis with cell blebbing and DNA cleavage characteristic of apoptosis. This premature lysis or apoptosis that occurs

at about 12 hours post infection interferes with the budding of infectious progeny virus which normally starts 10 hours post infection and continues to 48 hours. Marker rescue experiments identified the gene p35, responsible for inhibiting this apoptosis (Clem et al, 1991). The suppression of apoptosis by p35 correlates with increased yields of virus progeny and viral replication (Hershberger et al, 1992; Heshberger et al, 1994) indicating that apoptosis provides an antiviral defence mechanism. Cotransfection of SF-21 cells with vAcAnh and DNA from a variety of baculoviruses resulted in the identification of two genes that could functionally complement p35, Cp-iap and Op-iap (Crook et al, 1993; Clem and Miller, 1994). Surprisingly these two genes do not share any sequence homology with p35 but contain a repeated BIR (baculovirus iap repeat) motif necessary for the inhibition of apoptosis and a RING zinc finger whose exact function is not known. A third iap family member, Ac-iap, was identified based on its homology with Cp-iap and Op-iap however was unable to block cell death in cotransfection experiments with vAcAnh in SF-21 cells (Birnhaum et al, 1994).

Apoptosis can be induced in SF-21 cells by actinomycin D, an inhibitor of RNA synthesis, which is blocked by expression of p35 or the iaps (Clem et al, 1994). This indicates that rather than simply inhibiting the viral induction of apoptosis, p35 and the iaps directly block cellular apoptosis and act at a common point in the cell death pathway. Subsequently p35 has been shown to inhibit cell death in mammalian neural cells induced by various triggers (Rabizadeh et al, 1993), in developing embryos and eyes of transgenic

Drosophila melanoganster (Hay et al, 1994) and can rescue a ced-9 mutant in *C. elegans* (Sugimoto et al, 1994). Although no known homologs of p35 have been identified to date, its ability to suppresses apoptosis in various species suggests a conservation among the components of the cell death pathway. In keeping with this proposal, the viral iaps have been observed to block apoptosis in mammalian cells (Duckett et al, 1996; Uren et al, 1996)

ICE proteases

It is now firmly established that that proteases play a crucial role in the cell death pathway. The first evidence to implicate proteases in the apoptotic cascade came with the observation that the *C. elegans* cell death gene, *ced-3*, is homologous to ICE, a mammalian cysteine protease which cleaves pro-interleukin-1ß to its active form (Thornberry et al, 1992). Overexpression of ICE results in apoptosis which can be inhibited by the cowpox virus gene CrmA (Ray et al, 1992). ICE deficient mice, although having a defect in Fas mediated cell death, develop normally suggesting redundancy in the cell death pathway. Six members of this ICE/ced-3 family have now been isolated: Yama/apopain/CPP32 (Tewari et al, 1995; Nicholson et al, 1995); Nedd-2/ ICH (ice and ced-3 homolog) (Kumar et al, 1994; Wang et al. 1994); ICH2/ICE rel-II (Faucheu et al, 1995; Kamens et al, 1995), ICE rel-III (Munday et al, 1995); Mch2 (Fernandes-Almemri et al, 1995) and ICE-lap3 (Duan et al, 1996) all of which cause apoptosis when

overexpressed in cells. Each of these encode cysteine proteases which are initially synthesized as inactive precursors. Cleavage of these precursor forms at specific aspartic acid residues results in their activation consequently leading to apoptosis (Figure 1-2). The active site in all members is a QACRG pentapeptide in which the cysteine residue is catalytic. Not only are these inactive proteases cleaved at aspartate residues, but they in turn cleave their substrates at aspartate residues. As might be expected, activated ICE can cleave and activate its precursor form in addition to one of its family members, CPP32 (Tewari et al, 1995; Cerreti et al, 1992; Faucheau et al, 1995). This suggests that other proteases may act in a similar fashion.

The substrates of these cysteine proteases are now being elucidated. The 116 kDa nuclear protein poly(ADP-ribose) polymerase (PARP), involved in DNA repair and genome surveillance, is specifically cleaved at the onset of apoptosis to an 85 kDa fragment (Kaufmann et al, 1993) by a protease recently shown to be CPP32 (Nicholson et al, 1995; Tewari et al, 1995). While ICE is unable to cleave PARP directly, indirectly through its activation of CPP32, PARP cleavage occurs (Tewari et al, 1995). Poly-(ADP) ribosylation deficient mice develop normally indicating it is not the substrate to directly control apoptosis. Other substrates implicated in apoptosis include lamin B1 (Neamati et al, 1995), topoisomerase I (Voelkel-Johnson et al, 1995) and β-actin (Kayal et al, 1995).

Figure 1-2: ICE protease activation and cleavage

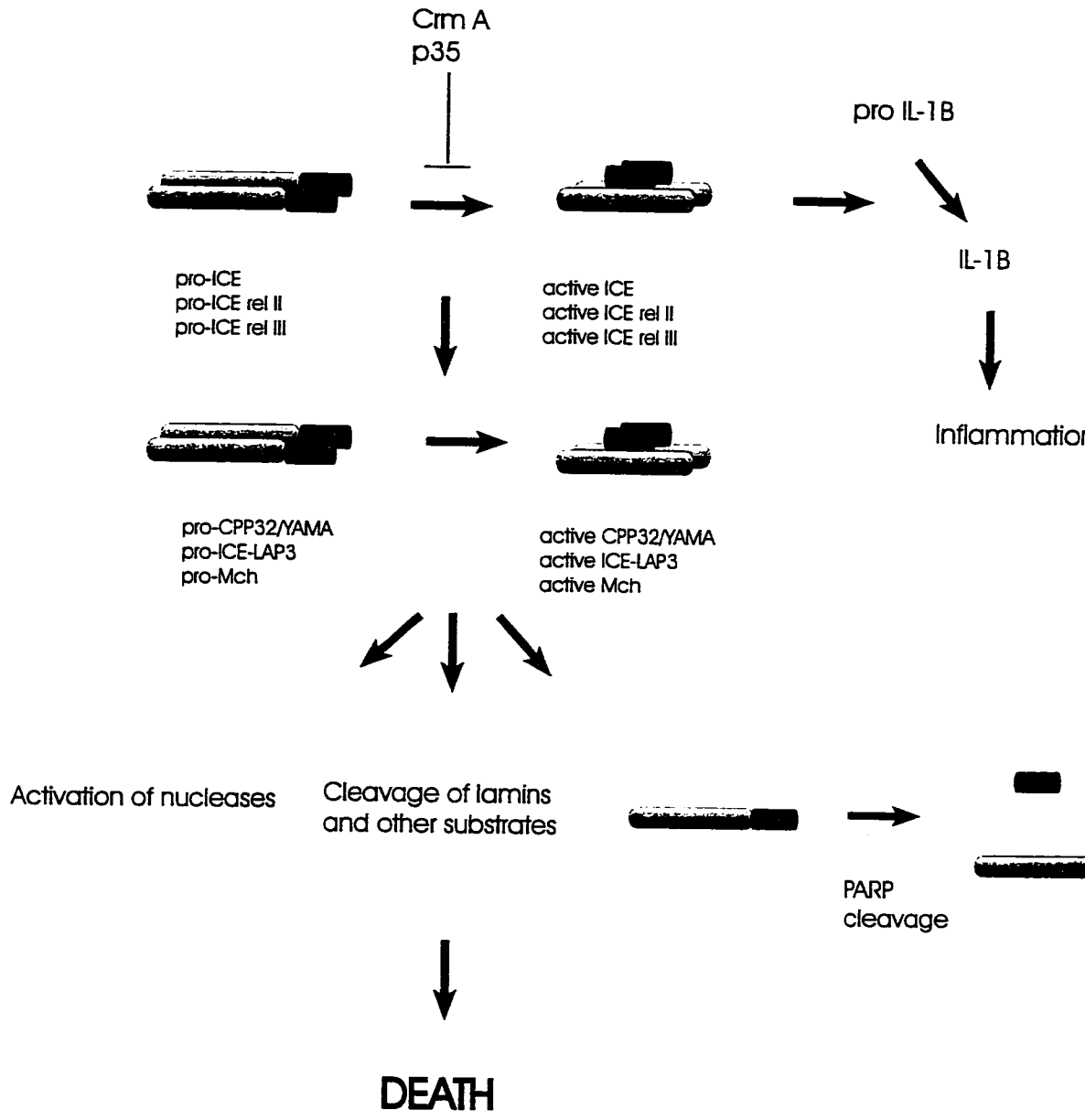
Crm A
p35
pro IL-1B
IL-1B
pro-ICE
pro-ICE rel II
pro-ICE rel III
active ICE
active ICE rel II
active ICE rel III
Inflammation
pro-CPP32/YAMA
pro-ICE-LAP3
pro-Mch
active CPP32/YAMA
active ICE-LAP3
active Mch
Activation of nucleases
Cleavage of lamins
and other substrates
PARP
cleavage
DEATH

The viral protein p35 has been shown to act as a competitive inhibitor of ICE and its other family members (including ced-3) consequently blocking apoptosis (Bump et al, 1995; Xue and Horvitz, 1995). This is achieved by the interaction with and the formation of a stable complex with these proteases, suggesting that other substrates may serve as competitive inhibitors. Although bcl-2 and bcl-xl do not directly act as substrates for these proteases, their overexpression inhibits activation of CPP32/ICE-LAP3 and the cleavage of PARP. These data indicate that these family members act upstream in the pathway (Chinnaiyan et al, 1996). The multiple ICE like proteases which cause apoptosis upon activation together with the multiple substrates which can either inhibit or promote cell death suggests a complex regulation at this level of the apoptotic pathway.

Increasing evidence suggests that proteases play a regulatory role in neuronal cell death. The demonstration that CrmA could inhibit death of neurons deprived of growth factor first implicated proteases in this process (Gagliardini et al, 1993). Furthermore peptide inhibitors of ICE, which mimic the aspartic acid in the P1 position of known ICE substrates, block the apoptotic death of cultured motoneurons deprived of trophic support (Milligan et al, 1995). Moreover, administration of these ICE peptide inhibitors reduces naturally occurring motor neuron cell death in the chick. In addition, the cysteine protease calpain I, is activated in the neuronal subpopulation that die by apoptosis during ischemia (Rami and Krieglstein, 1993). Serine proteases, that cleave after an arginine residue, may

additionally be involved in regulating the fate of neuronal cells. The serine protease thrombin, induces degeneration and death of neurons and astrocytes *in vitro* (Vaughan et al, 1994). Consistent with this data, the serine protease inhibitor nexin I (PNI) can inhibit thrombin and the death of spinal cord motoneurons during the period of programmed cell death in the chick and after axotomy in the mouse (Houenou et al, 1995).

The TNF family of receptors

A number of cell membrane receptors have recently emerged as proximal components of the cell death pathway which can either be protective or inductive. In contrast with most growth factor receptors, the two cell surface cytokine receptors, tumour necrosis factor receptor (TNFR) I and Fas/Apo-1 antigen activate apoptosis by binding of their ligands or specific agonist antibodies (Trauth et al, 1989; Yonehara et al, 1989). TNFR1 mediates cell death, antiviral activity and activation of NF-κB (Espevik et al, 1989; Tartaglia et al, 1991; Wong et al, 1992 and Pfeffer et al, 1993). Fas mediated cell death contributes to T cell mediated cytotoxicity and is required for negative selection, that is the normal elimination of potentially autoreactive peripheral T cells (Brunner et al, 1995; Ju et al, 1995). TNFR1 and Fas are members of the TNF receptor superfamily comprising both TNF receptors (TNFR1 [p60]and TNFR2 [p80]), the low affinity nerve growth factor (NGF) receptor p75, Fas, CD40, CD30, CD27 and OX40. (Smith et al, 1994). These receptors and their ligands are critical to the development and regulation of

lymphoid and hematopietic cells hence dysregulation of these gene products results in autoimmune disorders, immune deficiency syndromes and cancer (Gruss and Dower, 1995). Binding of these receptors by their ligands induces receptor oligomerization that initiates a cascade of downstream signalling events (Tartaglia and Goeddel, 1992). The cytoplasmic domains of these receptor family members differ in size with no discernible sequence homology to other catalytic domains to indicate how these receptors transduce signals. Only within the last year have two distinct classes of receptor associated proteins been identified which link these receptors to downstream signalling cascades.

Analysis of the two spontaneous mouse mutants, *lpr* (lymphoproliferation) and *gld* (generalised lymphoproliferative disease) which suffer from autoimmune disorders similar to systemic lupus erythematosus has helped delineate the role of the cytoplasmic domain of Fas in signalling (Cohen and Eisenberg, 1991). *Gld* mice result from a point mutation in the COOH terminus of the Fas ligand gene which abolishes the ability of the Fas ligand to bind its receptor while *lpr* mice were identified to have a point mutation in the cytoplasmic domain of the Fas receptor within a region that shares homology with the cytoplasmic domain of TNFRI. Both of these mutations abolish the ability of Fas to transduce the apoptotic signal (Watanabe-Fukunagata et al, 1992). The 80 amino acid region near the C-terminus of TNFRI and Fas, known as the death domain, was shown to be essential not only for the induction of cell death but antiviral activity and activation of NFκB (Tartaglia et al, 1993). The yeast two hybrid system demonstrated that the death domain was

involved in protein-protein interactions with other death domain containing proteins such as RIP (Stanger et al, 1995), FADD/MORT (Chinnaiyan et al, 1995; Boldin et al, 1995), TRADD (Hsu et al, 1995) and FAF (Chu et al, 1996). RIP and FADD associate with Fas while TRADD associates with TNFRI with the interactions occurring as homo and heterodimers (Figure 1-3). Overexpression of RIP, FADD or TRADD results in apoptosis yet the mechanism of signalling by these three proteins is not identical. Deletion analysis demonstrates that, as one would predict, induction of apoptosis by RIP or TRADD requires the death domain. Apoptosis is induced by FADD however not by the C terminal death domain but by a death effector domain at the N terminus. FADD induces apoptosis in a Fas ligand independent manner suggesting that it may be associated with Fas in a resting cell and is released upon receptor oligomerization. The N terminus of FADD may then interact with a downstream component (Chinnaiyan et al, 1995). Apoptosis induced by overexpression of these death domain proteins can be inhibited by CrmA implicating ICE involvement downstream in these pathways. Overexpression of TRADD not only leads to apoptosis but to activation of NF-κB (Rothe et al, 1995). These two signalling pathways were shown to be distinct as apoptosis induced by TRADD could be suppressed by crmA, however activation of NF-κB was not.

Figure 1-3: Apoptotic signal transduction of the TNF receptor superfamily. Extracellular cysteine rich repeats of the receptors are shown as shaded ovals. Death domains are shown as black rectangles. TRAF-N domains are depicted as stippled rectangles. IkB is shown as a lightly stippled circle and components of the NF-kB complex are depicted as darkly stippled circles

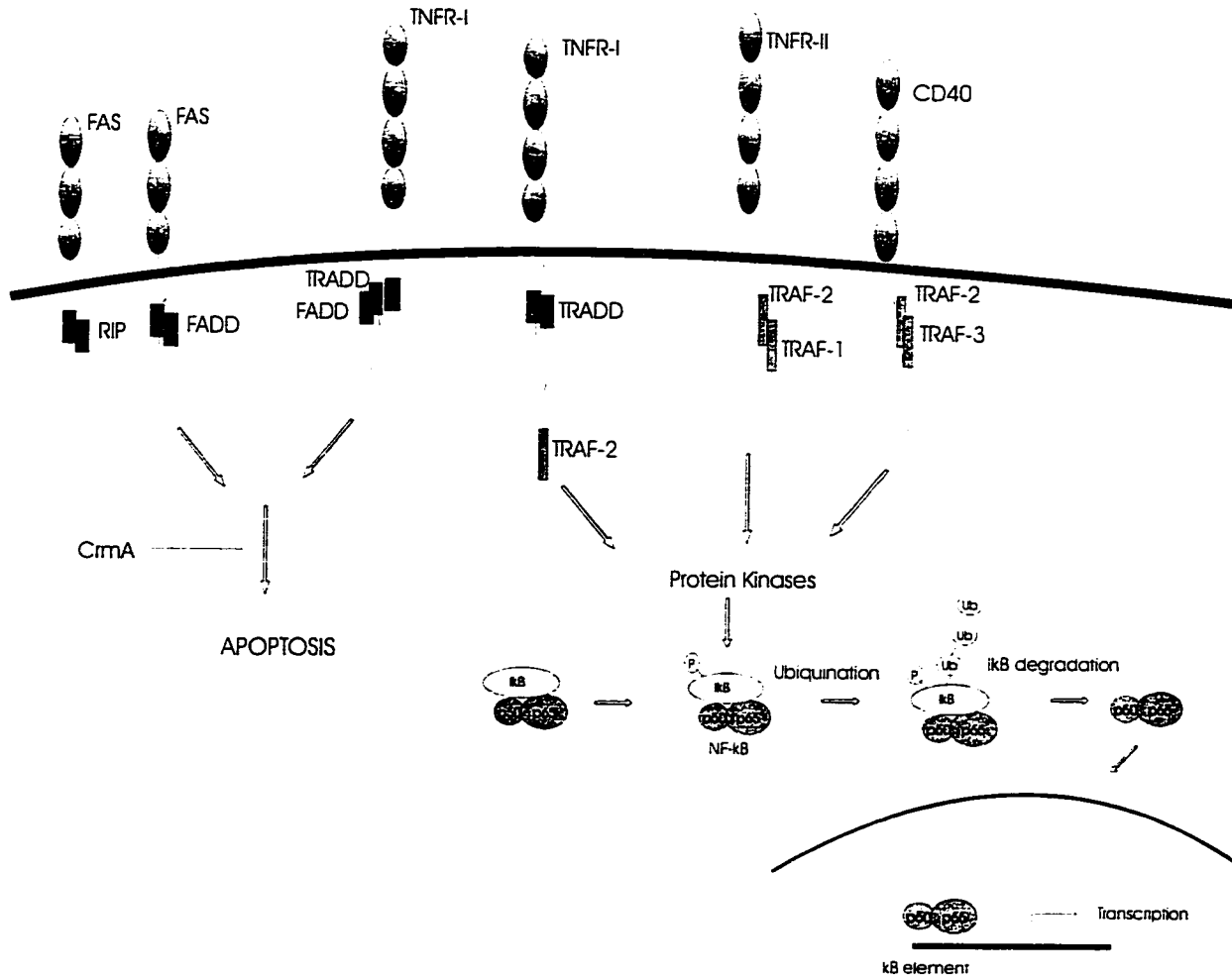
TNFR-I
TNFR-I
TNFR-II
CD40
FAS
FAS
TRADD
FADD
RIP
FADD
TRADD
TRAF-2
TRAF-1
TRAF-2
TRAF-3
TRAF-2
CrmA
Protein Kinases
APOPTOSIS
Ubiquination
ikB degradation
NF-kB
Transcription
kB element

. Figure 1-4: Schematic of the apoptotic cascade

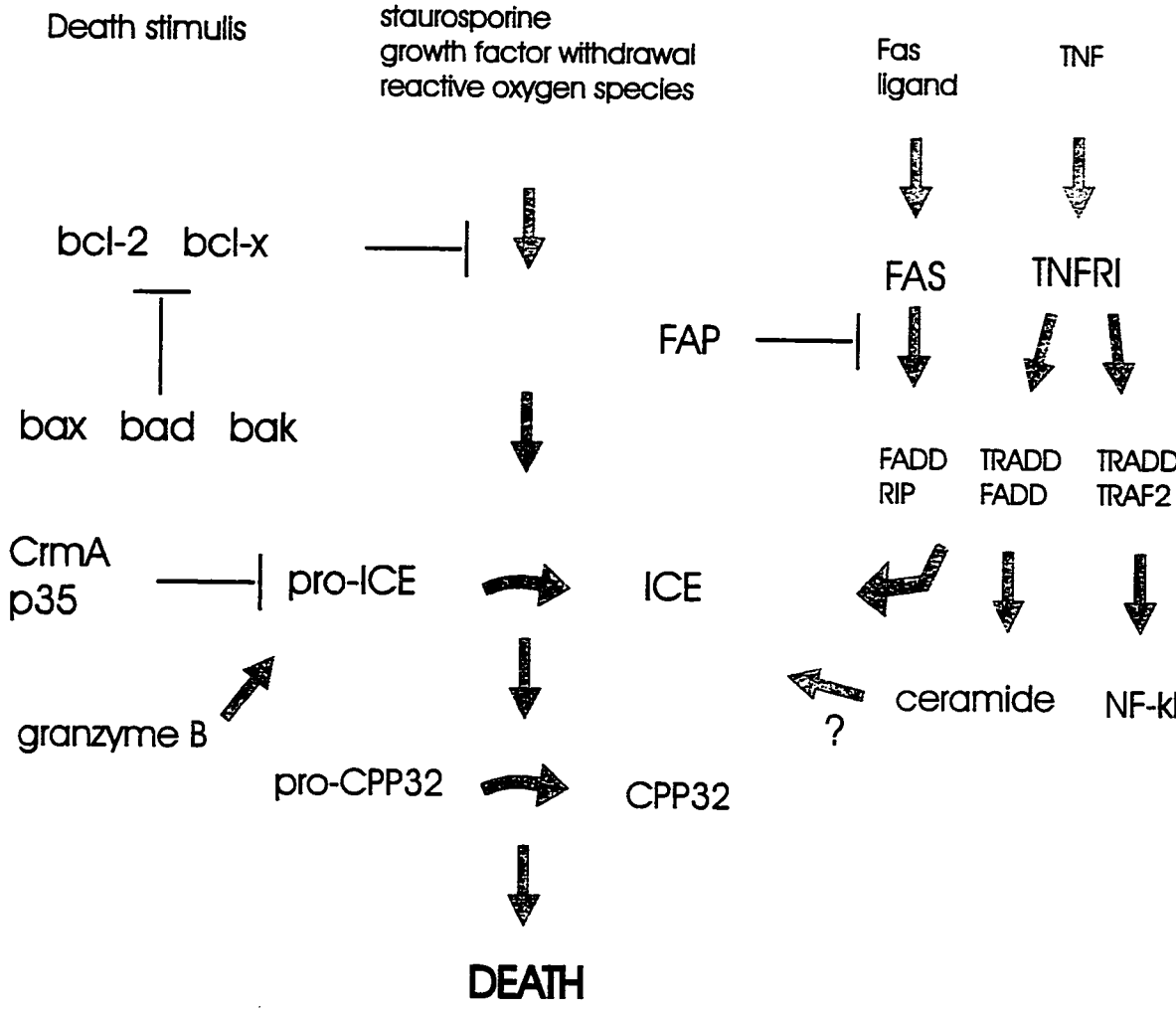
Death stimulis
staurosporine
growth factor withdrawal
reactive oxygen species
Fas ligand
TNF
bcl-2 bcl-x
FAS
TNFRI
FAP
bax bad bak
FADD RIP
TRADD FADD
TRADD TRAF2
CrmA p35
pro-ICE
ICE
granzyme B
ceramide
?
NF-kB
pro-CPP32
CPP32
DEATH

Stimulation of TNFRII or CD40 with agonist antibodies induces cellular proliferation (Tartaglia et al, 1991; Armitage et al, 1993). Mutational analysis has identified a C-terminal region of 78 amino acids within the cytoplasmic domain of TNFRII responsible for signal transduction (Rothe et al, 1994) that subsequently was shown to interact with two proteins TRAF1 and TRAF2 (TNFRII associated factor). TRAF1 and 2 interact with the signalling domain of TNFR2 in a heterodimeric complex via TRAF2. A third TRAF protein- TRAF3 (CD40 bp, CRAF1 or LAP-1) was identified which interacts with the cytoplasmic domain of CD40 and the EBV protein, latent infection membrane protein (LMP-1) (Hu et al, 1994; Cheng et al, 1995; Mosialos et al, 1995; Sato et al, 1995). TRAF3 and 2 were subsequently shown to associate with CD40 in a heterodimeric complex via TRAF2 (Rothe et al, 1995). Efforts to elucidate the two signalling events emanating from TRADD resulted in the identification of two associated proteins FADD and TRAF2 (Hsu et al, 1995). The NF-κB and apoptotic signalling components of TNFRI diverge at TRADD. Whether other downstream signalling components of TNFRI and TNFRII are shared is still unknown.

The three forms of SMA map to 5q11.2-q13.3:

The broad clinical spectrum observed in SMA led to the belief initially that TypeI and TypeII/II SMA were distinct disorders caused by non allelic mutations or different genes. Pearn first suggested that the lack of intrafamilial phenotypic variability was

evidence that genetic differences existed between the three forms (Pearn et al, 1973). However, close clinical examination of affected siblings has revealed heterogeneity indicating that all forms may be caused by the same gene with various allelic mutations (Emery et al, 1976; Benardy et al, 1978). In 1990 all three forms of SMA were mapped to the long arm of chromosome 5 at 5q11.2-13.3 confirming genetic homogeneity between the severe and chronic forms (Gilliam et al, 1990; Melki et al, 1990). Furthermore no cases of nonallelic heterogeneity have been reported supporting either a model of one gene with multiple phenotypic mutations or the involvement of different genes clustered at the 5q13 locus. No detectable chromosomal abnormalities such as translocations, large insertions or deletions are associated with SMA thereby precluding identification of the gene in this manner. However, the mapping of SMA to a specific chromosome permitted isolation of the gene(s) by positional cloning (reverse genetics). (Collins, 1991).

Positional cloning: an overview

Positional cloning of a human disease gene is a process of incremental refinement of the location of a gene by sequentially employing methods of increasing resolving power (summarised in Figure 1-5). The first step towards the identification of a disease gene is the collection of DNA samples from families affected by the illness. Subsequently a whole genome search is undertaken to link (map) the disease to a chromosome through

Figure 1-5: Sequential steps to identify a disease gene

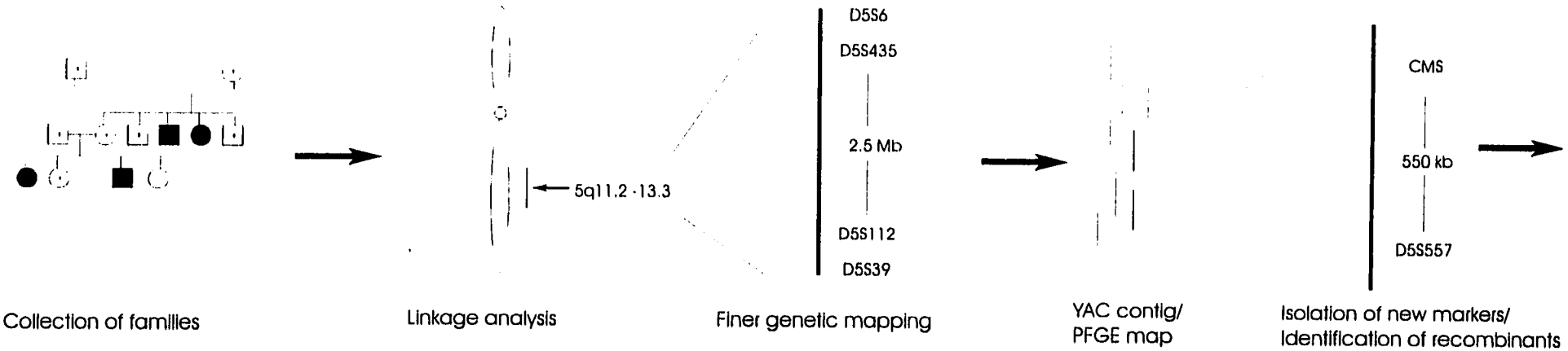
D5S6
D5S435
2.5 Mb
5q11.2 -13.3
D5S112
D5S39
CMS
550 kb
D5S557
Collection of families
Linkage analysis
Finer genetic mapping
YAC contig/
PFGE map
Isolation of new markers/
Identification of recombinants

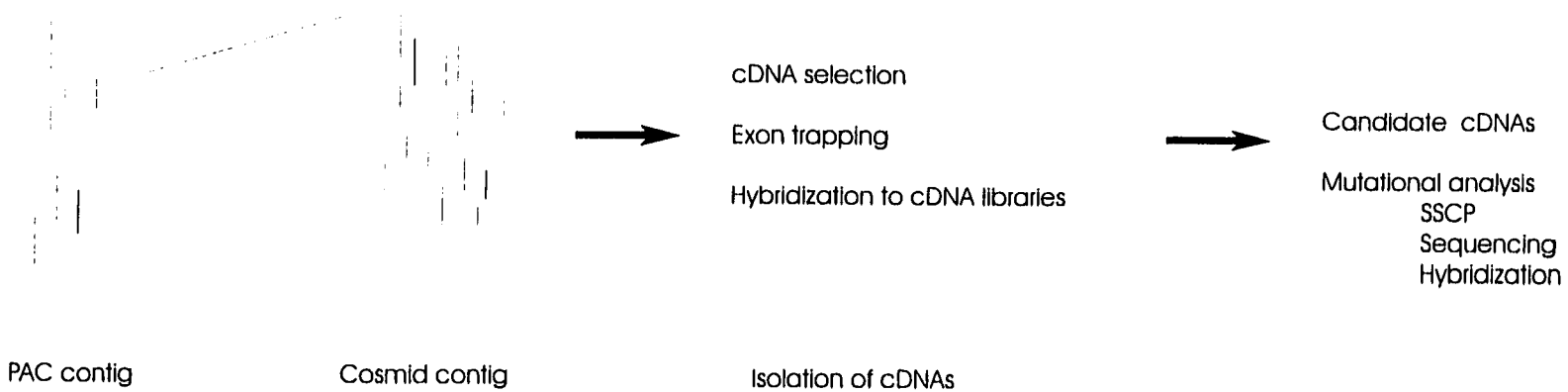
cDNA selection
Exon trapping
Hybridization to cDNA libraries
Candidate cDNAs
Mutational analysis
SSCP
Sequencing
Hybridization
PAC contig
Cosmid contig
Isolation of cDNAs

the use of polymorphic markers whose chromosomal location is known. Normally the disease gene is localised between a set of flanking genetic markers within a relatively small portion of a single chromosome. Linkage analysis in combination with physical mapping of the region leads to the isolation of the disease causing gene.

Markers utilised for genetic analysis take advantage of nucleotide variants or repetitive DNA sequences interspersed in the human genome. Nucleotide variants resulting in the disruption or gain of a restriction endonuclease site can be detected by hybridization with probes that span this region, detecting variations in the length of restriction endonuclease fragments. This type of genetic marker has been termed a restriction fragment length polymorphism (RFLP) (Robson, 1988). A second class of markers are based on repetitive DNA sequences that are polymorphic. One type of repetitive sequences that are highly polymorphic are microsatellites (MSR). They consist of a variable number of dinucleotide repeats where the number of repeat units can vary from 10 to 60 (Miesfeld et al, 1981; Weber and May; 1988). Each microsatellite can be specifically amplified by the polymerase chain reaction (PCR) using unique sequence oligonucleotides that flank the repeat.

Linkage analysis is based on the concept that markers and the disease phenotype will cosegregate (be passed on or be genetically linked) in families with that disease. If linkage between two markers is demonstrated then they are located on the same chromosome; the greater the degree of linkage between the two markers the smaller the

distance between them. Crossing over, or recombination, occurs randomly over the length of the chromosome between two loci on homologous chromosomes. It can be deduced that recombination is more likely when two loci are far apart from one another and is rare when two loci are in close proximity. The probability of recombination occurring is called the recombination fraction (θ). The value of θ denotes the genetic distance between two loci. A θ of 0.01 or a 1 % chance of recombination between two genetic markers is denoted as one centiMorgan (cM) which itself represents the equivalent distance of approximately one million base pairs. It follows then that the comparison between the value of θ between different sets of markers permits the orderering of loci on a chromosome and leads to the construction of a genetic map.

Linkage disequilibrium mapping offers a powerful approach for finer localisation of a disease gene. Linkage disequlibrium is based on the observation that in a given population affected chromosomes may have descended from a common ancestral mutation. Chromosomes descended from the original ancestral chromosome with the mutation would have, in the vicinity of the gene, a haplotype similar or identical to the original chromosome. Affected individuals then share a ccmmon haplotye that would be distinct from that found in unaffected individuals. This approach is most powerful if (i) there is a single disease-causing allele (ii) this allele was introduced into the population a long time ago and (iii) if the population under study is of genetic homogeneity. In general

the greater the linkage disequilibrium a marker shows for a given disease gene the closer it maps to the disease locus.

The identification of genetic markers on a chromosome which flank a disease gene allows one a starting point for the generation of a physical map. Once linkage analysis has been employed to the limits of its resolving power, physical mapping strategies must be utilised to clone the region encompassing the gene, an essential step in the identification of the gene. If the genetic flanking markers define a large physical distance (> 1 cM) then somatic cell hybrids and yeast artificial chromosomes are initially required to physically map the locus. Somatic cell hybrids containing either whole or irradiation-reduced chromosomes, in combination, provide a powerful method for ordering DNA markers that span millions of base pairs (Goss and Harrie, 1975; Cox et al, 1990). Linkage analysis of chromosome 5 markers demonstrated that SMA lies in a region close to the loci D5S6 and D5S39. Mapping studies using somatic cell hybrids deleted for the region 5q11.2 - q13.3 localised these markers within this deleted region (Gilliam et al, 1989).

The assembly of physical maps over large areas of a chromosome has been facilitated by the advent of large insert cloning technology. These include yeast artificial chromosomes (YACs) (Burke et al, 1987) which carry inserts that average several hundred kilobase pairs, and several bacterial artificial chromosome systems (BACs) which include, F-factor derived BACs (Shizuya et al, 1992) and various P1 derived BACs or

PACs (Sternberg et al, 1990; Ioannoue et al, 1994) which carry inserts of approximately 100 kb. Finer resolution can be achieved by the use of cosmids, having an average insert size of 40 kb.

A contiguous array of clones (known as a contig) encompassing a region of a chromosome, is assembled through the use of end-clones generated by *Alu*-vector PCR and internal single copy probes (or sequence tagged sites (STS)) generated by *Alu-Alu* PCR. These are utilised as hybridisation probes or, in the case of STS's, unique primers are generated such that PCR may be utilised to identify overlapping clones. The overlap of clones is confirmed by *Alu*- PCR fingerprinting, STS content and restriction mapping analysis.

Although YACs represent a powerful tool for physical mapping they are not without some limitations and thus are not always suitable for fine mapping of a region. Approximately 1% of YAC clones are unstable giving rise to clones which contain small or large scale deletions, duplications or inversions. Instability of certain genomic regions, due possibly to repetitive sequences, results in a high frequencyer of unstable clones. In addition, 10 % of YAC clones contain two different YACs due to cotransformation during preparation of the library and a high proportion of clones contain DNA from two different regions of the genome (chimeric clones). Furthermore often there is low transformation efficiency and only low yields of YAC DNA can be obtained. These

limitations can greatly hinder the construction of a contiguous array and require that the chromosomal location of YAC probes be verified by fluorescent in situ hybridization or somatic cell hybrid analysis.

The bacteriophage cloning systems were generated to provide a supplement and alternative to the YAC and cosmid based systems. The BAC system employs the*E. coli* F. factor, reducing the potential for recombination as the F plasmid is maintained in a low copy number. The P1 system was developed to obtain larger quantities of cloned DNA (Sternberg et al, 1990). With this system DNA is replicated as a low copy number plasmid in *E. coli* and then amplified to a high copy number through the use of a second replicon in the vector. The bacteriophage artificial chromosomes offer advantages over YACs due to their stable propagation, increased stability and increased yields of cloned DNA.

The YAC, PAC and cosmid clones serve as a resource to identify new polymorphic markers that are utilised for linkage analysis. The physical assignment of linkage markers and the identification of recombination events with these markers, define the minimum region anticipated to contain the disease gene while the physical mapping of markers which are in linkage disequilibrium with the disease denote the interval within that minimum region most likely to contain the disease gene. The identification of candidate genes from within a region can be achieved once the DNA which encompasses the disease

locus has been cloned and usually begins when a minimum region is defined. A variety of approaches now exist to identify candidate genes including the screening of cDNA libraries, cDNA selection and exon trapping utilising either YAC, PAC or cosmid inserts. Direct cDNA selection involves the hybridization of a library of cDNAs to an immobilised genomic clone followed by washing of non-specific cDNAs and elution of those which are encoded by the region of interest (Lovett et al, 1991; Parimoo et al, 1991). Coding sequences from genomic DNA can be isolated at a high efficiency by an exon trapping system based on the selection of functional splice sites (Buckler et al, 1994).

Summary of work

In 1990, all three forms of childhood SMA were mapped to the long arm of chromosome 5 at 5q11.2-13.3. The SMAs were mapped by genetic linkage analysis between the proximal marker D5S6 and the distal marker D5S39 within an approximate 10 cM interval (Figure 1-6) (Brustowicz et al, 1990; Melki et al, 1990; Gilliam et al, 1990). Recombinations with the distal marker D5S112 were subsequently identified reducing the genetic interval to 6 cM (Daniels et al, 1992, Brustowicz et al, 1992; Morrison et al, 1992). This region was further refined to a 4 cM region by a proximal recombination involving the marker D5S125 (Wirth et al, 1993; Melki et al, 1993). The order of these loci was based upon multipoint linkage analysis in addition to

Figure 1-6: Localisation of SMA to 5q11.2-13.3. The genetically defined 10 Mb region flanked centromerically by the marker D5S6 and telomerically by the marker D5S39, is shown. This interval was refined, based on the identification of recombinations in SMA individuals, to a 4 Mb locus flanked by centromerically by the marker D5S125 and telomerically by the marker D5S112

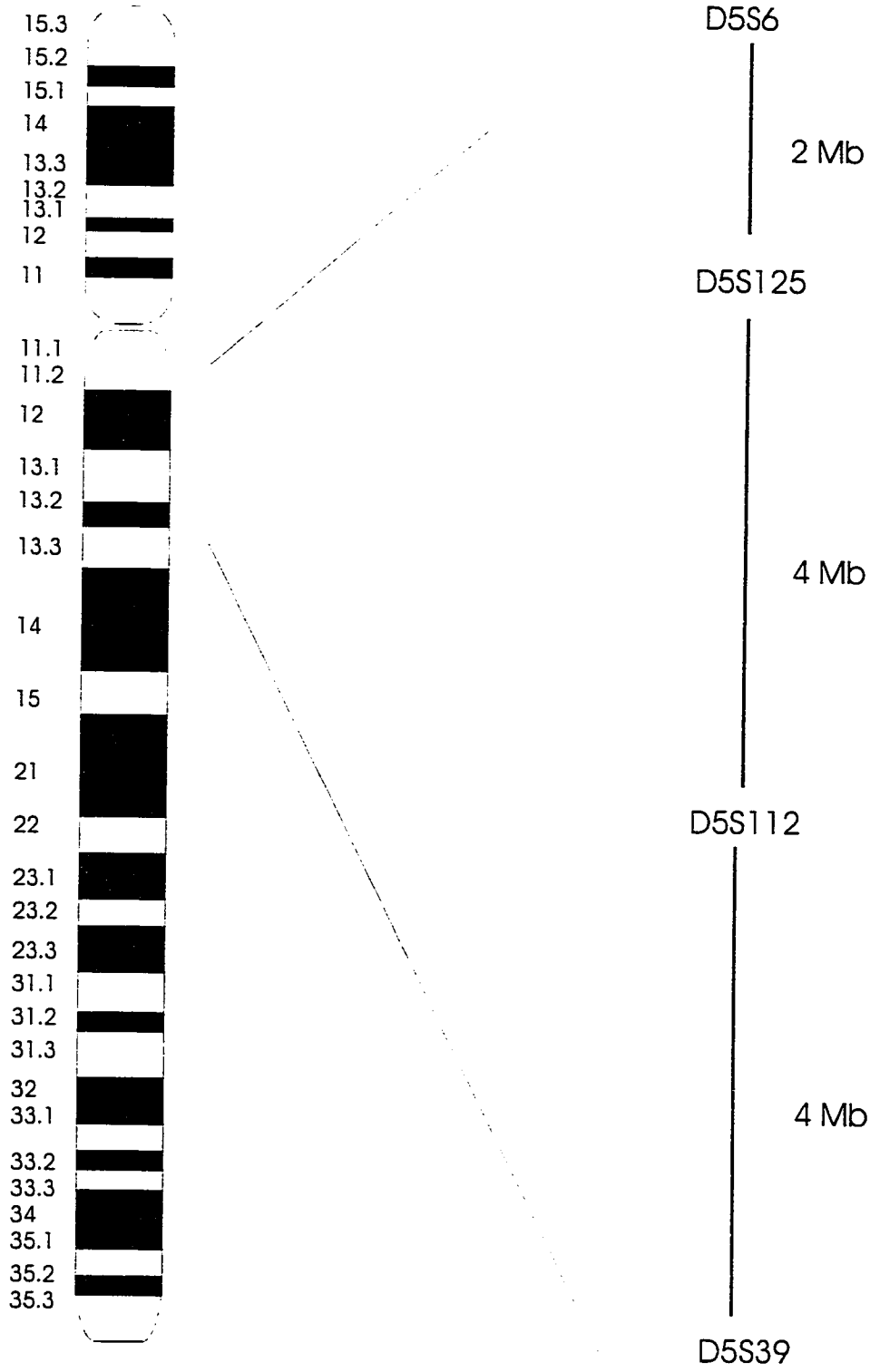
15.3
15.2
15.1
14
13.3
13.2
13.1
12
11
11.1
11.2
12
13.1
13.2
13.3
14
15
21
22
23.1
23.2
23.3
31.1
31.2
31.3
32
33.1
33.2
33.3
34
35.1
35.2
35.3
D5S6
2 Mb
D5S125
4 Mb
D5S112
4 Mb
D5S39

recombination results. A major objective of this thesis was to use physical mapping techniques to identify and clone the minimal region containing the SMA gene and subsequently isolate candidate cDNAs from this region to search for the SMA mutation. To this end we assembled a 3 Mb contiguous array of YACs encompassing the genetically defined SMA D5S435 - D5S112 region and established a long range restriction map of this region. This area of the genome is unusual in that chromosome 5 specific repetitive sequences are abundant hindering the isolation and ordering of clones. These sequences have homologies to other regions of chromosome 5 in addition to 5q11.2-13.3 including 5q31 and 5p (Francis et al, 1993; Thompson et al, 1993). The microsatellite repeat (MSR), CATT-1, mapping within the SMA D5S112-D5S125 interval, was isolated during the course of this study and was utilised to initiate a cosmid walk. This revealed the presence of multiple CATT-1 subloci within 5q11.2-13.3, encompassing 140 kb. One of these subloci demonstrated high linkage disequilibrium with Type I SMA indicating close proximity to the SMA gene. Given our genetic data in addition to the complexity of the region we constructed a PAC contig of approximately 500 kb encompassing the CATT region. These approaches resulted in the cloning of the entire SMA region. A key recombinant was identified in a Polish Canadian SMA family (Yaraghi et al, 1995) defining a proximal boundary which was mapped based on our YAC, PAC and cosmid contigs, reducing the minimal region harbouring the SMA gene from 1.1 Mb to approximately 600 kb. This work is presented in Chapter 2.

Given that one of the PAC clones contained the CATT-1 subloci, which demonstrates the maximum linkage disequlibrium with Type I SMA, and the marker CMS-1 which defines the proximal SMA boundary, we reasoned that the SMA gene was contained in this region. In an effort to identify candidate cDNAs, an exon trapping system was utilised to isolate exons spanning our PAC contig resulting in the identification of 36 exons. A number of these exons were contained within or extended cDNAs isolated in our lab. One of these demonstrated homology to the viral inhibitor of apoptosis proteins (IAP) which we termed, the neuronal apoptosis inhibitory protein (NAIP). The genomic organisation of this candidate gene was elucidated revealing a number of truncated and internally deleted versions of the *naip* gene in our YAC, PAC and cDNA clones. Mutational analysis revealed the homozygous deletion of exon 5 and 6 in our Type I population. These findings suggested that mutations in the *naip* locus may lead to the failure of normally occurring inhibition of apoptosis resulting in or contributing to the SMA phenotype. Concurrent with our isolation of *NAIP*, a second candidate gene, the survival of motor neuron (*smn*) gene was identified which also maps to the SMA locus at 5q13 and is deleted in a significant proportion of individuals with SMA (Lefevbre et al, 1995). We mapped this gene to the same 150 kb PAC clone containing *naip*. This work is presented in chapter 3.

In an effort to elucidate the role of NAIP in SMA pathogenesis we sought to determine the cellular distribution of NAIP and the role of NAIP in apoptosis. We

examined the distribution of NAIP in the spinal cord with a polyclonal antisera revealing a cytoplasmic distribution of NAIP in motor neurons. Furthermore, the ability of NAIP to suppress apoptosis upon serum deprivation, treatment with menadione or tumour necrosis factor- α (TNF) was investigated resulting in the confirmation of its ability to counter cell death. Taken together these data support a role for NAIP in the inhibition of naturally occurring motor neuron apoptosis during development and contributing to the SMA phenotype when absent. Futhermore we have isolated the first member of a novel class of human proteins which function to inhibit apoptosis.

CHAPTER II:

PHYSICAL MAP OF THE SPINAL MUSCULAR ATROPHY GENE REGION AT 5Q13 BASED ON YAC, PAC AND COSMID CONTIGUOUS ARRAYS

Introduction

In 1990, all three childhood forms of SMA (Types I, II and III) were genetically mapped to the long arm of chromosome 5 at 5q11.2 - 13.3 within an approximate 10 cM interval defined by the markers D5S6 and D5S39 (Brustowicz *et al.*, 1990; Gilliam *et al.*, 1990; Melki *et al.*, 1990). This suggested that different mutations in the same gene or contiguous genes account for the varying degrees of severity of the disorder. Subsequent multi-point linkage analyses and the identification of recombinant events have further localised the genetic defect to the region flanked centromerically by D5S435/D5S629 (Soares *et al.*, 1993; Wirth *et al.*, 1993, Clermont *et al.*, 1994)) and telomerically by MAP1B/D5S112 (Wirth *et al.*, 1994; MacKenzie *et al.*, 1993; Lien *et al.*, 1991). This interval has been refined by the more recent identification of recombination events indicating that the SMA gene lies distal to CMS-1 (Yaraghi *et al*, 1995, van der Steege, *et al.*, 1995) and proximal to D5S557 (Francis *et al* 1993).

We have established a contiguous array of YAC clones encompassing the SMA containing D5S435-D5S112 interval of 5q13.1. We and others have detected chromosome 5-specific repetitive sequences with particular abundance in the

D5S629/CMS-D5S557 region (Francis *et al.*, 1993; Thompson *et al.*, 1993) which has impeded the isolation and ordering of both clones and STRs. STR's, normally found at one chromosomal location are likewise repeated within this region of 5q13 and are located at various loci termed subloci. An array of cosmid clones spanning the 210 kb CMS-1 (Kleyn *et al.*, 1993)/CATT-1 (Burghes *et al.*, 1994, McLean *et al.*, 1994)/D5F150/D5F149/D5F153 (Melki *et al.*, 1994) region within this interval in addition to a 500 kb PAC contig encompassing this region has been constructed. The establishment of a high resolution physical map in this region, which we have shown to contain polymorphic loci demonstrating linkage disequilibrium with Type I SMA combined with the precise mapping of the distal boundary of the SMA locus were important steps in the cloning of the SMA candidate gene.

Materials and Methods

YAC libraries and screening

The libraries used in this study were constructed at the Imperial Cancer Research Foundation (ICRF) (Larin *et al.*, 1991), the National Centres of Excellance (NCE); cell line GM0684) and Centre d'Etude du Polymorphisme Humaine (CEPH) (Albertson *et al.*, 1990) The NCE library was screened initially by PCR of 34 pools, followed by PCR screening of rows and columns of the plates found to be positive. The ICRF library was screened by hybridization of high density robot spotted filters.

Cosmid and YAC DNA preparation

Cosmid DNA was isolated by alkaline lysis (Birnboim and Doiley., 1979). Yeast strains containing YACs were grown in 5 ml cultures of selective media lacking uracil and tryptophan for 24 hr at 30°C. Small scale DNA isolation for Southern blot analysis was performed as previously described (Scherer *et al.*, 1991). Yeast chromosomes were prepared in agarose blocks and stored at 4°C in 0.5*M* EDTA.

YAC end isolation and inter-Alu PCR

YAC end sequences were isolated by *Alu-vector* PCR. PCR primers for pYAC4 vector were:TAGCTCGAGGACTTTAATTTAACACTACGGAATTC;TAGCTCGAGCGCCC GATCTCAAGATTACGGAATC, corresponding to the pYAC4 left arm (*trp*) and right arm (*ura*) respectively. Each of these was used in combination with one of two human specific *Alu* primers corresponding to the 5' end of *Alu* GGATTACAGGCGTGAGCCAC and the 3' end of *Alu* GATCGCGCCACTGCACTCC (Tagle *et al.*, 1992). Reaction conditions were 7 min at 94°C followed by 30 cycles of 1 min 30 s at 94°C, 1 min 30s at 55°C, and 3 min at 72°C. Twenty microliters of each reaction was electrophoresed on 0.8 % agarose gels and both vector end products and inter-*Alu* products were isolated. Products were cloned using the TA cloning kit (Invitrogen) and subsequently sequenced to design primer sequences using M13 forward and reverse primers.

PCR primer sequences for STSs listed in Table 1 from this study were as follows: YD33, AGCCTTGGCGACAGAGCAAGA and TTCTCAGCAAGGAACATCCCT or TTAACCTAAGGACTCAGAGCT; Y13.1, AGGAGGGTGGATCCCTGGGA and CTCGAACTCCTGACCTCA; Y14.1, AGGAAGAAGTCAGGATTG and AGTTACACATGTATGCAT; Y15.1, CACAATGCAGGATCATCA and GAAGCGTTCAGTGGACAC, Y5.6, GCTGTGTGAAGTCTTCCT and GGAATTACTGAGCTGCTG; Y9.2, GTAAGGAATTGGTTGCAG and GTGCTGGGATTATAGGCA, and Y11.2, AGCTTAAATGTGCATTGT and ACAAGGATCTCACTGAGT.

Pulsed field gel electrophoresis

DNA was separated through 1% agarose gels in 0.5X TBE buffer using a CHEF DRII electrophoresis system at 200 volts with a 50s to 90s switch time. To determine the size of YAC clones, undigested YAC DNA was run for 20 hr. Various run times were used when DNA was digested with rare cutter restriction enzymes depending on the sizes of fragments to be resolved. Gels were depurinated for 10 minutes in 0.25M HCl, denatured for 1 hr and neutralized for 1 hr prior to transfer to nylon membranes (Hybond, Amersham) for 48 hr. For restriction enzyme digestion, YAC plugs approximately 25μl in volume were utilized in 100μl reactions containing 10X buffer, BSA, DTT and spermidine (Nelson *et al.*, 1993). Partial digestion of YACs was achieved by addition of 0.5U and 20U of enzyme. Reactions were placed on ice for 60 minutes prior to digestion for 4

hours. Filters were hybridized separately with a 2.7 kb *Pvu* II/*Bam* HI fragment or a 1.7 kb *Pvu* II/*Bam* HI fragment of pBR322 corresponding to the pYAC4 left (trp) end and the pYAC4 right (ura) end respectively.

PCR analysis and hybridization

YAC and cosmid DNA were diluted 1/10 for PCR analysis. For each STS and marker, one primer was endlabeled with [γ-^{32}P]ATP utilizing T4 polynucleotide kinase (GIBCO BRL) as described (Sambrook *et al.*, 1989). The DNA was amplified in 25µl reactions containing 0.4 m*M* dATP, 0.4 m*M* dCTP, 0.4 m*M* dGTP, 0.4 m*M* dTTP, 10 m*M* $MgCl_2$, 10 m*M* Tris pH 8.3, 50 m*M* KCL, 1 unit *Taq* polymerase (Perkin Elmer Cetus) 50 ng end labeled primer and 50 ng cold primers. Reaction conditions and primers for STS's and markers in Table 2 are as described in their corresponding references. Cycling conditions for Y15.1 were 95°C, 1 min. 60°C, 1 min 20 s, 72°C, 1 min; 72°C, 10 minute final extension. All other STSs from this study were amplified by the following conditions; 94° 1min, 55°C, 1 min, 72°C, 1 min; 72°C, 10 minute final extension. 4 µl of each product was run on 6 % polyacrylamide gels at 50 Watts for 4-7 hours. Gels were visualized by audioradiography after 1-24 hr exposure at -80°C. Cloned probes or total human DNA utilized for hybridization were radiolabeled with [α^{32}P]dCTP by random priming as described (Feinberg *et al.*, 1983).

Chromosome 5 cosmid library screening

A flow-sorted chromosome 5 cosmid library was utilised as a source of 5q13.1 cosmids. Duplicate colony filters of each microtiter dish (256 in all) were prepared on nylon membranes (Hybond, Amersham). The membranes were placed at 37°C overnight on LB agar to allow colonies to grow and subsequently prepared as described (Davis *et al.*, 1986). Pooled cultures of the 96 cosmids from each microtiter dish were utilized to prepare DNA . The DNA from each dish was digested with *Pvu*II, electrophoresed on 0.8% agarose gels and transferred to duplicate nylon filters overnight. Probes were hybridized to the filters containing the pooled DNA to identify positive microtiter plates. The corresponding colony filters were then hybridized to identify the cosmid address.

End fragments of cosmids were isolated by vector *Alu* PCR utilizing T7 and T3 primers in combination with one of two *Alu* primers: *Alu* 33, 5'-CTGGGATTACAGGCGTGAGCCA-3' (Shutler al., 1992) and Alu34, 5'CGCCAATGCACTCCAGCCTGGG-3' (Shutler al., 1992). Reaction conditions were: 1 min at 92°C, 1 min 30s at 50°C, and 2 min 30s at 72°C for 30 cycles. 15µl of each product was electrophoresed on 0.8% LMP gels and vector end or inter-*Alu* products isolated. Products for *Alu*-PCR fingerprinting were electrophoresed in a 2.5% Nusieve GTG gel.

Construction of cosmid library from YAC 76C1 and screening

High molecular weight DNA was prepared as described (Davis *et al.*, 1986). Cell lysates were fractionated on a sucrose step gradient and examined by pulsed field gel electrophoresis. The average size of inserts ranged from 100kb to 680kb. 1-2μg of YAC DNA was digested with *Mbo*I to clone into the *Bam*HI site of SuperCos 1. Inserts were size fractionated with a step sucrose gradient, fractions collected and run on an agarose gel. The *Mbo*I concentration and time of digestion which gave a mean size of 30-50 kb was chosen. Ligation of inserts to SuperCosI was as described (Stratagene, Davis *et al.*, 1986). Packaging of the inserts was performed with Gigapack as recommended by the manufacturer. Colony filters were prepared and hybridizations performed as described above.

Assembly of PAC contig

Three PAC libraries, constructed as in Ioannou et al (1994), with a combined total of 175,000 clones were screened by PCR with 5q13 STS's and STR's. PACs were aligned by further analysis with STS's and by hybridization of Southern blots with single copy genomic and cDNA probes. PAC clones were digested with *NotI* and resolved by pulsed field gel electrophoresis at 200 V with a 50 to 90 s switch time for 5 hr to determine their size. PACs were grown in LB containing 25 μg/ml kanamycin and DNA was prepared by alkaline extraction. PAC ends were isolated by *Alu*-vector PCR using the pCYPAC1 derived primers 1657 (GA GCT TGA CAT TGT AGG ACT) and 1658 (AAG CCC

TCC TAG CTT TGC CGT) in combination with the *Alu* 33 and 34 primers as described above.

RESULTS

Construction of YAC contig

YAC clones were isolated from three libraries, constructed at the National Centers of Excellence(NCE, Toronto), the Imperial Cancer Research Fund (ICRF, London) (Larin *et al.*, 1991) and the Centre d'Etude du Polymorphisme Humaine (CEPH, Paris) (Albertson *et al.*, 1990), all of which were prepared from partial *Eco*RI digests of total DNA ligated into the YAC vector pYAC4. ICRF YAC clones were identified by probing library filters with 5q13.1 probes. YAC DNA from the NCE library was screened by PCR amplification, electrophoresed, immobilized on to Southern blots and hybridized with the radiolabelled STS product to identify positives. Numerous positives were obtained repeatedly in both the initial round of PCR of pooled plates, and the second round with the plate(s) thought to contain the clone of interest many of which proved to be false positives. The number of false positives obtained, which appeared to be primer dependent, was reduced by radiolabelling PCR products and resolving these on 6% polyacylamide gels. The true positives could then be sized accurately without interference from spurious products.

Yeast strains with YACs positive for 5q13.1 STSs were grown on selective plates and examined for stability in the following manner: 4 colonies of each were grown for preparation in agarose blocks, yeast chromosomal DNA was separated by pulsed field gel electrophoresis and transferred to filters and the size and number of YAC clones contained within each yeast colony was determined by hybridization with radiolabelled total human genomic DNA. Positive clones were confirmed either by hybridization or PCR amplification with the original probe. Only YAC 24D6-2 contained some colonies with transformed or deleted YACs (Figure 2-1).

YAC end clones and inter-*Alu* products were isolated by vector-*Alu* PCR and inter-*Alu* PCR respectively. The location of these products within 5q11-13 was confirmed by hybridization to Southern filters of the somatic cell hybrids HHW105 (Dana*et al.*, 1982), containing the entire chromosome 5, and HHW1064 (Gilliam *et al.*, 1989), a derivative containing chromosome 5 with a deletion at 5q11.2-13.3. Many of these probes demonstrated hybridization profiles indicative of locations both within the 5q11-13 region and elsewhere on chromosome 5. In some cases primers specific for the ends of each YAC were generated from the sequences of YAC end clones isolated by vector-*Alu*-PCR. The mapping of each new STS to 5q11 - 13 was determined by PCR amplification of DNA from the somatic cell hybrids HHW105 and HHW1064 (Figure 2-2). In a few cases it was found that a primer pair contained a chromosome 5 repetitive sequence as the

TABLE 1-1: Origin and size of YAC clones

YAC	Size	Library
12H1	560 kb	NCE
12H4	270 kb	NCE
24D6	750 kb	NCE
27H5	630 kb	NCE
33H10	1.3 Mb	NCE
H0416	390 kb	ICRF
E0320	440 kb	ICRF
G1138	850 kb	ICRF
A0848	350 kb	ICRF
D06100	580 kb	ICRF
D0981	450 kb	ICRF
919C2	800 kb	CEPH
755B12	1 Mb	CEPH
754H5	500 kb	CEPH

Figure 2-1: Pulsed field gel electrophoresis and stability of YAC clones. Chromosomal DNA from YACs were separated by pulsed field gel electrophoresis (left panel). The location of the YAC clone, observed as an extra chromosome , is marked with a black dot. Many of the YAC clones cannot be detected by eye. Chromosomal DNA from four colonies of YAC 24D6 (right top panel) and 1281 (right bottom panel) were separated by pulsed field gel elctrophoresis and probed with total human genomic DNA. Cotransformation of YACs and deleted versions are both observed in the top panel.

24D6
700 kb
580 kb
460 kb
370 kb
1281
650 kb
754H5
919C2
755B12
12H4
76C1
D0981
27H5
184H2
235B7

Figure 2-2: Generation of YAC end STS. *Alu* PCR of YAC D06100. A 750 bp unique band can be seen upon amplification with the YAC vector (trp/left arm) and the *Alu* 5' primer (top panel). This band was cloned into the TA cloning vector, sequenced and internal primers were designed to generate a novel STS. The bottom panel shows amplification products in genomic DNA (G), YAC D06100 and the somatic cell hybrid HHW105 but not HHW1064, confirming its location at 5q11.2-13.3.

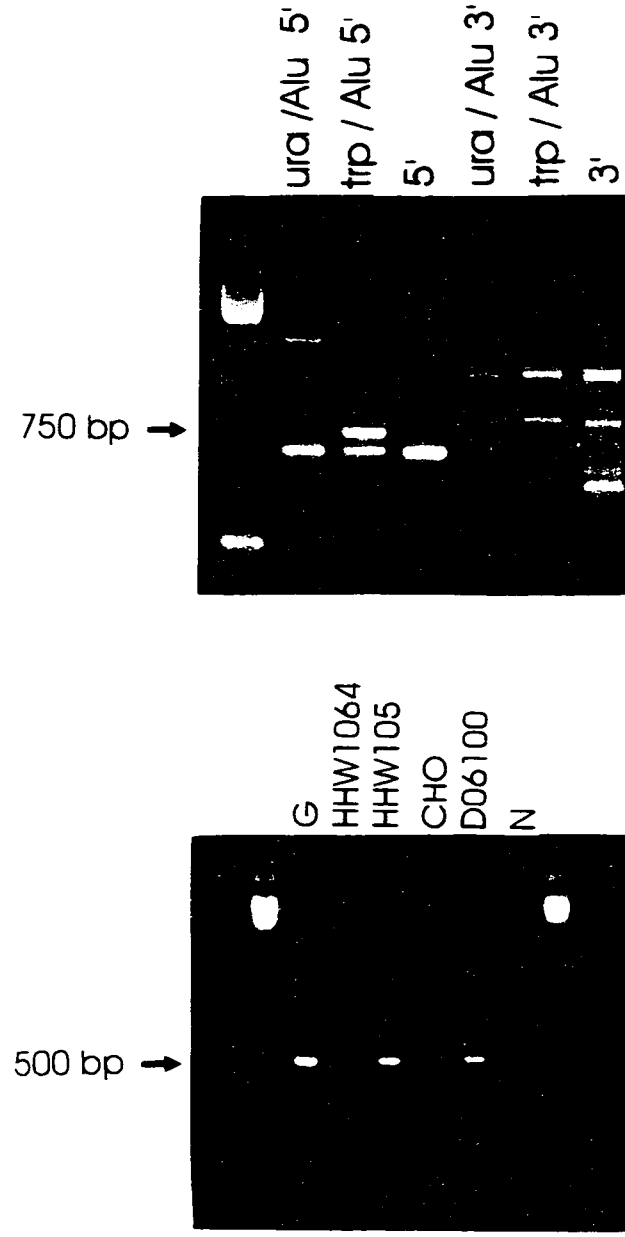
ura /Alu 5'
trp / Alu 5'
5'
ura / Alu 3'
trp / Alu 3'
3'
750 bp
G
HHW1064
HHW105
CHO
D06100
N
500 bp

PCR amplified products from both HHW1064 and HHW105 were positive. Formulation of new STS primers resulted in the amplification of products specific to the 5q11-13 region. End clone hybridization and STS analysis performed on all YACs confirmed the orientation and location of each YAC.

The assembly of a contiguous array of YACs covering the SMA interval was initiated from two markers which flank SMA; D5S125 (Mankoo *et al.*, 1991), which lies centromeric to D5S435 and the more telomeric marker D5S112 (Lien *et al.*, 1991) (see Figure 2-3). Six YACs were identified in the ICRF library by the telomeric marker pJK53 (D5S112). One of these YACs, D06100, was shown to extend the furthest centromerically based on end clone STS analysis. The centromeric end of this YAC identified two YACs from the NCE library, 12H1 and 12H4. YACs positive for the D5S125 or D5S435 markers were not found in the ICRF or NCE library thus the CEPH library was screened, from which clones containing D5S435 were isolated. A microsatellite polymorphism mapping into the center of the gap, CATT-1 (Burghes *et al.*, 1994), was utilized to detect three YACs, 24D6-2, 27H5 and 33H10. These YACs were shown to be linked to both the centromeric and the telomeric YACs (12H1, 12H4) by STS analysis. Internal YAC products generated by *Alu*-PCR were utilized to probe all YACs establishing the degree of overlap. STS sequences (Kleyn *et al.*, 1993) mapping between JK348 and D5S112 were utilized to confirm the degree of overlap and the

Figure 2-3: YAC contig of the SMA gene region. YACs are represented by solid lines. Open triangles represent polymorphic STRs, solid triangles represent STSs, open squares represent single copy probes. The genetically defined SMA interval, CMS-1-SMA-D5S557 (550 kb) and the previous D5S629-SMA-D5S557 (1.1 Mb) and D5S435-SMA-D5S112 (2.5 Mb) intervals, are indicated above the YACs. The location of the cosmid contig (Figure 3) is indicated below the schematic by a grey solid line.

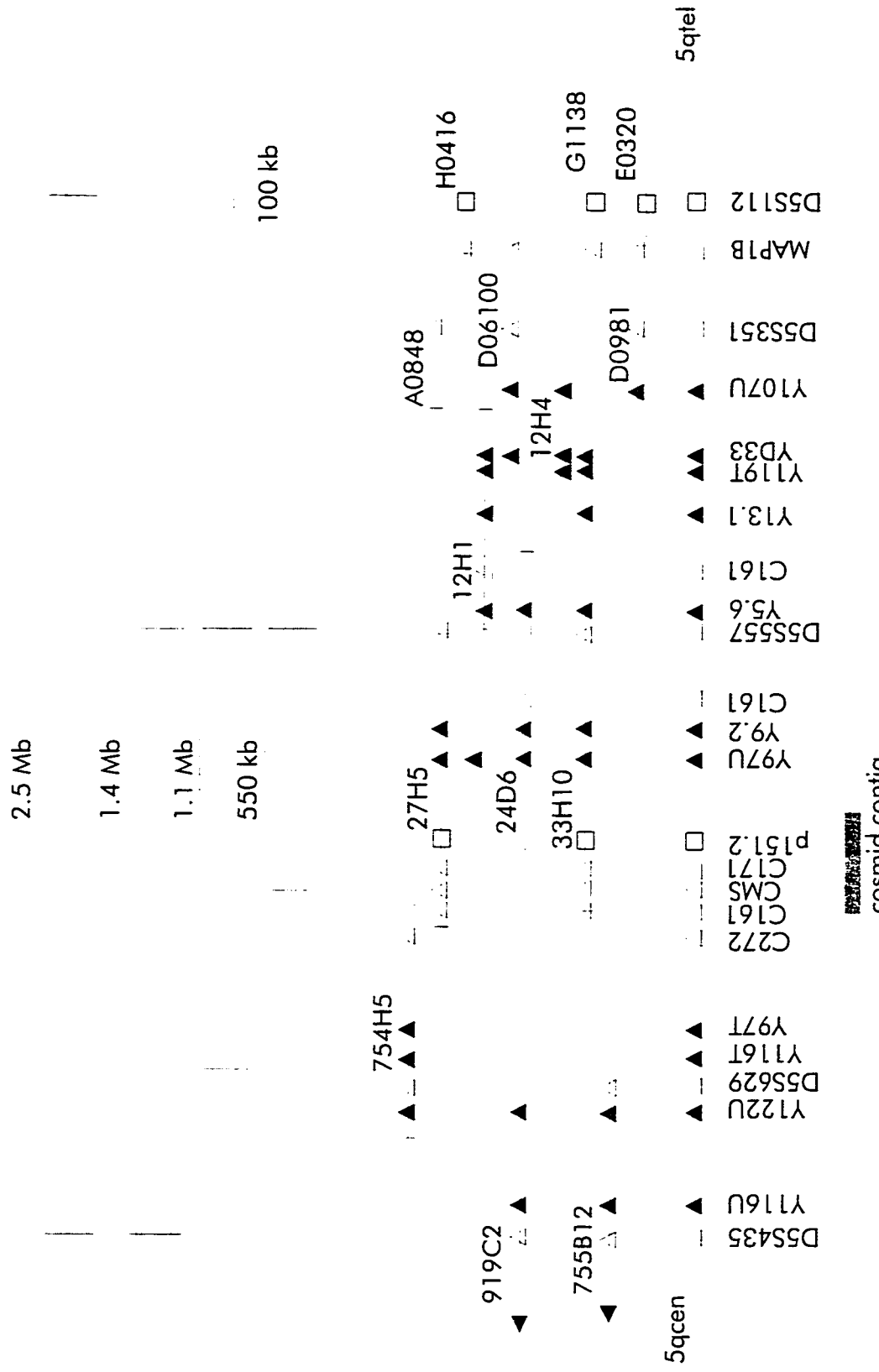
2.5 Mb
1.4 Mb
1.1 Mb
550 kb
100 kb
5qcen
5qtel
D5S435
Y116U
919C2
755B12
D5S112
MAP1B
D5S351
Y107U
Y119T
YD33
Y13.1
C161
D5S557
Y5.6
Y97U
Y9.2
C161
C272
C161
CMS
C171
p151.2
Y122U
D5S629
Y116T
Y97T
754H5
27H5
24D6
33H10
12H1
12H4
A0848
D06100
D0981
H0416
G1138
E0320
cosmid contig

TABLE 1-2: Markers and STS's utilised in this study

Probe	Source/reference	Probe	Source/reference
YD33	STS developed from *Alu*-5'-trp PCR product of YAC D06100 (this study)	Y13.1	STS developed from inter-*Alu*-5' PCR product of YAC 12H1 (this study)
Y14.1	STS developed from *Alu*-3'-ura PCR product of YAC 12H4 (this study)	Y15.1	STS developed from *Alu*-5'-ura PCR product of YAC 12H4 (this study)
Y9.2	STS developed from inter-*Alu*-5' PCR product of YAC 27H5 (this study)	Y5.6	STS developed from inter-*Alu*-3' PCR product of YAC 24D6 (this study)
Y11.2	STS developed from *Alu*-3'-trp PCR procut of YAC 33H10 (this study)	pZY8	subcloned 1.3 kb *Hind* III fragment from cosmid 250B6 (this study)
H7T733	*Alu* 33-T7 PCR product from cosmid 1H7 (this study)	p151.2	subcloned 1.2 kb inter-*Alu* PCR product of cosmid 15F8 (this study)
G10T333	*Alu* 33-T3 PCR product of cosmid 1G10 (this study)	p402.1	subcloned 2.1 kb *Bam* HI/ *Hind* III fragment of cosmid 40G1 (this study)
G3T733	*Alu* 33-T7 PCR product of cosmid 1G3 (this study)	pL7	liver transcript isolated with subcloned 1.1 kb *Bam* HI/ *Sal* I fragment from 58G12 (this study)
p2281.8	subcloned 1.8 kb *Hind* III fragment of cosmid 228C8 (this study)	F933	inter-*Alu* PCR product of cosmid 1F9 (this study)
pGA1	fetal brain transcript isolated with cosmid 250B6	β-glucuronidase	(Oshima *et al.*, 1987)
MAP1B	(Lien *et al.*, 1991)	Y122T	(Kleyn *et al.*, 1993)
D5S351	(Yaraghi, *et al* in press)	CMS-1	(Kleyn *et al.*, 1993)
D5S557	(Francis *et al.*, 1993)	Y98T	(Kleyn *et al.*, 1993)
D5S112	(Brzustowitcz *et al.*, 1990)	Y97T	(Kleyn *et al.*, 1993)
Y122U	(Kleyn *et al.*, 1993)	Y88T	(Kleyn *et al.*, 1993)
Y119T	(Kleyn *et al.*, 1993)	Y116U	(Kleyn *et al.*, 1993)
CATT-1	(Burghes *et al.*, 1994, McLean *et al.*, 1994)	Y55U	(Kleyn *et al.*, 1993)
D5S127	(Sherrington al., 1991)	Y38T	(Kleyn *et al.*, 1993)
D5S435	(Soares *et al.*, 1993)	D5S125	(Hudson *et al.*, 1992)
Y107U	(Kleyn *et al.*, 1993)	Y97U	(Kleyn *et al.*, 1993)
D5F149 (C212)	(Melki *et al.*, 1994)	D5F151 (C171)	(Melki *et al.*, 1994)
D5F150 (C272)	(Melki *et al.*, 1994)	D5F153 (C161)	(Melki *et al.*, 1994)
D5S637	(Clermont *et al.. 1994)*)	D5S629	(Clermont *et al.. 1994)*

orientation of YACs in the contig. Concurrently the order of each STS along 5q13 was confirmed. In all a total of 14 YACs were identified, anchored by the genetic markers D5S435, D5S629, CMS-1, CATT-1, D5F153, D5F149, D5F150, D5F151, D5S557 and D5S112.

Long Range Restriction Map and estimation of long range physical distance

A restriction map of the critical SMA region was constructed from the STS Y116U (Kleyn *et al.*, 1993), approximately 100 kb proximal to D5S629, to the STS Y107U (Kleyn *et al.*, 1993), which lies approximately 500 kb distal to D5S557 (see Figure 2-5). In order to detect any possiblity of deletions or rearrangements in our YACs, additional YACs isolated from the CEPH library (Kleyn*et al.*, 1993), mapping within this region were included in the analysis. YACs 24D62, 27H5, 33H10, 155H11, 76C1, 235B7, 184H2, 428C5, and 81B11 (Kleyn *et al.*, 1993) were partially digested utilizing the rare cutter restriction endonucleases *NotI, BssHII, SfiI,* and *RsrI.* Southern blots of the PFGE separated restriction products were hybridized with YAC left arm and right arm specific probes which revealed the positions of cleavage sites from both ends of each YAC (Figure 2-4). The orientation and overlap of the YACs had been previously determined based on STS analysis, therefore the position of the rare cutter sites among the overlapping YACs were compared. By aligning the overlapping YACs at their common rare cutter sites, the degree of overlap could be more precisely determined. The long range restriction map of the overlapping YACs derived from different sources was mostly

Figure 2-4: Partial YAC digestion map construction. YAC's 27H5 and 76C1 were digested with *NotI* utilising either 20 or 0.5 units of enzyme. The products were separated on a pulsed field gel and the resulting filter was hybridised with the pBR322 *PvuII/BamHI* 2.7 kb fragment or the pBR322 *PvuII/BamHI* 1.7 kb fragment corresponding to the pYAC4 left (trp) end or the pYAC4 right (ura) end. The 630 kb and the 550 kb bands present in both panels correspond to uncut DNA from YAC 27H5 and 76C1 respectively. The 220 kb band (upper panel) and the 410 kb band (bottom panel) of 27H5 correspond to the *NotI* site at its most telomeric end (see Figure 2-5). This *NotI* site is also detected in the bottom panel in YAC 76C1 (70 kb fragment). The 108 kb fragment of 76C1 corresponds to the centromeric *NotI* site of 76C1. The internal *NotI* site is detected by the 160 kb fragment in the bottom panel.

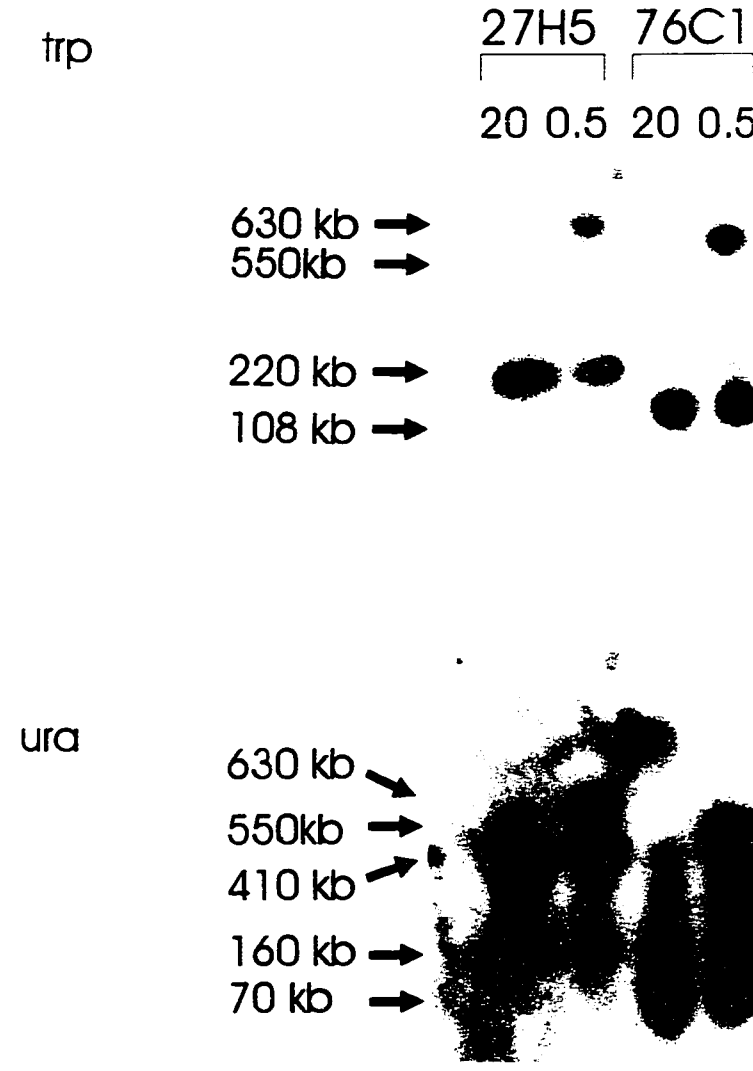
trp
27H5
76C1
20 0.5 20 0.5
630 kb
550kb
220 kb
108 kb
ura
630 kb
550kb
410 kb
160 kb
70 kb

Figure 2-5: Long range restriction map of the SMA region. Rare cutter sites are indicated above the solid line. A minimal set of markers are indicated below the solid line. t corresponds to the pYAC4 tryptophan or left end. u corresponds to the pYAC4 uracil or right end. The genetically defined CMS-1-SMA-D5S557 and the D5S629-SMA-D5S557 interval are estimated at 550 kb and 1.1 Mb respectively. YACs 184H2, 235B7, 428C5, 81B11, 155H11 and 76C1 are from Kleyn *et al.* (1993).

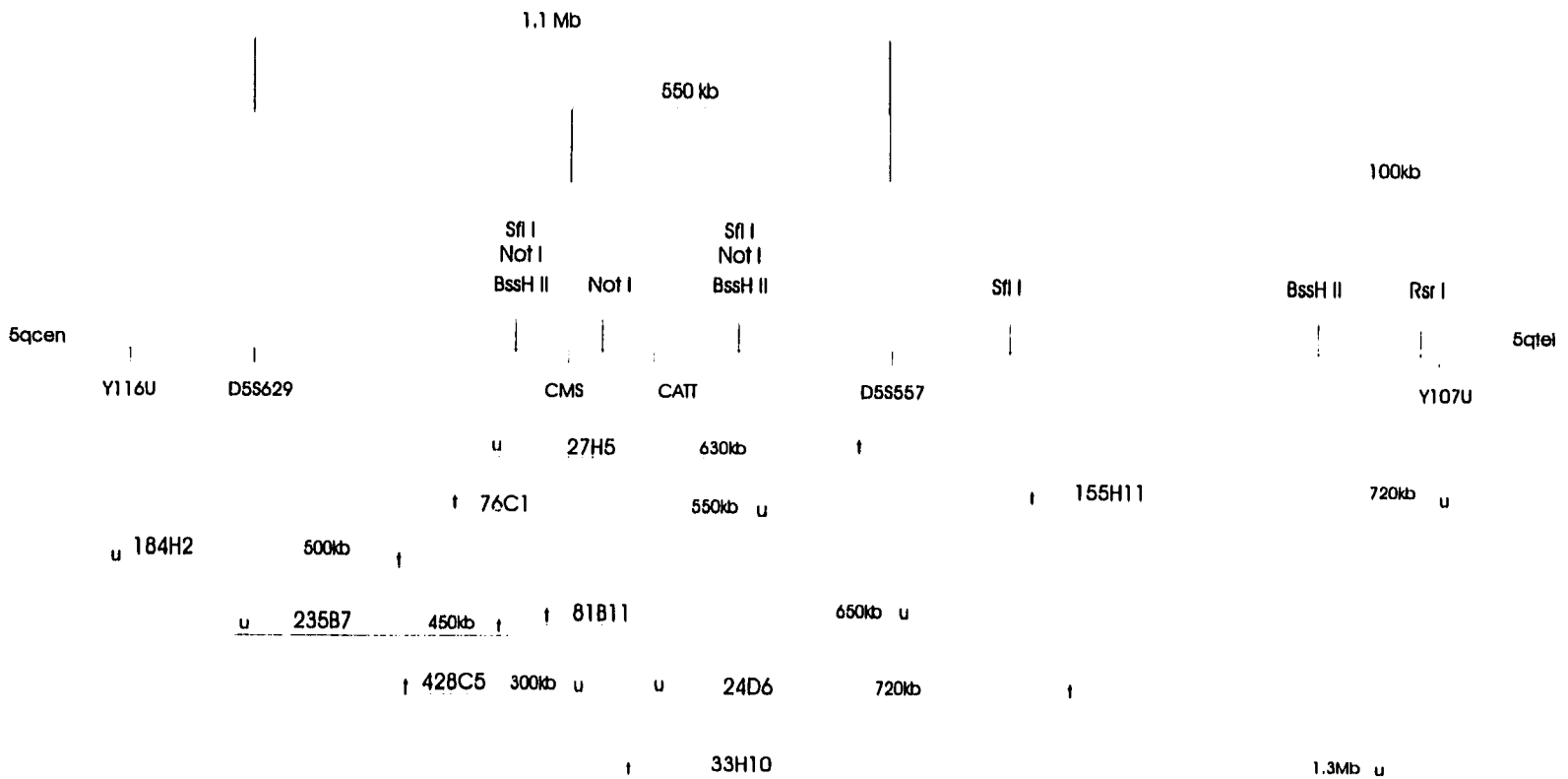
1.1 Mb
550 kb
100kb
Sfi I
Not I
BssH II
Not I
Sfi I
Not I
BssH II
Sfi I
BssH II
Rsr I
5qcen
5qtel
Y116U
D5S629
CMS
CATT
D5S557
Y107U
u
27H5
630kb
t
76C1
550kb
u
155H11
720kb
u
u
184H2
500kb
t
u
235B7
450kb
t
t
81B11
650kb
u
t
428C5
300kb
u
u
24D6
720kb
t
t
33H10
1.3Mb
u

in agreement with the exception of 33H10 and 428C5. 428C5 has previously been documented to contain a deletion (Kleyn *et al.*, 1993), evident by comparison of its STS content and its size of only 300 kb, indicating that it lies further centromeric than its placement in Figure 2-3. YAC 33H10, based on STS analysis contains an internal deletion and YAC 155H11 is chimeric at its centromeric end therefore rare cutter sites at the telomeric end of the map which could not be confirmed were not included. The results indicate the distance from the centromeric boundary D5S435 to the telomeric boundary D5S557 to be 1.4Mb in marked contrast to 400 kb as previously reported (Francis *et al.*, 1993) but in agreement with one other estimate (Wirth *et al.*, 1993). Furthermore, the D5S629-D5S557 interval can be estimated at 1.1 Mb and the distance of the genetically defined CMS1-SMA-D5S557 interval is approximately 550kb (Figure 2-5).

Cosmid contig assembly from the chromosome 5 library

Although the isolation of cosmids utilizing whole YACs as probes could be an expeditious method of constructing a cosmid contig, in this case the presence of chromosome 5 specific repeats would likely result in the isolation of cosmids mapping elsewhere on chromosome 5. A directed cosmid walking strategy was thus adopted. The CATT-1 MSR, which has been shown by irradiation hybrid analysis to map approximately midway between the two flanking markers D5S435 and D5S351 (Hudson *et al.*, 1992), was utilized as the initiation point for the construction of a cosmid clone array. Cosmids were subsequently isolated by the hybridization of *Alu*-end clones (Figure 2-6), STS's or

single copy clones.The complex pattern of amplification seen on genomic DNA, with two to eight alleles per individual (see Figure 2-7), suggested a variable number of copies or loci of the CATT-1 sequence in this region (Burghes *et al.*, 1994). Thirty CATT-1 positive cosmids were identified which upon PCR analysis were seen to contain one of four distinct alleles (see Figure 2-7). As the cosmid library was derived from a monochromosomal source, this confirmed that the CATT MSR exists at least in four locations, which we refer to as subloci. These subloci are referred to as CATT-40G1, CATT-192F7, CATT-58G12 and CATT-250B6-based on the cosmid addresses of the first cosmids identified containing alleles of 12, 19, 15 and 20 CA dinucleotides respectively. Bi-directional walking was initiated from these 4 cosmid subloci. Positive hybridization was observed for cosmid 250B6 with one end of 58G12 and for 192F7 with the other end resulting in the ordering of cen-192F7-58G12-250B6-tel (Figure 2-8). All cosmids which contained the CATT-192F7 allele were mapped to this location based on the size of their CATT-1 allele and their restriction enzyme profiles.

Due to the presence of chromosome 5 specific repetitive sequences, resulting in the identification of cosmids from another region of chromosome 5, the integrity of the contig was verified with each step taken. Cosmid end clones generated by vector-*Alu*-PCR were hybridized to somatic cell hybrid panels as described above. As repetitive sequences which map solely to the region of chromosome 5 that is deleted in the hybrid cell line HHW1064 have been observed, cosmids identified by end products which did not

Figure 2-6: Representative cosmid walking step. DNA from pooled plates of the chromosome 5 specific library were digested with *PvuII* and electrophoresed on 1 % agarose gels. Filters were probed with vector-*Alu* PCR products identifying plates 138, 147 and 149 as containing positive cosmid clones (top panel). The bottom panel shows the subsequent hybridization to the filter of plate 149 revealing the positive clone E11.

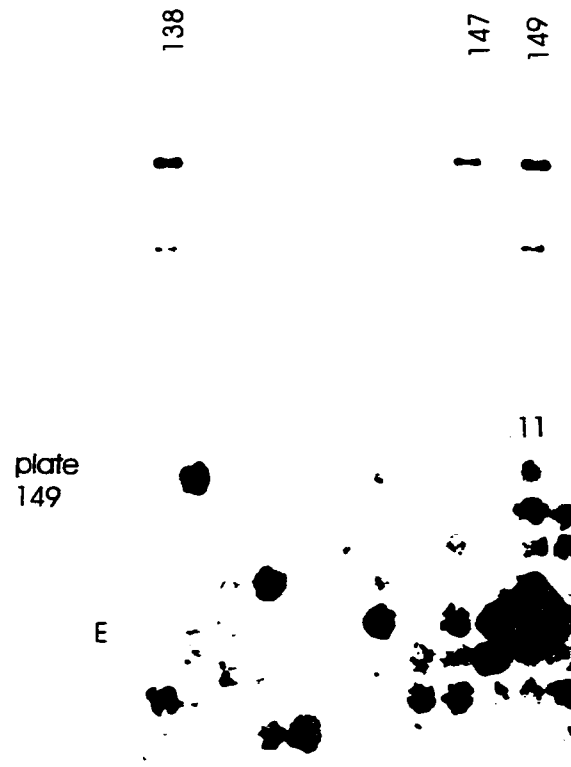
138
147
149
11
plate
149
E

Figure 2-7: Amplification of the CATT-1 locus. Allele sizes are shown below each lane and have been assigned according to McLean *et al.*, (1994).(left panel) Amplification of YACs. G: genomic DNA. (right panel) Amplification of cosmids derived from the chromosome 5 flow sorted library. The 4 distinct alleles are represented by cosmids 40G1 (allele 15), 58G12 (allele 12), 192F7 (allele 10) and 250B6 (allele 7).

G
G
D06100
12H1
12H4
24D6
27H5
33H10
76C1
155H11
184H2
235B7
81B11
6 6
7 7
9 9
11 11
12 12
15 15
12 7 15 15
15
10 12 12 15 12 10 7
108F4
126H11
123F6
40G1
58G12
192F7
250B6

hybridize to HHW1064 were analyzed further. Proof of overlap was shown by hybridization of end clones, single copy probe hybridization, STS content, and restriction enzyme profile comparison. Cosmids identified by end clones which hybridized to HHW1064 were eliminated and walking was continued by utilizing a different inter-*Alu* product from the clone of origin, which was verified in the same manner. Cosmids sizes were calculated by the addition of *Eco*RI restriction fragments and the extent of overlap was determined by the addition of those fragments in common. Both end products and inter-*Alu* products from cosmids, located at the most centromeric and telomeric ends of the contig contained repetitive sequences which identified cosmids outside the SMA region. One of these cosmids was analyzed based on its inclusion of an MSR and was shown to map to the beta subunit of the platelet derived growth factor receptor (PDGF) at 5q31 (Yaraghi *et al.*, 1995).

Cosmid contig assembly of YAC 76C1 cosmids

As extension of the cosmid contiguous array was prevented by the presence of chromosome 5 specific repeats, a 5X cosmid library was produced from YAC 76C1. The STSs CATT-1, CMS-1, Y122T (Kleyn *et al.*, 1993), Y97T (Kleyn *et al.*, 1993) and Y98T (Kleyn *et al.*, 1993), which are distributed along the YAC were utilized to identify cosmids to assemble the contig. As well, the previously developed markers, pZY8, pL7, pGA-1, p15.1, p402.1, p2281.8 and β-glucuronidase (Oshima *et al.*, 1987) (Table 2, Figure 4) were hybridized to the library providing an effective method of ordering the

cosmids. Cosmids demonstrating irregular hybridization patterns and thought to contain deletions and/or rearrangements were excluded.

The STS Y98T identified three cosmids including one previously identified by the probe p2281.8, derived from a chromosome 5 library clone, 228C8, also containing the STS Y98T. An end product of this cosmid hybridized to ten cosmids. Concurrently, an end fragment of a CATT-40G1 sublocus was shown to hybridize to four of these ten cosmids thus linking CATT-40G1 and CMS-1 with the more centromeric STS Y98T (Figure 2-8). We were unable to identify any clones containing the YAC end STS Y97T. Filter hybridization and STS mapping experiments indicated a second more telomeric location of the CATT40G1 sublocus. A duplication of this sublocus would agree with genotype data in our SMA kindreds (McLean *et al.*, 1994).

To ensure the reliability of the contig, we sought to integrate it with the contig constructed from the chromosome 5 specific library. Concordance of the contigs was evident by comparison of the restriction maps, the position of probes and STSs on the map and *Alu*-PCR fingerprinting (Figure 2-9). In this manner the size of the contig was estimated to be 210 kb. A directed walking strategy has thus resulted in the generation of a single contiguous set of cosmids containing the CATT-1 cluster of subloci with known centromere/telomere orientation.

Figure 2-8: A representative subset of mapped cosmids from our contiguous array. Vertical lines above the solid line are the positions of *Eco*RI sites. Open triangles represent polymorphic STRs, filled triangles represent STSs, filled squares represent single copy probes and open squares represent transcribed sequences. The STRs which demonstrate strong linkage disequilibrium with Type I SMA are indicated by stars. Cosmids 1G3 and 1B9 are from the YAC 76C1 cosmid library.

E
5qcen
228C8
1B9
40G1
15F8
192F7
58G12
250B6
1G3
10 kb
p2281.8
Y98T
C272
C212
F933
CATT-40G1
C161
p402.1
Y122T
CMS
p151.2
β gluc
CATT-192F7
CATT-58G12
C161
H77733
pZY8
pGA1
pL7
G37733
C272
G1013
CATT-250B6
C161
CATT-40G1
C161
p402.1
5qtel

Figure 2-9: *Alu* fingerprinting of cosmids to determine overlap. Cosmid DNA was PCR amplified with the *Alu* primer 33 (see Materials and Methods) and products were seperated on a 1 % agarose gel. *Alu* products that are in common between cosmids denote overlap.

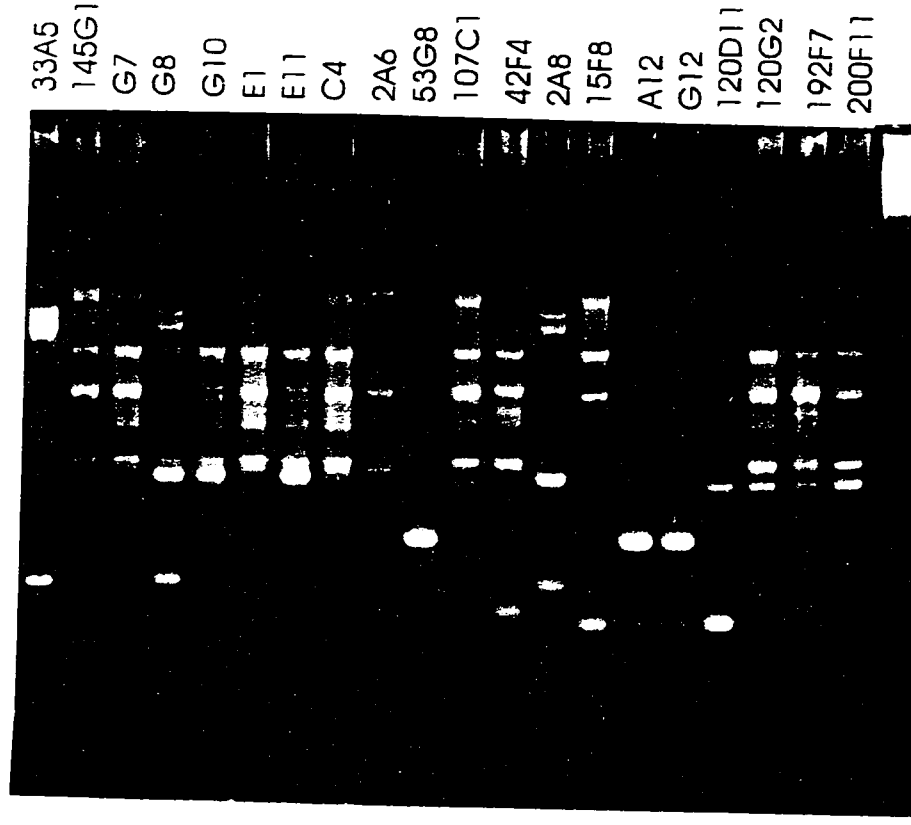
33A5
145G1
G7
G8
G10
E1
E11
C4
2A6
53G8
107C1
42F4
2A8
15F8
A12
G12
120D11
120G2
192F7
200F11

Assembly of PAC contig

The 5q13.1 STS's CMS-1, CATT-1, MAP1B Y119T, Y98T, Y112T, Y116T, D5S212, D5S161 and D5S637 were utilized to identify PAC clones within the SMA region. Three pooled libraries (LLNL, RPCI1 and RPC12) were screened by PCR resulting in the identification of 18 clones. Given the instability of STRs we observed in our YAC clones we sought to determine if our PAC clones were prone to deletion or instability. Glycerol stocks of the each PAC were streaked on LB kanamycin plates and 10 individual colonies of each PAC were isolated. Their profile upon digestion with *EcoRI* was compared revealing the absence of bands in approximately one third of clones. The PACs with the most *EcoRI* fragments were utilized in all subsequent analysis and clones were routinely checked for instability. The size of the clones was determined by pulsed field gel electrophoresis and the clones were arranged into a contiguous array utilizing the STS's and single copy genomic probes isolated previously (Figure 2-10). Given that the order of the complex multilocus microsatellite repeats and single copy sequences had been established by the construction of the YAC and cosmid arrays, the generation of a PAC contiguous array was expeditious. The CATT-1, Ag-1/C212 and CMS allele sizes of each PAC was determined, confirming the order of the CATT-1 and Ag-1/C212 subloci along 5q13. A recombination event was identified in a Polish Canadian families defining the location of CMS-1 allele 9 as the centromeric boundary of the SMA gene containing interval (Yaraghi et al, 1995). CMS-1 occurs in multiple copies and neither our YAC or

Figure 2-10: PAC contig of SMA locus. Open triangles represent polymorphic STRs, filled triangles represent STSs, filled squares represent single copy probes and open squares represent transcribed sequences. The CMS subloci of PAC 125D9 defines the distal SMA boundary.

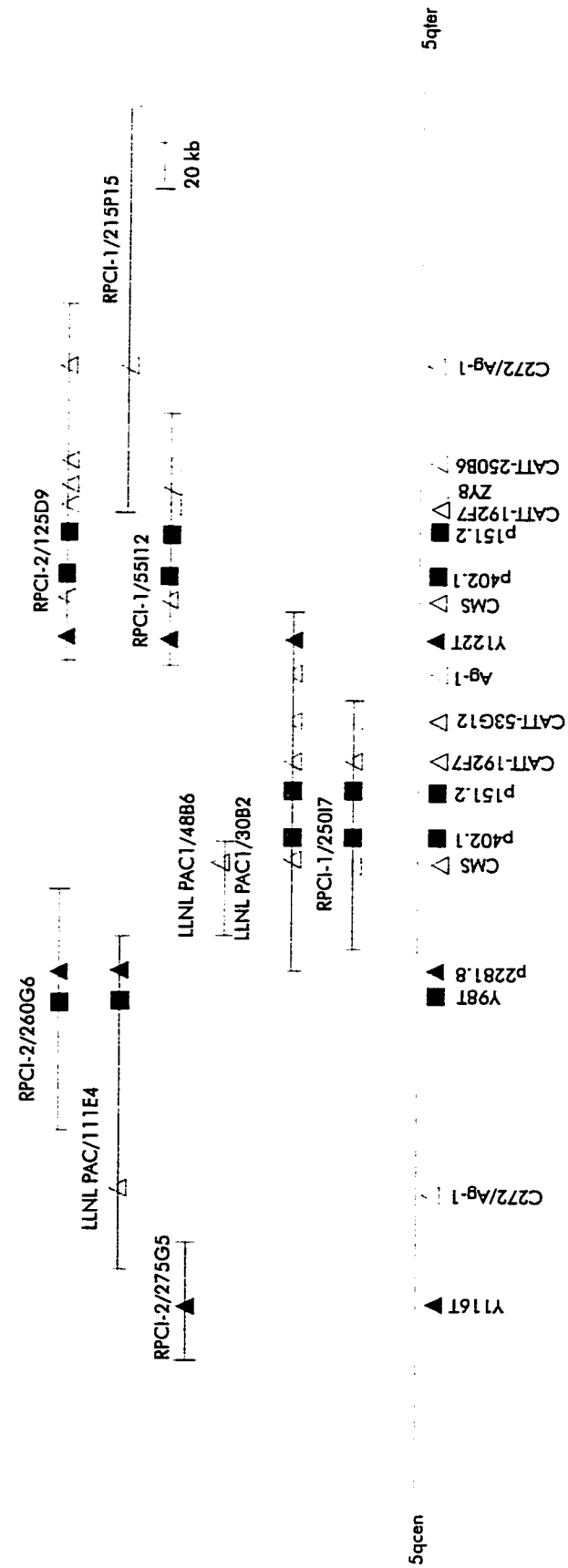
5qter
C272/Ag-1
CATT-25086
ZY8
CATT-1927F7
p151.2
p402.1
CMS
Y1221
Ag-1
CATT-53G12
CATT-1927F7
p151.2
p402.1
CMS
Y98T
p2281.8
C272/Ag-1
Y1161
5qcen
RPCI-2/260G6
LLNL PAC/111E4
RPCI-2/275G5
LLNL PAC1/48B6
LLNL PAC1/30B2
RPCI-1/25017
RPCI-2/125D9
RPCI-1/55I12
RPCI-1/215P15
20 kb

Figure 2-11: Linkage disequlibrium and physical mapping of SMA locus at 5q13. (A) Linkage disequlibrium analysis taken from Yaraghi et al, 1995. (B) YAC contig. The CMS subloci defining the CMS boundary is marked. (C) PAC contiguous array. (D) Cosmid contig.

A

Correlation of Type I SMA 5q13.1 marker linkage disequilibrium with 5q13.1 physical map

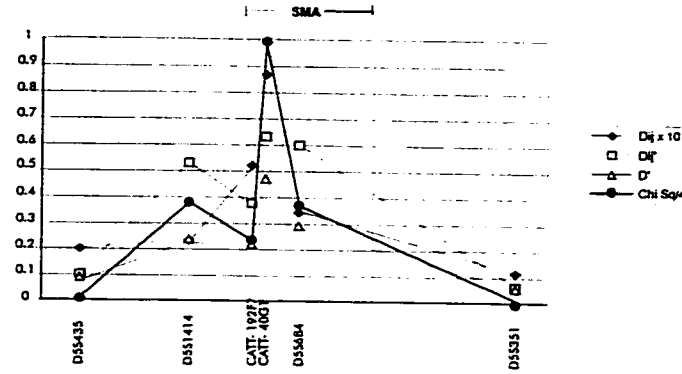

B

YAC array

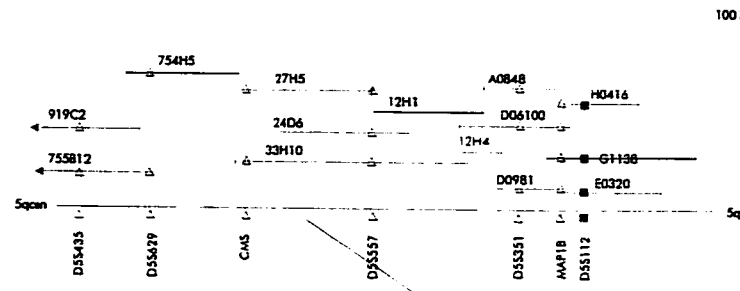

C

PAC array

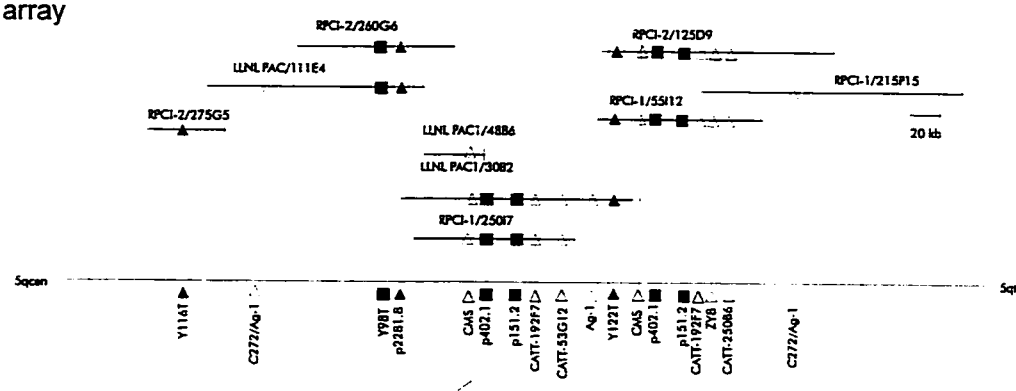

D

Cosmid contig

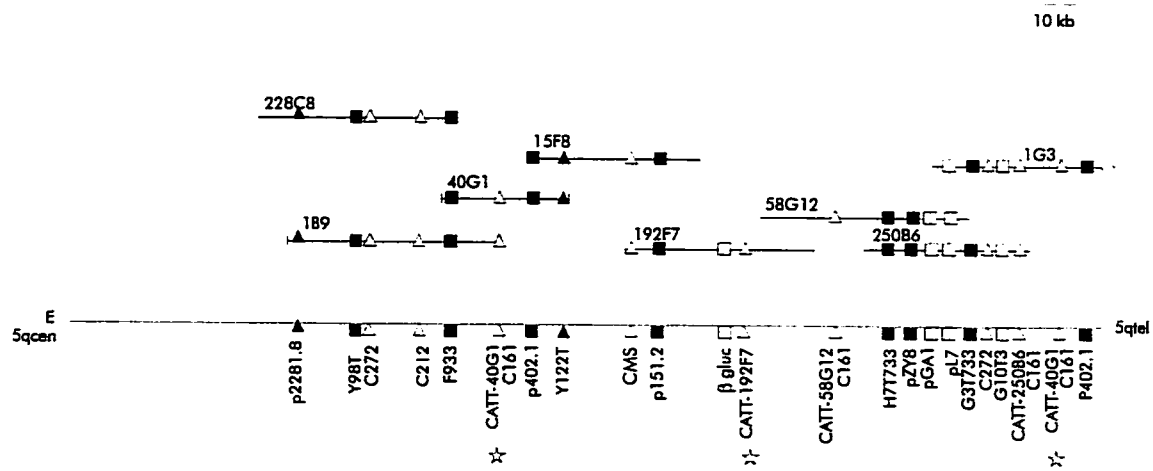

cosmid clones contained this particular subloci hence the precise location of this boundary could not be determined. Analysis of our PAC clones revealed the allele 9 CMS-1 sublocus PAC 125D9, suggesting that this clone contained the proximal boundary of the SMA containing interval.. This sublocus was mapped within 10 kb of the centromeric end of 125D9. Furthermore PAC 125D9 was shown to encompass the CATT-1 subloci demonstrated to be in high linkage disequilibrium with Type I SMA (McLean et al, 1994) (Figure 2-11). Although PAC 125D9 did not contain the CATT-40G1 sublocus it did contain the p402.1 single copy probe shown to be contiguous with this sublocus. This possibly reflects the precence of a null allele at this sublocus in the individual from which the library was made. Taken together, we believed these data indicated that the SMA locus would map within this PAC.

Duplications/Deletions

Several lines of evidence suggested the presence of genomic sequence duplications within our cosmid array. We provide evidence for the duplication of the CATT-40G1 sublocus in cosmids derived from a single chromosome 5. A centromeric location for this sublocus was established as the CATT-40G1 sublocus was found to be contiguous with the STSs Y122T , Y88T and CMS-1 in several cosmids, and the centromeric YAC 428C5 is positive for probes isolated from the CATT-40G1 containing cosmids. Although YAC 428C5 does not contain the CATT40G1 sublocus upon PCR amplification, this may be explained either by a null allele in the chromosome from which the YAC was derived or a

deletion in the YAC. We have previously observed null alleles in individuals at distinct CATT-1 subloci (McLean *et al.*, 1994). A second more telomeric location of CATT-40G1 was determined by the hybridization to CATT-40G1 cosmids of the probes pGA-1, pL7, and pZY8 all of which bind the more telomeric YACs 33H10, 24D62. The hybridization of p402.1, derived from cosmid 40G1, to cosmids at both locations would indicate that the duplication is not restricted to the CATT-40G1 subloci and likely encompasses a larger region. This has been confirmed by FISH analysis with the probe p401.2, derived from the CATT-40G1 cosmid, which indicates a duplication within an approximate 100 kb (Lemieux et al., personal communication). Southern blot analysis revealed distinct profiles of cosmids for the two locations however common bands were detected by *Alu*-PCR fingerprinting supporting a duplication.

Correlation of our YAC contig with the cosmid contig revealed that YACs 76C1, 81B11, and 27H5 span the 150 kb CATT region of 5q13. Despite this, CATT-1 genotyping of these YACs revealed only one allele size, raising the possibility that the chromosomes from which these YACs were derived (4 in all) contain null alleles at their remaining CATT-1 subloci. Our experience, however, with CATT linkage analysis of SMA families indicated that such a scenario is highly unlikely as none of the approximately 300 individuals genotyped had fewer than 2 alleles (Burghes *et al.*, 1994, McLean *et al.*, 1994). We consequently believe it is more likely that these CATT subloci are unstable and have been deleted during YAC construction and/or propagation.

Sequence comparison between the CATT-1 and D5F153 (Melki et al, 1994) primer sequences indicated that these two STRs were similar and possibly the same as one primer is identical and the other primer sequences overlap by eight nucleotides. YAC and cosmid clones which were positive for CATT-1 were also D5F153 positive. However, the centromeric YACs 428C5, 232F12, 235B7, 184H2, and the telomeric YACs 12H1, 155H11, 269A6 which were CATT-1 negative yielded D5F153 amplification products (data not shown) indicating that CATT-1 may be a derivative of D5F153. These data, in combination with D5F153 analyses of the cosmid contig, which contains three D5F153 loci (Figure 4), indicated that at least five D5F153 subloci exist.

In addition to the CATT-1 and D5F153 STRs , the STRs CMS-1 (Klyen et al, 1993) and D5F150 (Melki et al, 1994) were present in a variable number of copies per chromosome 5. STS analysis localized CMS-1 to YACs 428C5, 76C1, 81B11 and 27H5 with allele sizes of 5, 4, 4 and 3, and 4 respectively. PCR amplification of genomic DNA revealed up to four alleles per individual indicating as many as two copies per chromosome. D5F150 was present at two locations within the cosmid array yet only one location was detected in the YAC contig. D5F151 was not detected within our cosmid array nevertheless was placed at the centromeric end of YAC 33H10, which encompasses the cosmid array, based on the positive amplification of YAC 428C5. One location of D5F149 was detected on both our cosmid and YAC clones. We cannot confirm multiple

locations of both D5F151 and D5F149 based on these analyses in contrast to one other study (Melki *et al.*, 1994). Our data suggested that, as with CATT-1, the existence of null alleles and/or instability of the CMS-1, D5F150, D5F151, D5F149 sequences in YACs.

A deletion event was observed in hybridization with an 800 bp *Eco*RI fragment isolated as a single copy probe from the CATT-40G1 containing cosmid 234A1 from the chromosome 5 specific cosmid library. Probings of YAC DNA failed to detect this fragment in any of our YACs. Hybridization to genomic DNA of several individuals did not identify any deletion events thus this sequence may be susceptible to instability in the YACs. Sequencing of this fragment did not reveal any exons or coding region.

Further evidence of sequence duplication in the SMA region was identified with a 1.2 kb internal *Alu*- PCR product (p151.2) from cosmid 15 F8 (Figure 2-12)The probe identified three *Eco*RI fragments in YAC clones 76C1, 81B11 and 27H5 (20 kb, 12 kb and 3 kb) but only one in 33H10 and 24D6 (20 kb) and one in 428C5 (12 kb). An internal *Eco*RI site divided this marker into 500 bp and 700 bp probes. The larger probe identified the 12 kb and 20 kb fragments while the smaller probe identified the 3 kb and 20 kb fragments (Figure 2-12). We ruled out instability of this sequence in YACs as they are from different libraries and the hybridization patterns reflected their physical location. The 12 kb and 3 kb fragments were localized on the *Eco*RI restriction map, however we were unable to position the 20 kb fragment as there were no positive cosmids for this fragment.

Figure 2-12: Sequence duplication in the SMA region identified by p151.2. Hybrization of YACs with (A) the 700 bp fragment and (C) the 500 bp fragment. YACs are arranged from left to right, centromeric to telomeric. Hybridization of cosmids with (B) the 700 bp fragment and (D) the 500 bp fragment. (B) The 12 kb fragment is detected in the cosmids however the 20 kb fragment is not present. The 2.5 kb and 600 bp fragments detected in 3B3 and 1E1 respectively are end fragments.(D) Only the 3 kb fragment is detected in the cosmids. Note the absence of the 20 kb band in 24D6 in (A) but its presence in (C). The 700 bp fragment may be deleted in 24D6.

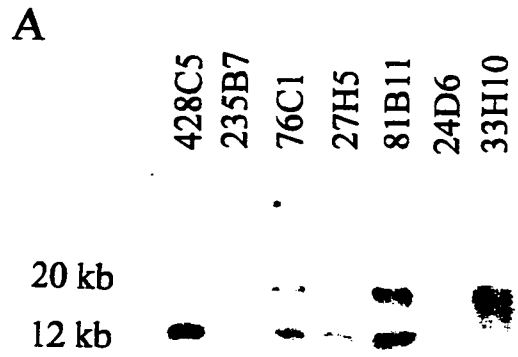
A
428C5
235B7
76C1
27H5
81B11
24D6
33H10
20 kb
12 kb

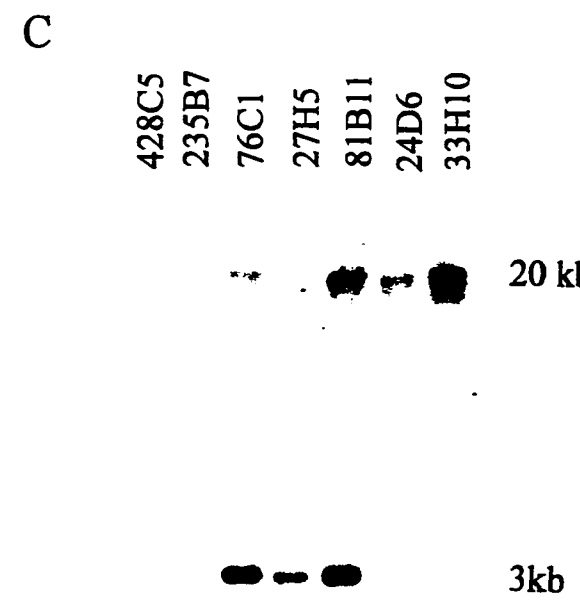
C
428C5
235B7
76C1
27H5
81B11
24D6
33H10
20 kb
3kb


B
1C4
3A5
3B3
3B4
3B5
200F11
1G7
1G8
1E1
1A8
1G4
1E7
1C1
12 kb
2.5 kb
600 bp

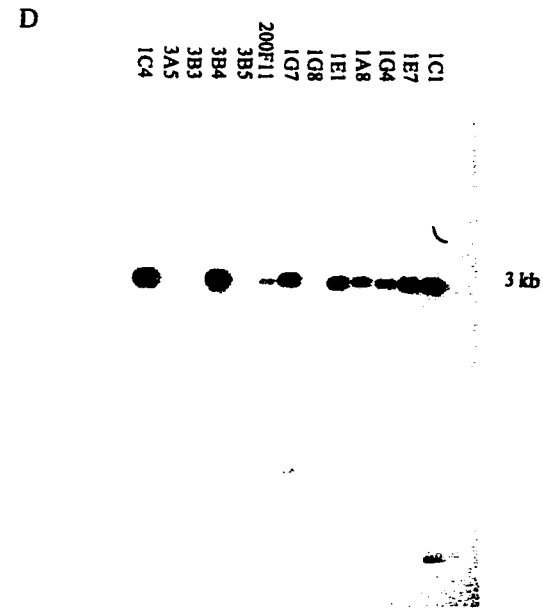
D
1C4
3A5
3B3
3B4
3B5
200F11
1G7
1G8
1E1
1A8
1G4
1E7
1C1
3 kb

Figure 2-13: Sequence duplication detected in our PAC array. Hybridization of PAC DNA with p151.2. The 12 kb and 3 kb fragments are located in the PACs confirming that they lie in tandem. The 20 kb fragment is not detected within the 500 kb PAC array.

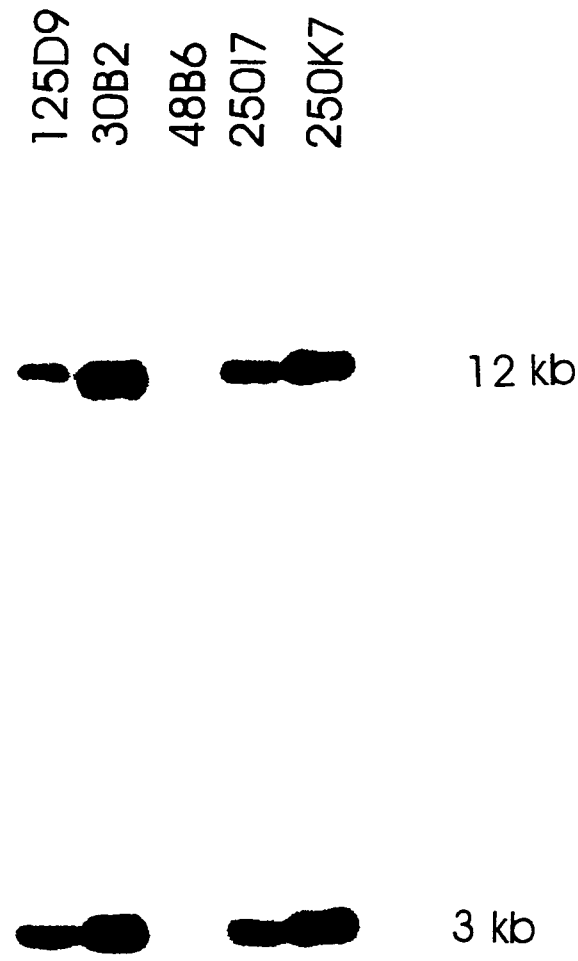
125D9
30B2
48B6
250I7
250K7
12 kb
3 kb

Taken together these findings suggest the 12 kb and 3 kb lie in tandem with a centromeric/telomeric orientation respectively. In support of these data, the 12 kb and 3 kb fragments were detected in our PAC clones (Figure 2-13). A location of the 20 kb fragment distal to our contiguous array of cosmids may be inferred from the data based on the location of the YACs which were positive. The duplication was confirmed by hybridization to genomic DNA digests revealing all three fragment sizes.

DISCUSSION

We have established a YAC contig of the SMA disease gene region, incorporating the D5S435-D5S112 interval, encompassing 3 Mb. Orientation of the contig along 5q13 has been confirmed by analysis of seven genetic markers and STSs in combination with PFGE analysis. The long range restriction map revealed neither major deletions nor rearrangements among the YACs within our contig, and was utilized to refine the estimates of the size of the contig. Our YAC map establishes physical linkage of the markers D5S629, D5F153, D5F151, D5F150, D5F149, CMS-1, CATT-1 and D5S557 to a 1.1 Mb region, a region of the genome characterized by low copy repetitive sequences and multilocus STRs. Furthermore, we estimate the new genetically defined CMS1-SMA-D5S557 to be 550 kb. Estimates of the physical distance of the D5S435-D5S557 interval range from 400 kb to 2.8 Mb (Carpten *et* al., 1994; Kleyn *et* al., 1993; Francis *et al.*, 1993; Melki *et* al., 1994) have been reported. In contrast to these studies our estimation

of 1.4 Mb for the D5S435- SMA-D5S557 interval and 550 kb for the CMS-SMA-D5S557 interval, employs clones derived from three sources, comprised of 6 chromosomes. Moreover, the determination of both the size of clones and the position of rare cutter sites has enabled us to determine more precisely the extent of overlap of the YACs and the size of the contig providing a reliable estimation.

We also report the assembly of a single contiguous array of cosmid clones derived from both a chromosome 5 specific library and a YAC (76C1) specific library in conjunction with a restriction map of the CMS-1/CATT-1/D5F153/D5F150/D5F149/ region encompassing 210 kb. We and others have detected homology of the 5q13 region at 5q31, q33 and p13 (Francis *et al.*, 1993, Thompson *et al.*, 1993). The repetitive sequences prevented extension of the cosmid contig when utilizing a chromosome 5 specific library necessitating construction of a cosmid library the YAC 76C1 in the critical region. The contiguous cosmid array was constructed by a directed walking strategy with validation of cosmid overlap established by restriction fragment enzyme overlap,*Alu* fingerprinting, and analyses involving STSs, cosmid end clones and single copy probes. In a similar fashion we assembled an array of PAC clones encompassing this region spanning 500 kb. The PAC contiguous array helped to confirm the order and STR's and STS's within our cosmid clone array. Moreover the CMS-1 allele 9, which establishes the proximal boundary containing the SMA locus was identified in one of our PAC clones,

125D9. This sublocus maps in close proximity of the CATT-1 subloci which are in significant linkage disequlibrium with Type I SMA (McLean et al, 1994).

Physical and genetic mapping analyses have revealed a complex region of genomic DNA comprising duplications and the presence of repetitive sequences. Genotyping of genomic DNA with complex STRs from this region reveals the presence of a polymorphic number of bands ranging as high as eight per individual. This suggests the presence of multiple copies, or subloci, for the STRs CATT-1, CMS-1, D5F153, D5F150. Our physical mapping data confirms the presence of these subloci except in the case of D5F151 and D5F149 which reveal only one location. Four of the CATT-1 subloci map to our cosmid array within a 140 kb region; at least one of these subloci, CATT-40G1, is duplicated. D5F153 and CATT-1 are related STRs which appear to have diverged from a common ancestor. Genotype data for both CATT-1 and CMS-1 reveals Mendelian inheritance of stable null alleles at many of these subloci in both Type I patients and the normal population, with a variable number observed in chromosomes among individuals (McLean *et al.*, 1994). We have localized one CMS-1 sublocus to our cosmid array, however, we are unable to determine from our data whether other subloci exist on other chromosomes within this 200 kb interval, as the chromosomes from which the YAC/cosmid libraries were derived may either contain null alleles at the remaining subloci or have sustained deletions.

The CATT-1, D5F153, D5F150 and D5F149 MSR , although present in multiple copies on chromosomes in the population were observed as single sublocus markers on all YACs, as evidenced by single allele PCR products for each, suggesting instability and deletion of these sequences. This is supported by the absence in our YACs of an 800 bp fragment, derived from the chromosome 5 cosmid library based contiguous array. Instability of these sequences does not appear to result in large deletions as additional unique sequence probes located between the multiple subloci are retained in the YACs.

The basis of the YAC clone instability may be due to the novel class of STRs which exist at multiple loci, and the chromosome specific low copy repetitive elements, both distinctive features of this region. These may be prone to deletion or instability in this yeast host system or during yeast propagation and transformation. Internal deletions may occur in YACs during transformation or propagation possibly due to tandemly repeated elements as demonstrated in clones containing alphoid sequences (Neil *et al.*, 1990) or due to interactions among repeat DNAs (Kouprina *et al.*, 1994). Recombination will lead to clones harboring either a deletion or tandem duplication of sequences and hence have been suggested as a cause of this instability, a model supported by the reduction in transformation associated deletions in clones propagated in recombination deficient host strains (Kouprina *et al.*, 1994). Furthermore, regions of extensive homology or clusters of repetitive elements, such as *Alu* sequences, are more prone to recombination. Sequence analysis reveals the presence of *Alu* elements both within the

duplicated and deleted regions and adjacent to the CATT-1 and CMS-1 STRs. It may therefore be that the low copy repetitive sequences specific to chromosome 5 with particular abundance in this region, and/or the *Alu* sequences, mediate successive insertions or deletions by recombination or gene conversion.

In summary, I present the first high resolution physical map of the critical SMA region. Two of the CATT-1 subloci which we map to our cosmid array are in significant linkage disequilibrium with SMA, (McLean *et al.*, 1994) indicating close proximity to the gene. CATT-40G1 which shows a greater allelic association with SMA relative to CATT-192F7 is duplicated, flanking CATT-192F7. As a result, delineation of the precise region which contains the SMA gene was not possible based on these data alone. However, analysis of our PAC contiguous array has established the proximal SMA boundary reducing the region containing the SMA locus from 1.1 Mb to 600 kb. Moreover this boundary is in close proximity to the CATT subloci.. We therefore commenced the screening of cDNA libraries with cosmids and PACs from our contig in an effort to clone the SMA gene.

CHAPTER III:

ISOLATION OF THE SMA CANDIDATE GENE THE NEURONAL APOPTOSIS INHIBITOR PROTEIN (NAIP)

INTRODUCTION

In 1990 all three childhood forms of SMA were genetically mapped to 5q11.2 - q13.3 by linkage analysis (Brustowicz et al, 1990; Gilliam et al, 1990; Melki et al, 1990). These results support a model in which allelic mutations of the same gene or nonallelic mutations of contiguous genes lead to the manifestation of the three clinically diverse forms. Recombination events have progressively positioned the gene to the interval defined centromerically by the marker CMS (Yaraghi et al, 1995) and D5S557 (Francis et al, 1993). We and others have constructed YAC contiguous arrays encompassing the SMA locus and in so doing, have all documented the presence of chromosome 5 specific sequence repeats. These repetitive sequences include both single tandem repeat markers (MSR) and transcribed sequences which occur in a polymorphic number between individuals. These sequences map within the genetically defined SMA region at 5q11.2 - q13.3 in addition to 5p13 and 5q33 (Francis et al, 1993; Kleyn et al, 1993; Wirth et al, 1993; Roy et al, 1995). The polymorphic nature of the region has consequently confounded the ordering of genetic markers and STS's on the physical maps and have resulted in discrepancies between groups in the estimates of physical distances. We have additionally constructed a high resolution physical map consisting of a PAC and cosmid

array within the genetically defined SMA region that has helped to confirm the order of loci within this region. We have defined one of the CMS subloci as the proximal SMA boundary by the identification of a recombination and this sublocus has been mapped to our PAC clones (Yaraghi et al, 1995; Roy et al, 1995). Additionally we have demonstrated a clear linkage disequlibrium peak with the Type I SMA phenotype at the CATT-40G1 sublocus which lies adjacent to the proximal SMA boundary (Mclean et al, 1994; Roy et al, 1995). Similar allelic association with Type I SMA has been observed for the Ag-1 and C272 MSR's (DiDonato et al, 1994; Melki et al, 1994). These MSR's are clustered within our PAC and cosmid arrays clearly indicating that this region contains the gene responsible for SMA.

The highly variable and polymorphic structure of the SMA region including the presence of chromosome 5 specific repetitive sequence that may also be transcribed has rendered the isolation of candidate cDNAs problematic. These structural features have led to the identification of transcribed sequences that map outside of the 5q11.2-q13.3 region and of unprocessed pseudogenes (Francis et al, 1993; Theodosiou et al, 1994). We decided to isolate coding sequences from our PAC clones utilising the exon trapping system (Buckler et al, 1993). This system offered advantages over other approaches to isolating cDNAs. Coding sequences are isolated from genomic DNA when subcloned into the pSPL3 vector based on the presence of functional splice sites reducing the possibility of recovering pseudogenes. Additionally genes whose RNA expression patterns are

developmentally regulated, tissue specific or at expressed at a low level will be recovered with the same efficiency as those that are ubiquitously or highly expressed. Concurrent with this approach , PAC 125D9, containing the CATT subloci and CMS the proximal boundary, in addition to the cosmid 250B6, containing the CATT sublocus with high linkage disequlibrium, were utilised to screen cDNA libraries by other members of the group. These strategies led to the isolation of a novel gene mapping to the SMA locus, the neuronal apoptosis inhibitor protein (NAIP) that is deleted in a significant majority of Type I chromosomes. NAIP is homologous to the previously characterised viral inhibitor of apoptosis proteins (IAP) suggesting that NAIP may also function to suppress apoptosis. In keeping with the cell death of motor neurons that typifies SMA, mutations in *naip* would result in the impairment of cell death suppression resulting in excessive motor neuron apoptosis leading to the SMA phenotype.

MATERIALS AND METHODS

Exon trapping

pSPL3 DNA (0.25 μg) was linearized with *BamHI*, phosphatase treated, ligated with and without PAC DNA (0.25 μg) digested with *BamHI* or *BamHI* and *BglII* and transformed into E.coli. 10 % of each transformation was plated onto LB amp plates to determine the non-recombinant frequency while the remainder was inoculated into LB

amp medium. Plasmid DNA was prepared by alkaline extraction. COS-1 cells were passaged one day prior to transfection by plating 4 X 10^5 cells into 2 ml of DMEM (Gibco) (with 10% fetal calf serum) in 3.5 cm dishes. Cells were transfected by lipofectace. 5 µl of lipofectace were added to 100 µl Opti-MEM without serum for 5 min and 1 µg of DNA was added to 100 µl of Opti-MEM prior to the two mixtures being combined for 10 min. COS cells were rinsed with serum free media, the DNA/lipid/Opti-MEM mixture was added and the cells were incubated overnight. The cells were supplemented with 2 ml of DMEM with fetal calf serum and total RNA was extracted after 24 hr utilising TRIzol reagent as recommended by the manufacturer (Gibco). cDNA was synthesised in a 20 µl reaction utilising 2 µg of RNA. The RNA was denatured at 70°C for 5 min in the presence of the primer SA2 (ATC TCA GTG GTA TTT GTG AGC) and then cooled to 42°C. Reverse transcription was performed at 42°C for 30 min with 200 units of Superscript II reverse transcriptase (Gibco), 4 µl of 5X first strand buffer, 2 µl of 0.1 M DTT and 1 µl of 10 mM dNTPs.. The cDNA was incubated at 55°C for 5 min and 1 µl of RNase H was added. 8 µl of the reverse transcriptase reaction were utilised in a primary PCR reaction with primers SA2 and SD6 (TCT GAG TCA CCT GGA CAA CC) with the following conditions for 6 cycles: 94°C, 1 min, 60°C, 1 min and 72°C, 5 min. Half of the primary PCR reaction was treated with 20 units of BstXI overnight at 55°C. Both the BstXI digested and undigested PCR products were subjected to a second round of PCR with the primers dUSA4 (CUA CUA CUA CUA CTG AGG AGT GAA TTG GTC G) and dUSD2 9CUA CUA CUA CUA GTG AAC TGC ACT

GTG ACA AGC TGC) for 30 cycles at: 94°C, 1 min, 60°C, 1 min and 72°C, 3 min. 5 µl of each reaction were resolved on a 2% low melting point agarose gel and unique bands isolated. These products were cloned into the pAMP10 vector by the addition of 1 unit uracil DNA glycoslylase (UDG) and incubation at 37°C for 30 min. Exons were sequenced utilising the SD2 primer on an ABI 373A automated DNA sequencer. DNA sequence data was edited with the TED program (Gleeson and Hillier, 1991) and analysed using the GCG sequence analysis package (University of Wisconsin Genetics Computer Group).

PCR analysis and hybridisation

Primers used for *naip* mutational analysis and determination of the genomic organisation were selected for T_ms of 60°C and were utilised with the following conditions for 30 cycles: 94°C for 60 s, 60°C for 60 s and 72°C for 90 s. PCR primer sequences were as follows: 1145 CGCTGC ATA TCCC ATA TAG CTC, 1240, CTA TCT GAA TCC AGG AGT TCA; 1258, ATG CTT GGA TCT CTA GAA TGG; 1267, TCA CAG ATG ATA CTG GCC AG; 1285, AGC AAA GAC ATG TGG CGG AA; 1342, CAC TTG CTG GGC TGT GAT CTG; 1343, CCA GCT CCT AGA GAA AGA AGG; 1401, ACC TGG GAC CCT TCT GGA AG; 1842, GAA ATG GCA GGA AGG TGA TGA; 1843, AAA AGA GTC CAG CCG TAG TTC; 1844, GAA CTA CGG CTG GAC TCT TTT; 1857, CAT TTG GCA TGT TC TTC CAA G; 1863, CTC TCA GCC TGC TCT TCA

GAT; 1864, AAA GCC TCT GAC GAG AGG ATC; 1865, CAA GTG GGC ACA ACC TAC TGA; 1882, CTG AGT CAG ACA CTT ACA GGT AA; 1884, CGA CTG CCT GTT CAT CTA CGA; 1885, CCA GTG GAA GGA AAG TAT GTG; 1886, TTT GTT CTC CAG CCA CAT ACT; 1887, CAT TTG GCA TGT TCC TTC CAA G; 1892, TTA AAG GAA TGC CTG GAA TTT CAA C, 1893, GTA GAT GAA TAC TGA TGT TTC ATA ATT; 1894; GAC AGC TCT ATC ACA GTA CTG G; 1910, TGC CAC TGC CAG GCA ATC TAA; 1915, GAG AGG TGG AGG TTG CAG TGA; 1919, TAA ACA GGA CAC GGT ACA GTG; 1923, CAT GTT TTA AGT CTC GGT GCT CTG; 1926, TTA GCC AGA TGT GTT GGC ACA TG; 1927 GAT TCT ATG TGA TAG GCA GCC A; 1933, GCC ACT GCT CCC GAT GGA TTA; 1974, GCT CTC AGC TGC TCA TTC AGA T; 1979, ACA AAG TTC ACC ACG GCT CTG; 2048, ATG GAG GAG TGT CAT ATA CGC ACT; 2050, TGC TCC TCA CTC TTC TAC CTT TTC.

The 5' and 3' ends of *smn* were amplified using primers GCT AGT CCA GCT ATG GCC CAT TTA and GGA ACC TCA CGT AGC TTG AGG TGT TGT respectively with the following conditions. An aliquot of each reaction was run on a 0.8 % low melting point agarose gel and fragments were isolated. These were utilised to probe Southern blots of genomic DNA digested with *EcoRI* in addition to Southern blots of PAC clones digested with *EcoRI* or *BamHI*.

RT-PCR

RNA was isolated using TRIzol reagent as recommended by the manufacturer (GIBCO BRL). cDNA was synthesised in a 20μl reaction utilising 7μg of total RNA. The RNA was denatured for 5 min at 95°C and cooled to 37°C. Reverse transcription was performed at 42°C for 1 hr after addition of 5 μl of 5 X reverse transcription buffer (GIBCO BRL), 2 μl of 0.1 M DTT, 4 μl of 2.5 mM dNTPs, 8 U of Rnasin, 25 ng of cDNA primer (1285) and 40 U of MMLV (GIBCO BRL). cDNA was subsequently utilised as template in 50 μl PCR reaction. Of this primary PCR, 1 μl was used as template for secondary PCR amplification using nested primers. Products to be sequenced were subcloned into the TA vector (Invitrogen) and sequenced using M13 forward and reverse primers.

RESULTS

Exon trapping and identification of *naip*

PAC's 125D9, 250K7, 275G5, 238D12, 111E4 and 260G6 were utilised in an exon trapping system to isolate coding sequences within the SMA region (Figure 3-1). PAC 125D9 was emphasised as a source of coding sequences as it encompasses the proximal boundary CMS and the CATT-1 subloci that shows a linkage disequlibrium maximum with Type I SMA. *BamHI* and *BamHI/BglII* fragments of these PACs were

Figure 3-1: Exon trapping protocol. The HIV tat sequences of the pSPL3 vector are shown. The multiple cloning site (MCS) is flanked by functional splice donor (SD-V) and slice acceptor (SD-A) sites. Genomic DNA is subcloned into the multiple cloning site and transfected into COS cells. The DNA which contains exons in the proper orientation will allow splicing to occur. The two types of splicing that can occur are depicted. The MCS is flanked by two *BstXI* half sites such that vector/vector spliced products can be detected. SA-G: slice acceptor genomic. SD-G: splice donor genomic.

Exon Trapping Protocol

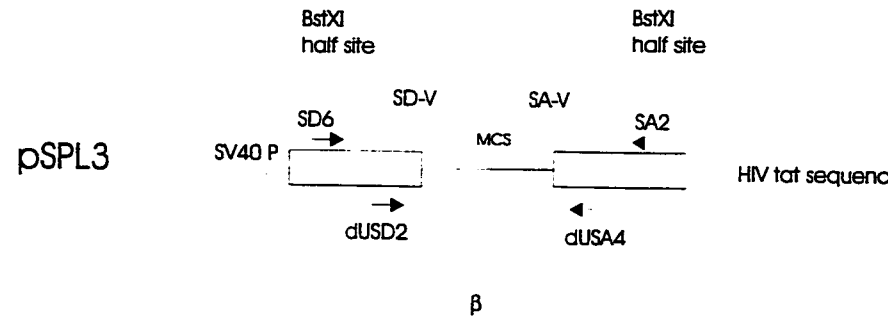

β

Subclone genomic DNA into pSPL3

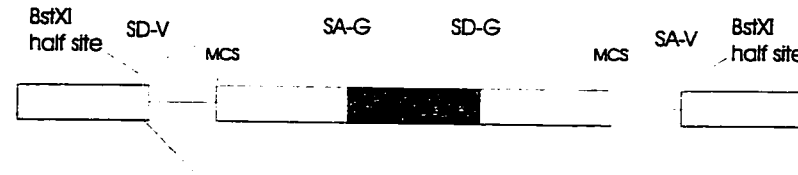

α α

Transfect into COS cells

(α) vector/genome splicing (β) vector/vector splicing

Isolate RNA/ Synthesize cDNA

Primary PCR amplification (SD6 - SA2)

BstXI treatment

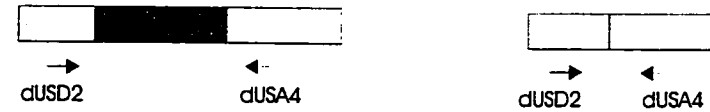

Secondary PCR amplification (dUSD2 - dUSD4)

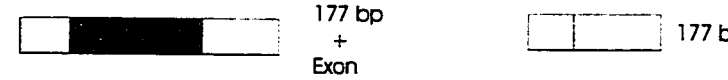

Clone PCR products Sequence

cloned into the multiple cloning site of pSPL3. This vector contains the HIV-1 tat gene, an intron, functional splice donor and acceptor sites and flanking exon sequences. Pooled genomic subclones from each PAC were transfected into COS-1 cells resulting in the identification of 68 exons. Sequence analysis revealed that 32 of these exons (47 %) were HIV vector derived products. The remaining exons did not show any striking homology at the nucleotide level to any known genes in the data base.

Genomic libraries had been constructed in our laboratory from complete and partial Sau3AI, *BamHI* and *BamHI-NotI* digests of PAC 125D9 and termini from these 200 clones were subsequently sequenced. This permitted the construction of contiguous and overlapping genomic clones covering most of PAC 125D9. Additionally a sequence database of the region was established including any sequences obtained from cDNAs concurrently being isolated. Exon 9-23 was shown to be contained within a previously isolated cDNA. The cosmid 250B6 which contains one of the CATT-1 subloci had been utilised to screen a human fetal brain cDNA library resulting in the detection of a 2.2 kb coding transcript that did not share any homology to any known proteins. This transcript was extended by screening the cDNA library and shown to encompass exon 9-23. Sequence analysis detected similarity between the protein encoded by this cDNA and two baculoviral inhibitor of apoptosis proteins (IAP). Given the suggestion that the motor neuron degeneration observed in individuals with SMA could be the result of apoptosis,

efforts were focused on this candidate cDNA eventually designated the neuronal apoptosis inhibitory protein (NAIP). The 2.2 kb exon isolated with the cosmid 250B6 and the trapped exon 9-23 ultimately proved to be exons 13 and 10 of *naip* respectively. The trapped exon 9-11 overlapped with the cDNA CC21.4B at its most 3' end, defining exon 14. This exon was utilised to screen a cDNA library resulting in the identification of a cDNA incorporating the trapped exon 9-7 (exon 15) and extending beyond to include exon 16.

Naip gene structure

Hybridization of *naip* exons to Southern blots containing DNA from our PAC array revealed that PACs 125D9 and 55I12 contained all of the *naip* exons. The genomic architecture of the *naip* locus was then elucidated by the subsequent hybridization of *naip* exons to Southern blots containing genomic DNA and DNA from PAC 125D9 digested with *BamHI*, *EcoRI* and *BamHI/EcoRI*. In addition, these exons were used to probe the libraries that had been constructed from PAC 125D9. Many of these clones had been ordered into contiguous arrays based on sequencing of their ends, permitting a rapid construction of the *naip* genomic organisation. The genomic structure of the region is shown in Figure 3-2 .

The *naip* gene contains at least 16 exons comprising 6 kb and spans approximately 90 kb of genomic DNA. The localisation of *naip* within the PAC and YAC array and

Figure 3-2: Physical mapping of the NAIP region at 5q13. The gene structure of the NAIP is depicted in (D). Of note is the genetically defined proximal SMA boundary (CMS) just centromeric to NAIP.

A

Correlation of Type I SMA 5q13.1 marker linkage disequilibrium with 5q13.1 physical map

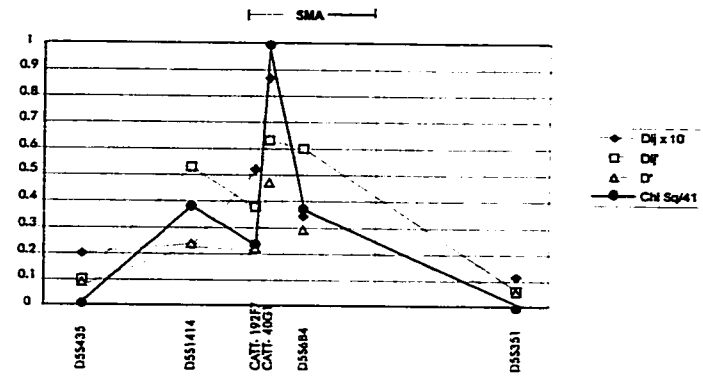

B

YAC array

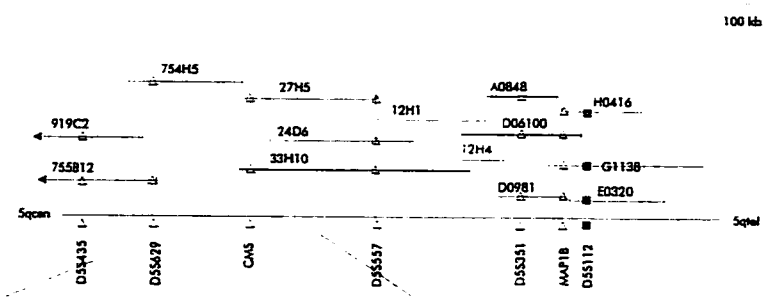

C

PAC array

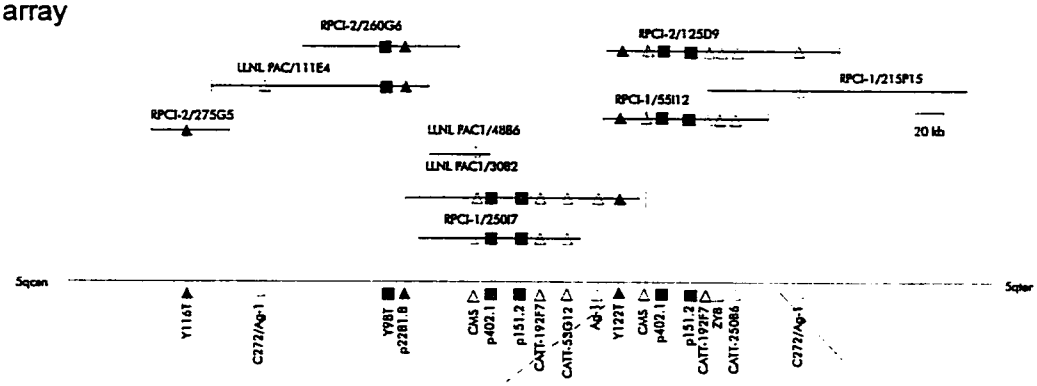

D

NAIP gene structure

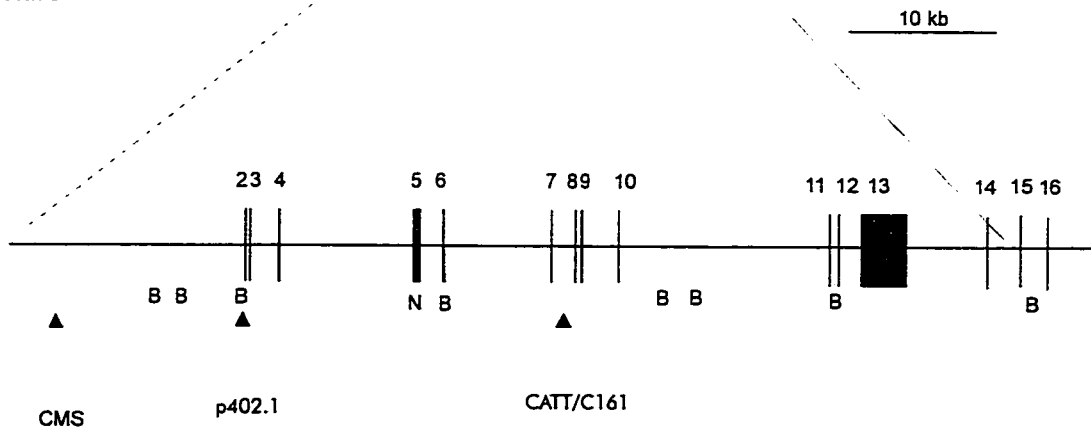

Figure 3-3: cDNA sequence and predicted amino acid sequence of NAIP. Sequence comparison with the viral IAPs is shown. The defined BIR motifs are in brackets. Darkly stippled regions denote identical regions. Similar regions are lightly stippled. The first BIR motif of NAIP that is not found in the viral IAPs is located in exon 5. Cp-iap: Cydia pomonella granulosis virus. Op-iap: Orgyia pseudotsugata nucleur polyhedrosis virus.

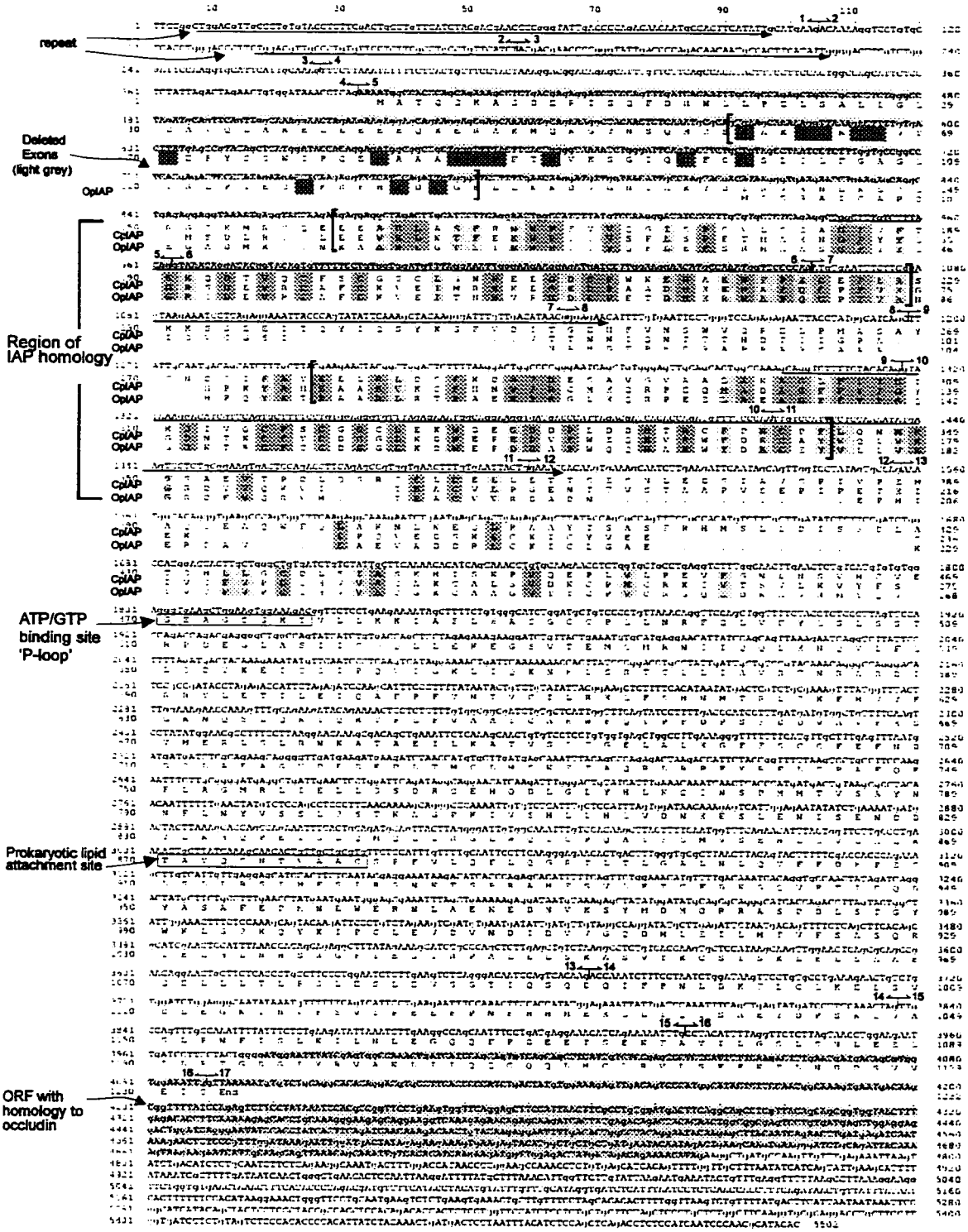
repeat
Deleted Exons (light grey)
OpIAP
Region of IAP homology
ATP/GTP binding site 'P-loop'
Prokaryotic lipid attachment site
ORF with homology to occludin

Figure 3-4: Domain structure of NAIP and viral IAPs. The position of the BIR motifs are shown bystipled boxes. The ring finger domain that is absent in NAIP is represented by black boxes. The proteins are drawn to scale except for the C-terminus of NAIP

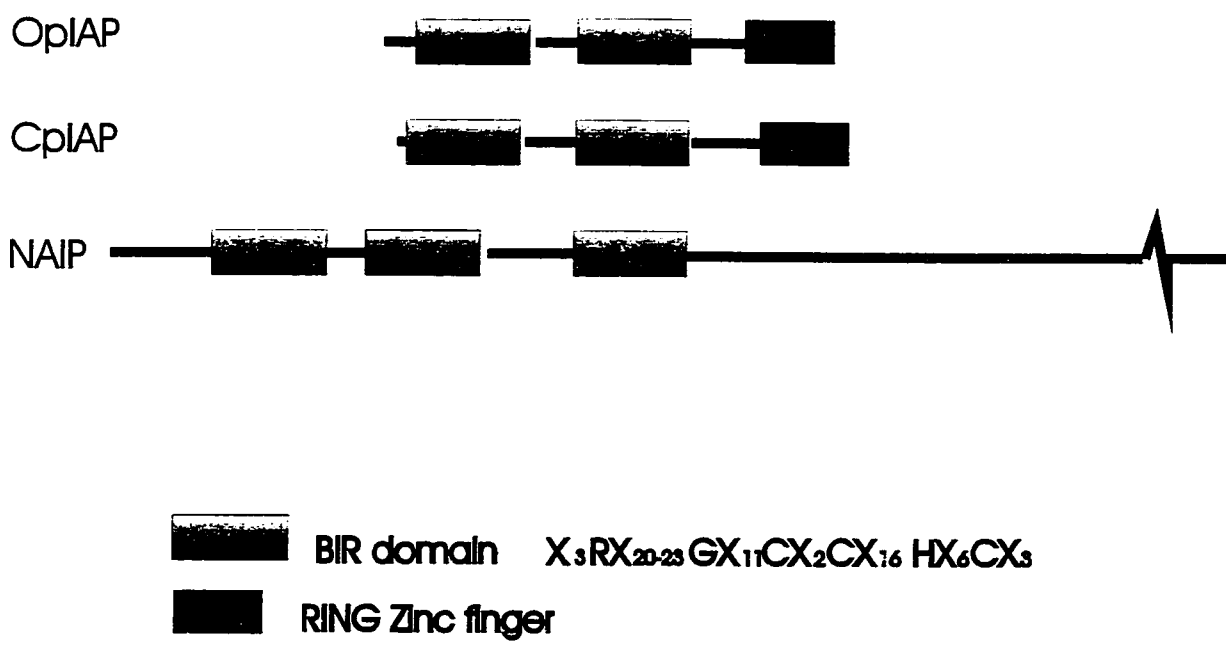
OpIAP
CpIAP
NAIP
BIR domain $X_3RX_{20-23}GX_{11}CX_2CX_{16}HX_6CX_3$
RING Zinc finger

relative to our linkage disequilibrium peak is depicted in Figure 3-2. The initiating methionine is localised to exon 5 and *naip* encodes a 1232 amino acid (3696 nt), 140 kDa protein (Figure 3-3). Further analysis indicates that *naip* is composed of 18 exons encoding a 155 kDa protein (Anne Besner, unpublished data). DNA and protein data base searches using the BLAST network service revealed significant amino acid similarity with two viral IAPs, Cydia pomonella granulosis virus (Crook et al, 1993) and Orgyia pseudotsugata nuclear polyhedrosis virus (Birhaum et al, 1994), with 33 % identity over 189 and 180 amino acids respectively. This homology is located in the 80 amino acid baculovirus IAP repeat (BIR) motifs, with the consensus sequence $X_3RX_{20-23}GX_{11}CX_2CX_{16}HX_6CX_3$, that occurs as a tandem repeat separated by approximately 30 amino acids at the N terminus of the viral IAPs (Birhaum et al, 1994). Although the viral IAPS are comprised of two BIR domains , NAIP contains three such motifs corresponding to amino acids 60-126, 159-228 and 278-344. These three BIR motifs of NAIP are approximately 35 % identical and have intervening sequences of 33 and 50 amino acids. The C-terminal domain of the viral IAPs contains a RING zinc finger motif that is absent in NAIP (Figure 3-4).

In addition to the homology with the viral IAPs, our analysis of NAIP structure predicted two hydrophobic possibly membrane spanning domains (residues 92-110 and 479-496), an ATP/GTP binding site (residues 470-477) and four N-linked glycosylation

sites in addition to a prokaryotic lipid attachment site in the carboxy region (Figure 3-3). We have identified three exons of the 5' untranslated region (5'UTR) however more may exist. Of note in the 5'UTR is the presence of a 90 bp duplication. Exon 17 which comprises the 3'UTR has a 550 bp region with high homology to the chicken integral membrane protein occludin (Furuse et al, 1993). This exon has been seen only in the deleted forms of *naip* and is thus thought not to represent the 3'UTR of the intact version of *naip*.

Deleted and truncated forms of *naip*:

Analysis of our PAC and YAC clones by PCR with primers spanning the *naip* locus and hybridization with *naip* exons revealed a variety of truncated and deleted versions of *naip* within the 5q11.2-13.3 region (Figures 3-5; 3-6). Hybridization of *naip* exon 10 to Southern blots containing DNA from the PAC clones is shown in Figure 3-8. A 14.5 kb *BamHI* fragment that spans exons 7-10 of the *naip* locus located on PAC 125D9 and 55I12 was observed (Figure 3-8(A); Figure 3-7). The 14.5 kb *BamHI* fragment is contiguous with a second 14.5 kb *BamHI* fragment encompassing exons 2-5 in the intact *naip* locus as depicted in Figure 3-7. However, a 23 kb *BamHI* fragment, not a 14.5 kb *BamHI* fragment, was detected in PACs 30B2 and 250I7 upon hybridisation of *naip* exon 10 (Figure 3-8(A)). PCR analysis across the *naip* gene and probings of Southern blots of these PACs with *naip* revealed a deletion of exons 5 and 6 (Figure 3-7). The deletion of exon 5 and 6 in PACs 30B2 and 250I7 incorporates 6 kb of DNA that

Figure 3-5: Schematic of NAIP deleted and truncated loci found in YAC and PAC clones.

Exon content of PAC and YAC clones

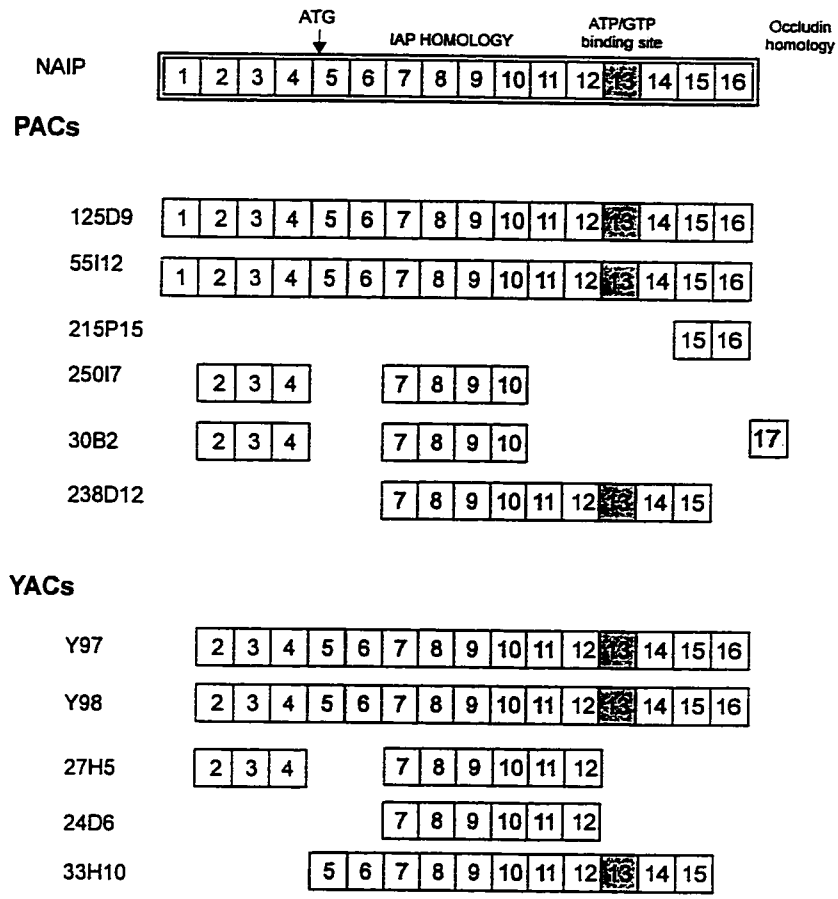

Figure 3-6: Exon probings of Southern blots containing PAC clones. The probes utilised and the endonucleases employed are indicated on the left. Note the presence of the centromeric probe Sf2 and the absence of exons 5 and 6 in PAC 238D12. PAC 30B2 and 250I7 also contain a deletion of exons 5 and 6.

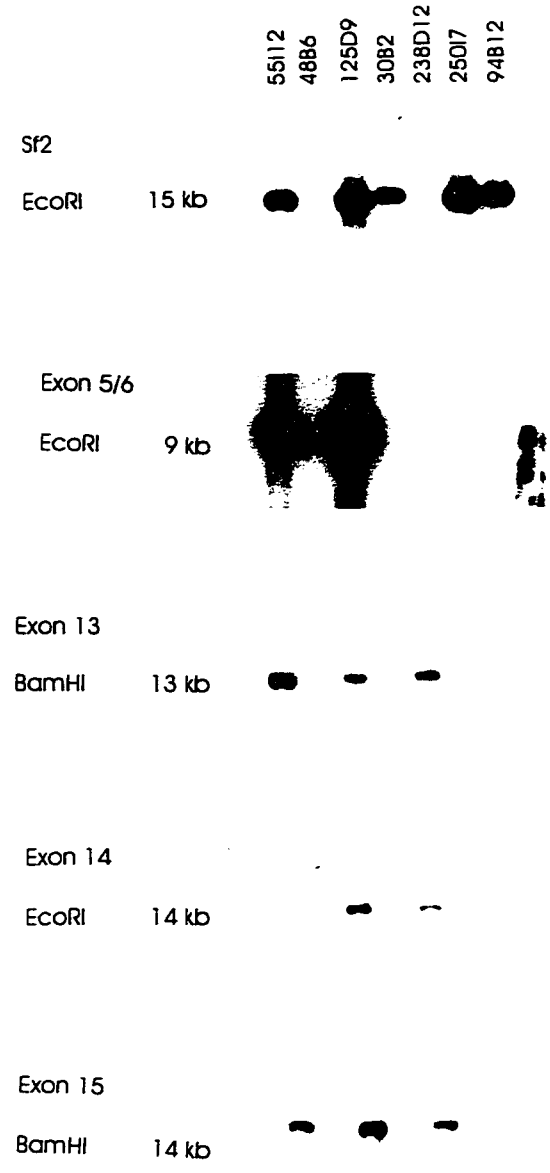
5112
48B6
125D9
30B2
238D12
2501?
94B12
Sf2
EcoRI
15 kb
Exon 5/6
EcoRI
9 kb
Exon 13
BamHI
13 kb
Exon 14
EcoRI
14 kb
Exon 15
BamHI
14 kb

Figure 3-7: Structure of intact and internally deleted and truncated NAIP loci at 5q13. The intact NAIP loci is shown with the location of the two contiguous 14.5 kb *BamHI* fragments. The deleted 6 kb region in PAC 30B2 and the resulting 23 kb *BamHI* fragment are depicted. The 9.6 kb *BamHI* fragment that arises due to the deletion of exons 1-6 is also shown. Th location of PCR primers utilised in the analysis are shown. N: *NotI* site. B: *BamHI* site. E: *EcoRI* site.

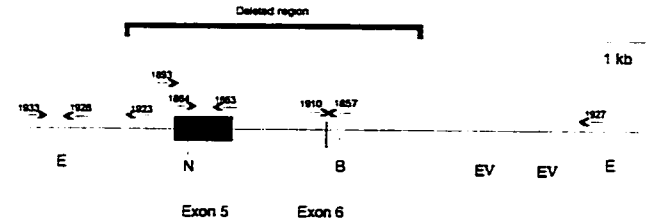
Deleted region
1 kb
E
N
B
EV
EV
E
Exon 5
Exon 6

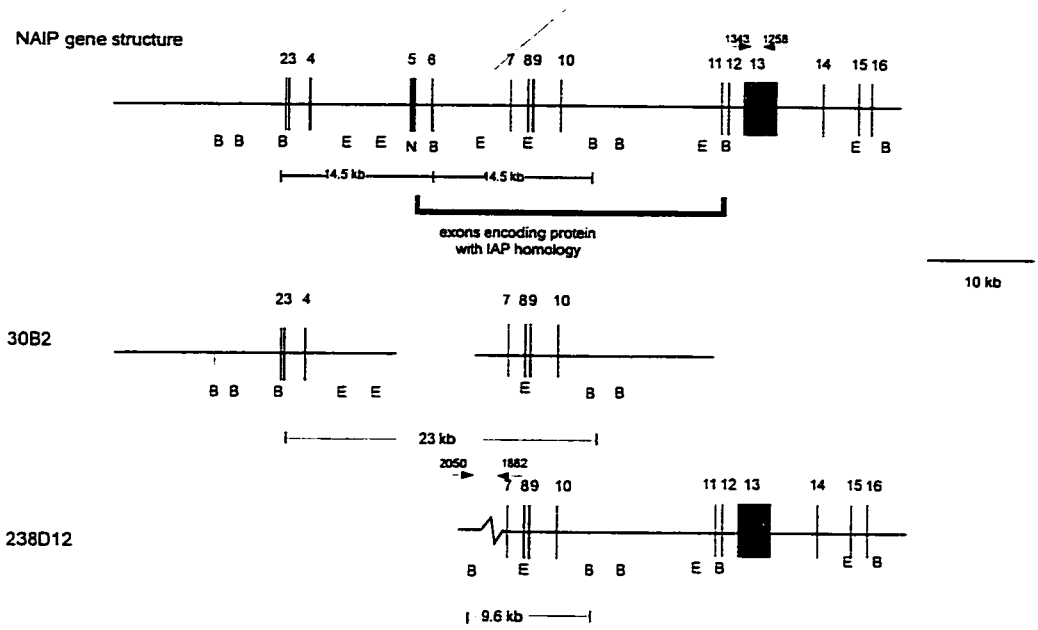
NAIP gene structure
23 4
5 6
7 89 10
11 12 13
14
15 16
B B B E E N B E E B B E B E B
14.5 kb
14.5 kb
exons encoding protein
with IAP homology
10 kb
30B2
23 4
7 89 10
B B B E E E B B
23 kb
2050
1882
238D12
7 89 10
11 12 13
14
15 16
B E B B E B E B
9.6 kb

Figure 3-8: Hybridization of PACs and genomic DNA to elucidate genomic architecture. (A) Southern blot of PAC DNA probed with *naip* exon 10. The 14.5 kb *BamHI* fragment corresponding to the intact *naip* loci are found in PAC 125D9. The 23 kb *BamHI* fragment corresponding to the deleted exon 5-6 *naip* loci is observed in PACs 30B2 and 250I7. PAC 238D12 contains a 9.6 kb *BamHI* fragment representing a deletion of exons 1-6. (B) Southern blot analysis of a French Canadian Type III family. There is an absence of the 14.5 kb *BamHI* fragment in affected individuals corresponding to the homozygous deletion of exons 5 and 6. The 23 kb and 9.6 kb *BamHI* fragments are present in all individuals at variable dosage.

A

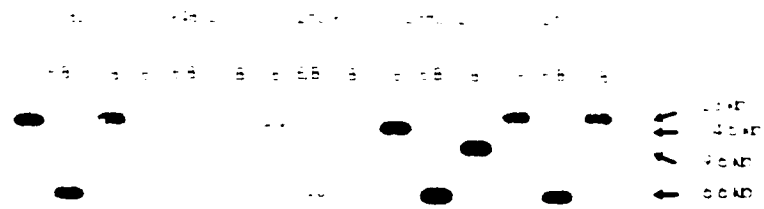

B

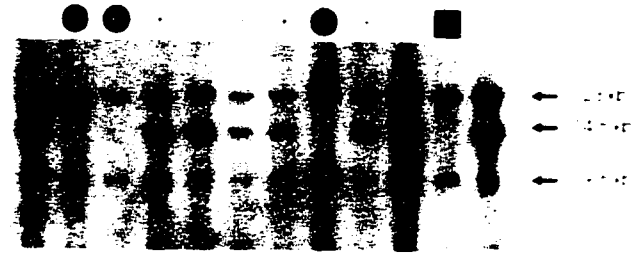

Figure 3-9: PCR analysis of the 6 kb, exon 5-6 deletion. Primers 1927 and 1933 were employed to amplify a junction fragment spanning the deletion (see Figure 3-7) in PACs 30B2 and 250I7. Note the presence of this 4.2 kb fragment in both normal and affected SMA genomic DNA.

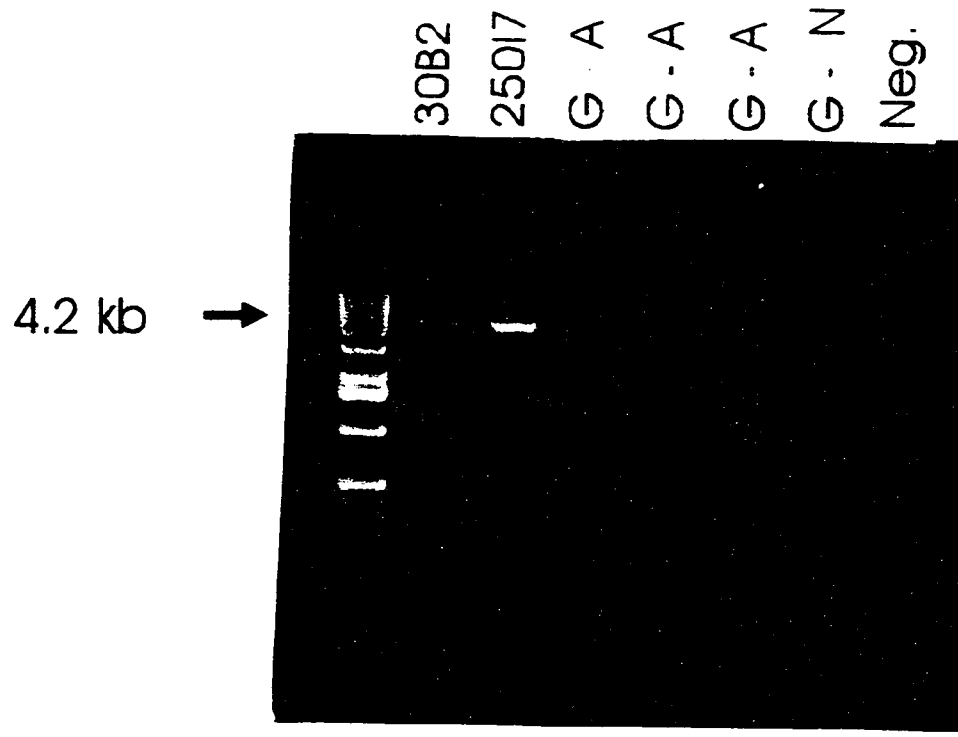
30B2
25017
G - A
G - A
G - A
G - N
Neg.
4.2 kb

contains a *BamHI* site as displayed in Figure 3-7. The loss of this 6 kb of DNA which contains a *BamHI* site, results in a 23 kb *BamHI* fragment detected upon hybridization with exon 10 (Figure 3-8(A)). The deletion of 6 kb of DNA was confirmed by PCR with primers 1927 and 1933 which amplify a 4.2 kb fragment spanning the deletion in PACs 30B2 and 250I7 (Figure 3-9). As shown, this junction fragment was also observed in genomic DNA confirming that it is not the result of clone instability. Moreover the junction fragment spanning the deletion of exon 5 and 6 is found in unaffected individuals suggesting that this deleted *naip* locus is contained in the general population

A second deleted *naip* locus was observed in PAC 238D12. This locus lacks *naip* exons 2-6 as determined by PCR and Southern blot analysis (Figure 3-6). The possibility that this PAC clone only spanned exons 7-15 was assessed by hybridisation with the centromeric probe Sf2. The presence of Sf2 in this PAC clone argued against this possibility. The genomic organisation of the *naip* locus on PAC 238D12 is depicted in Figure 3-7. A loss of approximately 20 kb incorporating two *BamHI* sites results in a 9.6 kb *BamHI* fragment spanning exons 7-10 (Figure 3-7; Figure 3-8(A)). This deletion was confirmed by PCR amplification of a 2.6 junction fragment with primers 2050, located upstream of exon 2, and 1882, located in exon 7 (depicted in Figure 3-7). As with the *naip* locus deleted for exons 5 and 6 this second *naip* locus was also present in genomic DNA of unaffected individuals suggesting that it is dispersed in the general population and not the result of clone instability.

***Naip* gene mutational analysis:**

Initial probings of genomic Southerns of SMA families with *naip* exons 2-9 revealed the presence of a deletion in affected individuals. To confirm this deletion and determine its extent, PCR analysis was conducted across the gene (Figure 3-10). The homozygous deletion of exons 5 and 6 was observed in individuals with SMA. PCR amplification of exon 5 from the Type I family 24561 and the Type III SMA family 21470 revealing the co-segregation of a deletion of exon 5 with the SMA phenotype is shown in Figure 3-11. Hybridization of *naip* exons 2-10 to Southern blots containing DNA from SMA families revealed the homozygous deletion of the contiguous 14.5 kb *BamHI* fragments in SMA affected individuals confirming the deletion of exons 5 and 6 (Figure 3-8(B)). A total of 110 SMA families were analysed revealing the homozygous deletion of exon 5 and 6 in 17 of 38 (45 %) of Type I SMA individuals and 13 of 72 (18 %) of Type II and Type III individuals.

Further assessment revealed that the deletion events corresponded to the *naip* loci found in PACs 30B2 and 238D12. PCR analysis was conducted around exon 5 and 6 in the anticipation of detecting a unique junction fragment and to determine the extent of the deletion in those individuals with homozygous deletions of exons 5 and 6. A unique junction fragment was never observed. PCR analysis revealed the loss of 6 kb of DNA and the amplification of the 4.2 kb junction fragment spanning the deletion as in PAC

Figure 3-10: Schematic of PCR mutational analysis performed across NAIP. The absence of amplification products detected are denoted by asterisks

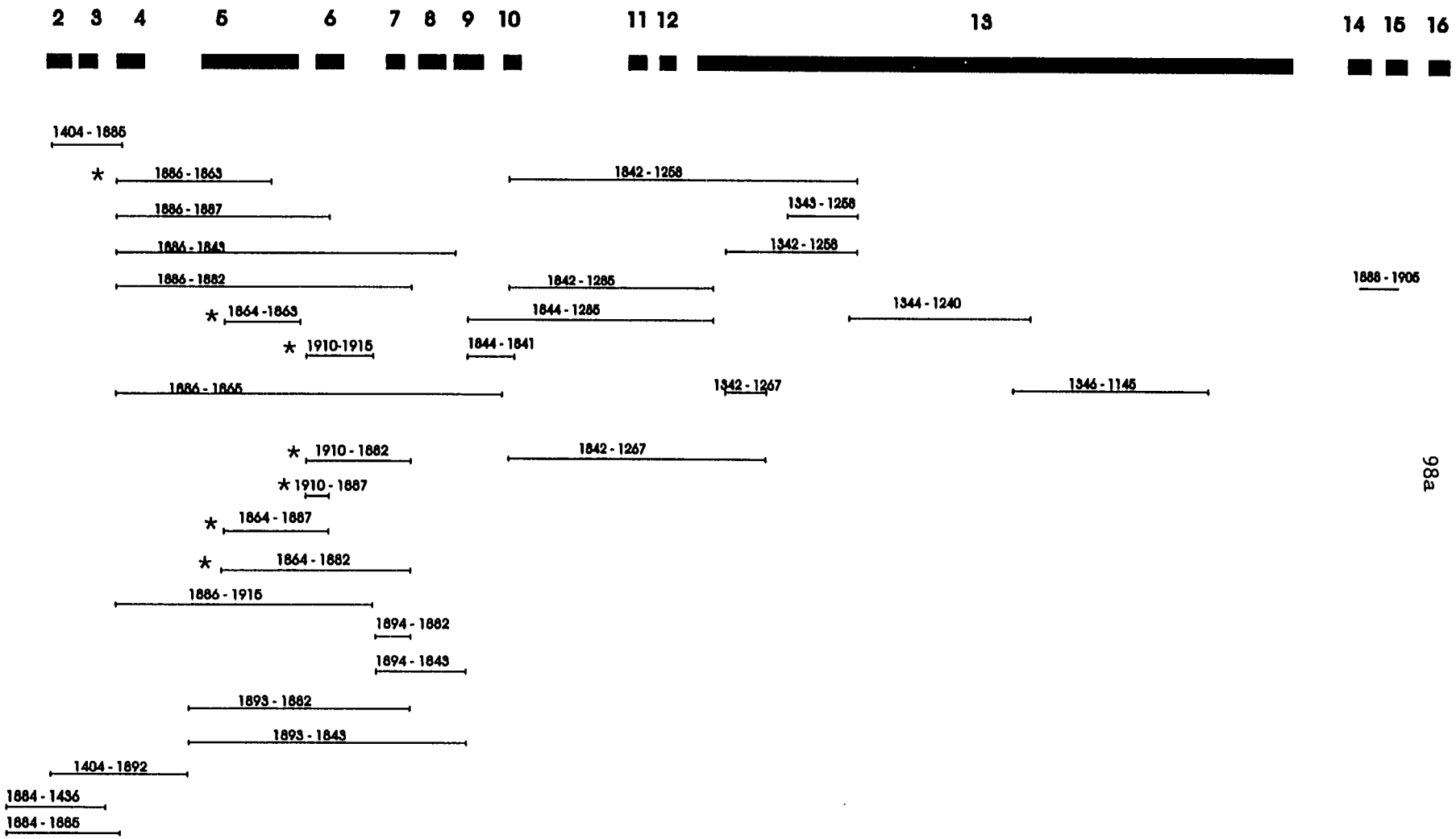
2
3
4
5
6
7
8
9
10
11
12
13
14
15
16
1404 - 1885
1886 - 1863
1842 - 1258
1886 - 1887
1343 - 1258
1886 - 1849
1342 - 1258
1886 - 1882
1842 - 1285
1888 - 1905
1864 -1863
1844 - 1285
1344 - 1240
1910-1915
1844 - 1841
1886 - 1865
1342 - 1267
1346 - 1145
1910 - 1882
1842 - 1267
1910 - 1887
1864 - 1887
1864 - 1882
1886 - 1915
1894 - 1882
1894 - 1849
1893 - 1882
1893 - 1849
1404 - 1892
1884 - 1436
1884 - 1885

Figure 3-11: Multiplex PCR analysis of exon 5 and exon 12 in a Type III family. The 435 bp product corresponds to the exon 5 amplification product. A failure of amplification is observed to cosegregate with the disease phenotype. Exon 12 amplification (241 bp product) was performed as a control.

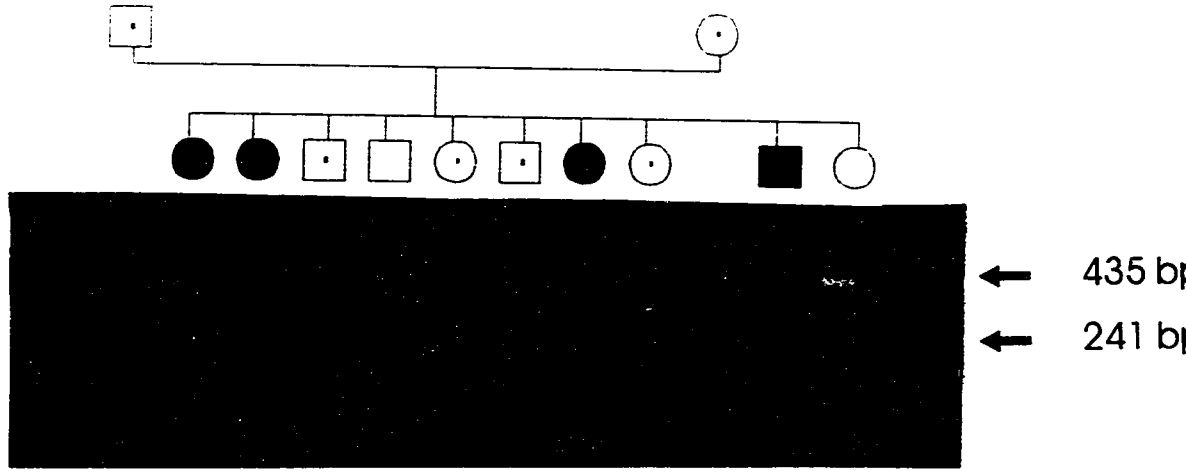
435 bp
241 bp

30B2. Additionally the 2.6 kb fragment spanning the deletion event in PAC 238D12 was also observed. In agreement with this data, the 23 kb and 9.6 kb *BamHI* fragments corresponding to the variant *naip* loci were observed in these individuals (Figure 3-8(B)). As can be observed in Figure 3-8(B) there is a variable dosage of these fragments suggesting the presence of a polymorphic number of each *naip* loci in individuals. Moreover SMA carriers and those individuals affected with SMA show reduced dosage of the various forms of *naip*. These results suggest that the number of copies of *naip* is polymorphic and that SMA chromosomes are characterised by a reduction of *naip* loci.

Reverse transcription PCR analysis

RT-PCR analysis of RNA from both non-SMA individuals and SMA individuals confirms that some of the deleted and internally truncated *naip* genes are transcribed (Figure 3-12). PCR amplification of reverse-transcribed products from exon 4 to exon 13 resulted in the amplification of multiple bands. Sequencing of these products revealed that they correspond to the full length transcript, the deleted exon 5-6 transcript and a deleted exon 5-6/exon 11-12 transcript. Failure of amplification was observed in several individuals with SMA. The amplification of β-actin RNA from these same samples indicated that this was not the result of RNA degradation but rather is in keeping with our hypothesis of the absence or reduction in *naip* loci. Although one of the SMA individuals shows amplification of the intact version of *naip*, since this RT-PCR is not quantitative it

Figure 3-12: RT-PCR amplification of RNA on tissues from SMA and non-SMA individuals. Primary PCR was performed with exon 1 primer 1884 and exon 13 primer 1285. Secondary PCR was performed with exon 4 primer 1886 and exon 13 primer 1974. A full length product in addition to the exon 5-6 and exon 5-6/11-12 deleted products are observed. A failure of amplification is observed in several affected individuals (a). n: normal.

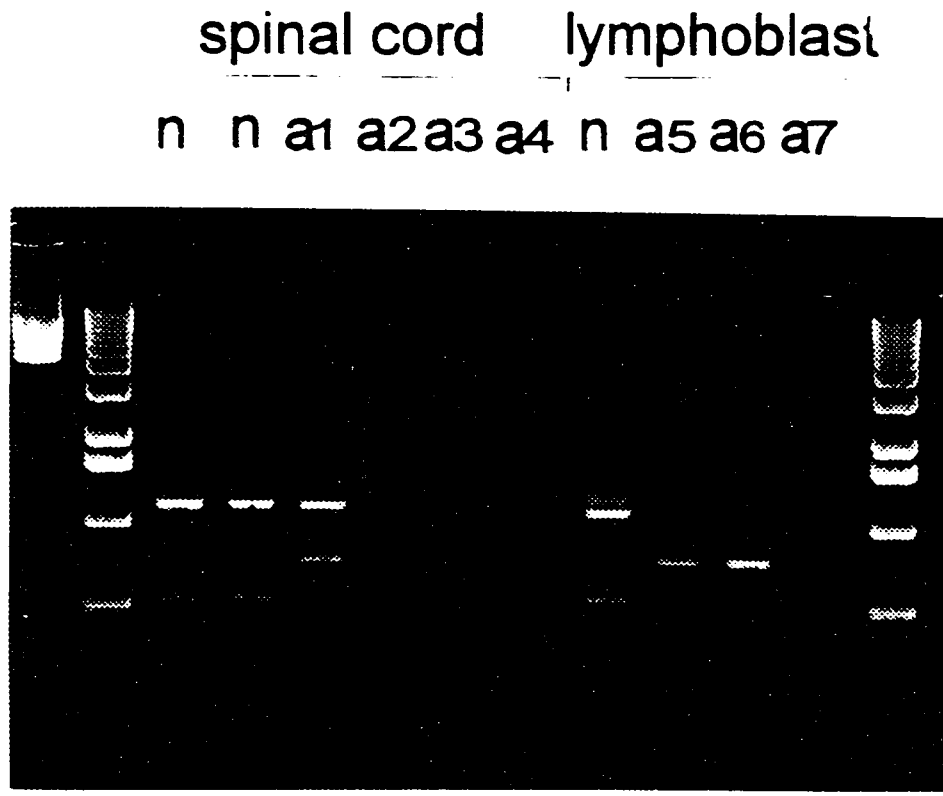
spinal cord
lymphoblast
n
n
a1
a2
a3
a4
n
a5
a6
a7

may be that there is a reduction in this transcript. Those SMA individuals that showed amplification of intact *naip* were examined for point mutations. One individual affected with Type I SMA showed a G to A change in exon 5 that resulted in an amino acid residue change of a cysteine to an arginine. This cysteine (amino acid 98) is one of the conserved amino acid residues within the first BIR motif suggesting that is may have a pathogenic consequence. A second amino acid conversion was observed in a Type II individual that results in a change from a proline to a leucine. This amino acid residue lies just outside the third BIR motif in exon 11 (amino acid 356) and is not conserved among the iaps. Site directed mutagenesis and in vitro functional studies will have to be performed to elucidate the consequences of these changes.

Mapping of *Smn*

Concurrent with our isolation of *naip* a second candidate gene for SMA which also mapped to 5q13 was identified, the survival of motor neuron (SMN) gene. Two copies of *smn* were reported to be located within the 5q13 region. Homozygous deletions of the last two exons of the telomeric version are found in 97% of individuals with SMA. PCR with primers corresponding to the 5' and 3' most ends of *smn* in combination with Southern blot analysis of our PAC clones revealed that *smn* also maps to the PAC clone (125D9) which contains *naip* (Figure 3-13; Figure 3-14). A second *smn* locus was detected in the PAC 111E4 and likely corresponds to the centromeric pseudogene as reported by Lefevbre et al (1995). The mapping of the functional *smn* locus telomeric to our CMS proximal boundary supports our genetic data. Analogous to the *naip* loci,

probings of Southern blots revealed variable dosage of *smn* suggesting that is also present in a polymorphic number.

Figure 3-13: *Smn* analysis of PACs and genomic DNA. *EcoRI* southern blots were hybridised with a 5' and 3' *smn* PCR product. The 5.5 kb and 7.5 kb *EcoRI* fragments correspond to the 5' and 3' ends of the gene respectively. Only the 3' end of *smn* is located on the PAC 111E4. Note the variable dosage of the two *EcoRI* fragments within each individual and between different individuals implying a polymorphic number of copies.

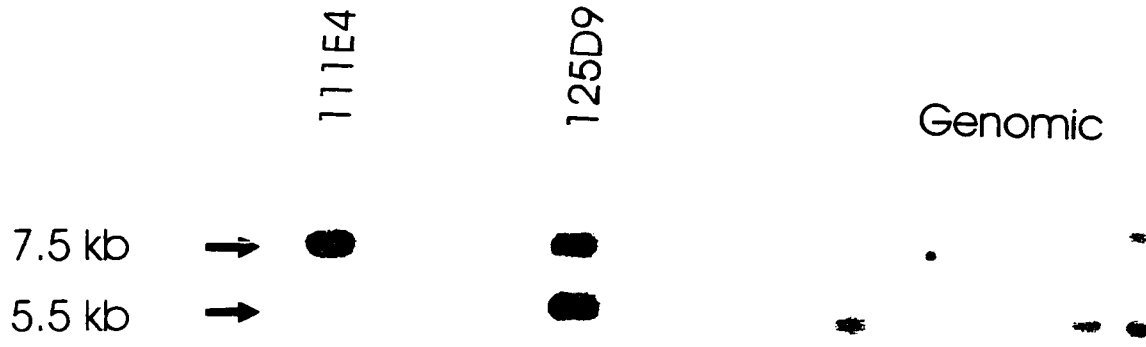
111E4
125D9
Genomic
7.5 kb
5.5 kb

Figure 3-14:. Location of SMN in our PAC contiguous array.

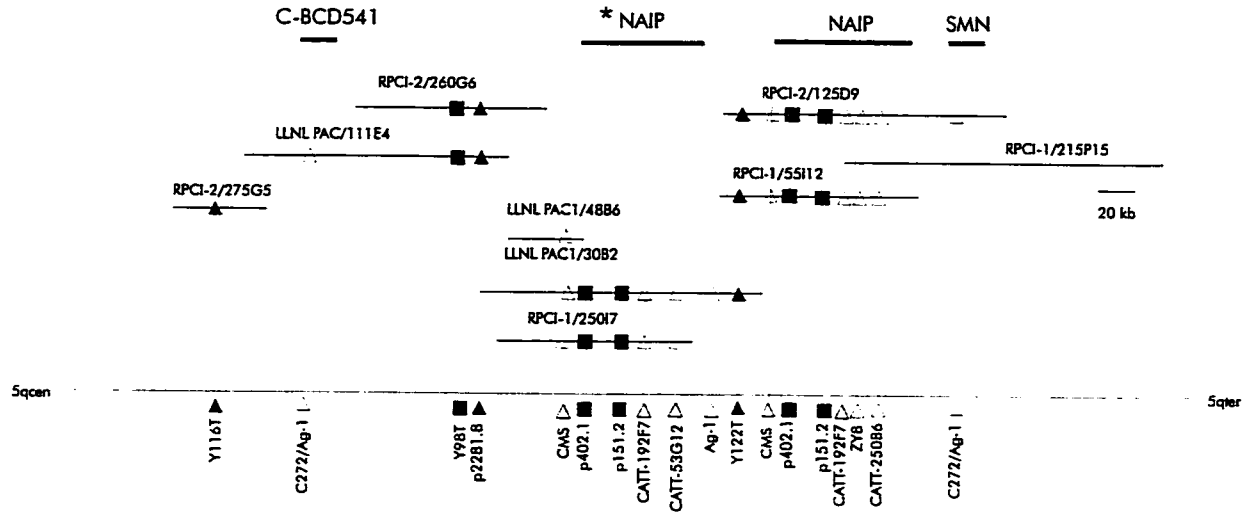
C-BCD541
* NAIP
NAIP
SMN
RPCI-2/260G6
RPCI-2/125D9
LLNL PAC/111E4
RPCI-1/215P15
RPCI-1/55I12
RPCI-2/275G5
20 kb
LLNL PAC1/4886
LLNL PAC1/30B2
RPCI-1/250I7
5qcen
5qter
Y116T
C272/Ag-1
Y98T
p22B1.8
CMS
p402.1
p151.2
CATT-192F7
CATT-53G12
Ag-1
Y122T
CMS
p402.1
p151.2
CATT-192F7
ZY8
CATT-25086
C272/Ag-1

DISCUSSION

Analysis of recombinant individuals narrowed the region of 5q11.2-13.3 containing the SMA gene to an interval of approximately 550 kb. We present the identification and characterisation of a candidate gene for SMA encoding the protein for neuronal apoptosis inhibitory protein (NAIP) which maps within this genetically defined interval. In addition to mapping within the recombination defined interval, the *naip* loci are located near the type I SMA linkage disequilibrium peak (Melki et al, 1994; DiDonato et al, 1994; Mclean et al 1994). Consistent with the complex genomic structure of the 5q13 region, *naip* is found in a variable number of intact and internally deleted forms within 5q13. Individuals have multiple copies of *naip* and this copy number is polymorphic between individuals and chromosomes. We have found homozygous deletions of exons 5 and 6 in 67% of type I SMA chromosomes and 42 % of type II/III SMA chromosomes.. We propose that a reduction in the number of *naip* loci or a complete absence of full length *naip* results in the SMA phenotype. NAIP shares homology with the baculovirus iaps Cp-iap and Op-iap that are known to inhibit apoptosis suggesting that NAIP also functions to inhibit apoptosis. Mutations in *naip* that lead to the loss of anti-apoptotic function would be in keeping with the insufficiency and morphology of motor neurons observed in SMA.

In keeping with this model, we have previously shown that the CATT-40G1 CTR that is duplicated on non-SMA chromosomes is deleted in 45 % of non-SMA

chromosomes in contrast to 80 % of SMA chromosomes (Mclean et al, 1994). Additionally a reduction in the number of C272 subloci and Ag-1 subloci in individuals with type I SMA has also been observed supporting chromosomal deletions at the 5q13 locus in affected individuals (Melki et al, 1994; DiDonato et al, 1994).

An issue raised by the spectrum of deleted and truncated *naip* loci is the transcriptional and translational activity of these forms. The deletion of exon 5 and 6, encoding the first BIR motif, results in an in frame deletion with a start methione in exon 2. At present it is unknown if this protein is translated and if so whether a protein lacking two BIR motifs may function to suppress apoptosis, assuming that NAIP functions in an anti-apoptotic manner. Alternatively, this protein may lack the ability to associate with other proteins that are crucial to NAIPs ability to suppresses cell death or it may retain this ability and act as a competitive inhibitor by sequestering an interacting protein. The deletion of a single copy of exon 5 and 6 might then result in a mild phenotype while deletion of multiple copies of exon 5 and 6 would result in a more severe phenotype. Additional internally deleted or truncated *naip* loci have been identified and more may exist. The relative levels of these proteins may determine the cells susceptibility to death and invokes a complex mechanism.

Southern blot analysis of over 900 non-SMA individuals failed to detect homozygous deletions of exon 5 and 6 however PCR analysis on parents of SMA children

resulted in the identification of homozygous deletions of exon 5 and 6 in 3 individuals. These data would suggest that mutations in *naip* may not be required for manifestation of the SMA phenotype or might reflect the involvement of a second tightly linked gene. Homozygosity for deletion of exon 5 and 6 is found predominantly in individuals affected with Type I SMA and would support a model in which mutation in two genes lead to the SMA phenotype with *naip* determining the severity of the phenotype.

Consistent with this hypothesis, a second candidate gene for SMA, the survival of motor neuron gene (SMN), was isolated (Lefebvre et al, 1995). *Smn* does not share significant homology to any known proteins giving no indication of its function. The *smn* gene is present in two copies (centromeric and telomeric) at 5q13 that can be distinguished by base substitutions in exons 7 and 8 neither of which affects the coding of the protein. PCR products analysed by single strand conformational polymorphism (SSCP) detected homozygous deletion of exons 7 and 8 in the telomeric version of *smn* in 97 % of individuals with SMA. Healthy individuals were reported to have a least one copy of the telomeric form of *smn*. One might expect that the centromeric version of *smn*, which is transcribed, would provide redundancy and consequently deletion of the telomeric copy would not result in the disorder. However the fact that 10 % of the general population lack the centromeric copy of *smn* with no discernible phenotype suggests that a functional difference may exist between the two forms.

RT-PCR analysis of RNA from muscle of both unaffected and SMA individuals demonstrates that a number of *smn* isoforms are transcribed (Gennarelli et al. 1995). Transcripts of the centromeric form of *smn* lacking exon 7 or exon 5 and 7 are observed and more abundant in SMA patients. The absence of exon 7 results in a loss in the number of amino acids which confer a coil and helical confirmation and it is possible that these structural changes may also confer functional changes. Additional alternatively spliced products have been identified which do not contain a potential N-myristoylation site (Gennerelli et al, 1995). The functional consequence of these transcripts and potential protein products is unknown at present. Possibly some of these products act as negative regulators and similar to *naip* invokes a complex mechanism.

The high frequency of deletions in the telomeric form of *smn* observed in all SMA individuals, strongly suggests that this mutation may be a prerequisite for the SMA phenotype. However, because of the lack of correlation between *smn* genotype it appears that mutations in *smn* alone are not sufficient to result in the more severe forms of the disorder. This would support the existence of a modifying gene such as *naip*, contiguous with *smn* that determines the degree of severity in patients. Consistent with this hypothesis homozygous deletions of *naip* are found predominantly in individuals with Type I SMA. This might also support a model in which the extent of the deletion would determine the severity of the phenotype. Individuals affected with Type I SMA may have larger deletions encompassing both *naip* and *smn* loci. Furthermore the number of *naip*

and/or *smn* loci which are lost may be greater in those individuals with the most severe form of the disease. The numerous copies of both genes has confounded the analysis and we have been unable to determine the copy number of each form.

Although homozygosity of deletions in the telomeric copy of *smn* were described only in SMA patients initially, as with *naip*, healthy individuals have since been identified who also harbour this deletion (Cobben et al, 1995). Within each family the healthy sibs which show homozygosity for an *smn* deletion share the same 5q haplotype as their affected siblings. The possibility that these unaffected *smn* individuals have not yet reached the age of disease onset is doubtful as the age between affected and unaffected siblings is greater than 15 years. Such a temporal discordance in age at onset for SMA siblings has not been reported (Rudnik-Schoeneborn et al, 1994) and these healthy individuals do not have any neurophysiological signs of SMA. Deletions of either *naip* or *smn*, in unaffected individuals would indicate that the SMA phenotype does not require mutation of either gene. However, healthy individuals deleted for both genes have not been observed and would support the model in which mutations in both *naip* and *smn* are required for the presentation of the SMA phenotype.

A gene conversion event may have reversed the mutation in the healthy individuals or caused the mutation in the affected individuals. Alternatively the affected individuals may harbor a larger deletion than their unaffected siblings, however the repetitive nature

of the region has rendered this analysis difficult. The organisation of this region containing highly repetitive sequences that are clustered within a relatively small area would facilitate gene deletion and addition events by unequal crossingover . These events would contribute to the instability of the region and furthermore might indicate that a chromosome structure or haplotype would be at a higher risk for generating a severe mutation by facilitating these events.

The genomic structure and instability leading to these types of mutations in the region encompassing *naip* and *smn* is analogous to the HLA class region located on chromosome 6p21.3. This 600 kb segment contains the genes for steroid 21-hydroxylase (CY21) and its pseudogene (CYP21P), serum complement C4A, serum complement C4B, ribosomal protein (RPL32) and its pseudogene (RPL32P) and gene X (Belt et al, 1984; Carroll et al, 1985; Shen et al, 1994). These four tandemly arranged genes form a modular structure (RCCX) and are present in 1 to 3 or more copies in the general population (Shen et al, 1994). Congenital adrenal hyperplasia, a disorder of cortisol biosynthesis, is caused by deletions or gene conversion events that occur between the functional steroid 21-hydroxylase gene (CYP21) and its pseudogene (CYP21P) which result in an inactive enzyme (Collier et al, 1993; Wedell et al, 1993). The organisation of the region has been proposed to promote these events. Moreover, similar to SMA, steroid 21-hydroxylase deficiency displays a wide range of clinical manifestations as a consequence of the various allelic mutations (Weddell et al, 1992).

The variability in the clinical phenotype observed in SMA as a result of mutations in either *smn* or *naip* or both genes may parallel the deletion mutations in the α-globin gene cluster that lead to the α-thalassemias. This cluster consists of two functional genes and their pseudogenes. Deletions that encompass both genes on both chromosomes result in the most severe phenotype. Those individuals which are heterozygotes and are deleted for both copies of the two genes on just one chromosome in combination with a mutation in one of the genes on the other chromosome, display an intermediate phenotype. The mildest phenotype is observed when both chromosomes have mutations in one of the genes. The complexity is increased at 5q13 since the 'pseudogenes' of *naip* and *smn* contain mutations which do not affect their coding ability highly indicating that they are functional. Polymorphisms which can distinguish the five or more *naip* loci in combination with rigorous genetic analysis will aid in elucidating the phenotype/genotype correlation.

NAIP shows significant homology with the baculoviral IAP genes Cp-iap, and Op-iap, two proteins isolated based on their ability to functionally complement the gene p35 of Autographa californica nucleur polyhedrosis virus (AcMNPV). p35 suppresses death of the host cell thus allowing the virus to replicate to a high titre. Mutations in p35 lead to the premature lysis of cells that demonstrates the hallmarks of apoptosis. The mechanism of action of p35 appears to be conserved as it can block cell death in mammalian cells ,

Drosophila and C. elegans (Rabizadeh et al, 1993; Sugimoto et al, 1994; Hay et al, 1995). The viral IAPs have been demonstrated to suppress apoptosis in Drosophila and mammalian cells (Hay et al, 1995; Duckett et a, 1996; Uren et al, 1996). A third iap Ac-iap (Birnbaum et al, 1994) was isolated based on its homology with Cp-iap and Op-iap however it its unable to block cell death. Cp-iap and Op-iap are 60% identical at the amino acid level however Ac-iap shares only 30% identity with these two iaps.

The BIR motifs which are the common structural feature of the iaps have been postulated to be involved in nucleic acid binding and metal ion co-ordination given the spacing of the cysteine and histidine residues (Birnbaum et al, 1994). It is intriguing that the viral iaps contain 2 BIR motifs while 3 are found in NAIP. Additionally these BIRs are separated by a variable number of amino acids which do not share any homology. Domain swapping experiments replacing the BIR-1 (N terminal BIR), both BIRs or both BIRs and the region upstream of the RING finger of Cp-iap with that of Ac-iap failed to rescue the wild type phenotype in SF-21 cells indicating the necessity of the BIR motifs in the suppression of apoptosis (Clem et al, 1994). With the exception of NAIP, the iaps contain a RING finger domain which is also found in a wide variety of proteins including several mammalian oncogenes such as; ret, mel-18,bmi, PML and herpes simplex virus E110, Drosophilia neu, Psc, Suz . The RING finger is thought to form two zinc-binding structures possibly involved in protein-protein or protein-DNA interaction (Schwabe and Klug, 1994). Swapping of the Cp-iap RING finger with the Op-iap RING finger

generated a protein that suppressed apoptosis. In contrast replacement of the RING finger of Cp-iap with that of Ac-iap resulted in a fusion protein that had no effect on apoptosis suggesting that the RING finger may also be required for the suppression of apoptosis.

In conclusion, we present the identification of a novel gene, *naip*, that maps to the genetically defined SMA locus. A variable and polymorphic number of internally deleted and truncated copies of *naip* are found within the 5q13 region. Homozygous deletions of the first two coding exons of *naip* are found in a significant number of SMA Type I chromosomes. A second candidate gene, *smn*, is deleted in 97 % of individuals with SMA regardless of the phenotype. Deletions in these two tightly linked genes lead to the SMA phenotype with the different nonallelic mutations presumably contributing to the manifestation of the three forms. NAIP is homologous to viral proteins that inhibit apoptosis indicating it may function in a similar manner. Mutations that abolish the anti-apoptotic ability of the protein would lead to the death of motor neurons, a phenomena that characterises SMA. SMN does not show any homology to any known proteins hence its function is unknown. Genetic and functional analysis will help elucidate the contribution of these two proteins to SMA .

CHAPTER IV:

NAIP INHIBITS CELL DEATH AND IS EXPRESSED IN MOTOR NEURONS OF THE SPINAL CORD.

INTRODUCTION

The loss of motor neurons in SMA, has led to suggestions that an inappropriate continuation or reactivation of normally occurring motor neuron apoptosis may underlie the disorder (Sarnat 1983, 1992; Oppenheim 1991). In keeping with this hypothesis, we have isolated a gene encoding the neuronal apoptosis inhibitor protein (NAIP) , which is homologous to baculoviral inhibitor of apoptosis proteins (IAP) (Clem and Miller, 1994a; Clem and Miller, 1994b) and is partially deleted in individuals with Type I SMA . Concurrently, a second candidate gene encoding survival motor neuron (SMN), which is contiguous with the *naip* locus on 5q13.1 was also reported (Lefebvre et al, 1995). *Smn* is deleted in a significant majority of SMA individuals, leaving unclear the precise role of the two genes in SMA causation. In an effort to delineate the role of NAIP in SMA pathogenesis, we have studied the effect of NAIP on cell death induced by different apoptotic triggers and determined the cellular distribution of the protein in human spinal cord. We report that overexpression of NAIP in Rat-1, HeLa and CHO cells suppresses apoptosis induced by menadione, tumor necrosis factor alpha (TNF-α) and serum withdrawal. Immunocytochemistry employing polyclonal antiserum raised against human NAIP demonstrates immunoreactivity in motor neurons. NAIP mediated inhibition of cell death and the immunolocalization of the protein to motor neurons are consistent with a

role for NAIP both in the naturally occurring programmed motor neuron death, and , when defective, in the pathogenesis of SMA. Moreover, NAIP appears to be the first member of a novel family of human genes with anti-apoptotic activity (Rothe et al, 1995; Liston et al, 1996).

MATERIALS AND METHODS:

Antibody production.

A cDNA encoding amino acids 254 to 664 was subcloned into the GST- fusion vector pGEX-KG. Rabbits were immunized with IPTG induced purified bacterial produced fusion protein (~ 100 μg) in complete Freunds adjuvant. Serum was pre-cleared with GST protein, ammonium sulfate precipitated to isolate the immunoglobulin fraction, dialysed against PBS and anti-NAIP immunoglobin (E1.0) purified with immobilised GST-NAIP fusion proteins.

Immunoblotting.

Cos cells were transfected by Lipofectace, collected after two days and dissociated in sample buffer (50mM Tris [pH6.8], 5% SDS, 5% β-mercaptoethanol, 10% glycerol). Total protein extracts from fresh frozen tissues were prepared by homogenizing with a Polytron homogenizer in lysis buffer (150 mM NaCl, 50 mM Tris-Cl [pH 8.0], 5% SDS), boiled for 5 min and sonicated. Proteins were resolved using 8 % polyacrylamide on

BioRad mini-Protean II apparatus and electrophoretically transferred to immobilon using BioRad TransBlot cells. Western blot analysis was performed using mouse anti-human myc monoclonal antibody (1:200) or rabbit anti-human NAIP (E1.0) (1:2000)polyclonal antibody.

Immunohistochemistry

For immunofluorescence, cells were grown on glass slides and fixed with formaldehyde for 10 minutes. Cells were subsequently incubated with anti-NAIP (1:200) or anti-myc (1:20) in PBS, 0.3% Triton X-100 for 1 hour at room temperature followed by incubation with secondary antisera, FITC-labeled donkey anti-rabbit immunoglobulin (Amersham), or biotinylated goat anti-mouse immunoglobulin (Amersham) and streptavidin Texas-Red (Amersham) at 37°C for 30 min. Human tissues were obtained at autopsy from infants that died of non-neurological causes and stored at -80°C. 14 μm cryostat sections were fixed in formaldehyde for 20 minutes, rinsed in PBS and incubated in blocking solution (2% horse serum, 2% casein, 2% BSA in PBS) for 15 min prior to overnight incubation with anti-NAIP antisera diluted in this blocking solution. CY3-labeled donkey anti-rabbit immunoglobulin (Sigma) was utilised as secondary antisera.

Adenovirus construction, purification and titre

For construction of the adenovirus, a 3.7 kb fragment of *naip* was cloned into the SwaI site of the adenovirus expression cosmid pAdex1CAwt . Orientation of the constructs was determined by restriction digest analysis. 293 cells (2 X 15 cm dishes) were infected with 3rd seed virus for 1 hr and then incubated for 3 days. Cells were harvested, sonicated and subjected to centrifugation (10k rpm, 10 min, 4°C) to collect the virus solution. Recombinant adenovirus was purified by cesium chloride gradient (25k rpm, 2 hr, 4°C, SW28 rotor), collected and subjected to a second purification on a cesium chloride gradient (35K rpm, 3 hr, 4°C, SW41 rotor). The virus band was collected and dialysed overnight against PBS-10% glycerol. The titre of the viruses were determined as follows: each recombinant adenovirus solution was diluted 10^{-1} with medium; 25µl of the diluted virus was aliquoted into lane 1 of a 96 well titre plate containing 50µl of media; 25µl of this diluted virus (3^{-1} x 10^{-1}) was transferred to lane 2; dilutions were continued to lane 11; 50µl of 293 cells from a 10 cm dish suspended in 6 ml was aliquoted into each well; cells were incubated for 2 weeks and fed 50 µl of media at day 3, day 6 and day 10; at day 14 the number of wells that show greater than 50% of cell death were counted. The titre was calculated according to the following formulas:

PFU (plaque forming unit) = $1/TCID_{50}$

$TCID_{50} = 10^{x}$

$X = \log a - (\Sigma\, n/N - 0.5) \times \log b$

a: dilution factor of first lane ($3^{-1} \times 10^{-4}$)
b: number of wells that showed . 50% of cell death
N: number of wells in the lane (8)
n: dilution fold to next lane (3)

To generate a 3.7 kb *naip* construct tagged with the myc epitope, MTG-SP3.7, a 2.5 kb Bsu36I/SalI fragment of *naip* cloned into Bluescript and Bsu36I/XhoI cut MTG-SE1.7, the expression vector pcDNA3 containing a 300 bp myc epitope with a 1.7 kb fragment of *naip* were ligated. This construct lacks the last exon of NAIP. The human Bcl-2 clone pB4 (ATCC) was digested with *EcoRI* and ligated into the *EcoRI* site of pcDNA3.

Cell death assays

HeLa, CHO and Rat-1 cells were transfected by lipofection (GIBCO BRL) with 8 μg DNA as described in the previous chapter. To generate pooled stable cell lines HeLa, CHO and Rat-1 cells were selected in 250 μg/ml, 400 μg/ml and 800 μg/ml G418 respectively resulting in resistant transformants. All cells were maintained in Eagles medium containing 10 % fetal calf serum. Three separate experiments for each assay were performed and each was done in triplicate. For each assay cells were plated at 5 x 10^4 ml-1 the day prior to the commencement of the experiment. The day of the assay cells were counted again and this value was taken as the starting number. All cell counts were performed in the same fashion; cells were trypsinised and live cells scored in 18 fields on a hemocytometer by trypan blue exclusion. For serum deprivation assays, cells were

washed 5 times in PBS and maintained in media with 0% fetal calf serum. Cell counts were performed at 24 and 48 hr. CHO or Rat-1 cells were treated with menadione for 1.5 hours, washed 5 times in PBS and subsequently maintained in normal media. CHO and Rat-1 cells (10 μM) were assayed at 3.5, 12 and 24 hr post treatment. Rat-1 cells exposed to 5μM menadione were assayed at 3.5, 24 and 36 hrs. HeLa cells were treated with 20 units ml^{-1} TNF in combination with 30 g ml-1 cyclohexamide for 17 hours and cell counts taken at 17 and 48 hours. Adenovirus infected cells were subjected to apoptotic insults 36 hours post infection. LacZ expression was confirmed histochemically by 5-bromo-4-chloro-3-indoyl-β-D-galactoside (X-gal) as described (Ellison et al, 1991). Transcription of *pian* was determined by in situ hybridization. Cells grown on slides were fixed in 4 % paraformaldehyde and probed with a sense oligonucleotide . 35 piocmoles of oligo was 3' end-labelled with digoxigenin-11-dUTP (Boehringer Mannheim) at 37°C for 5 min. Cells were prehybridized for 1 hour in 50% formamide, 4X SSC, 10% dextran sulfate, 1X Denharts, 5 mg yeast tRNA and 5 mg herring sperm prior to hybridization in the same solution overnight at 37-- C. Detection was accomplished using an anti-digoxigenin antibody conjugate (Boehringer Mannheim) (1:500) followed by incubation with colour solution (NBT, X-phosphate). The colour reaction was stopped after 4 hrs.

RESULTS

Assesment of anti-human NAIP antibody

A glutathione-S-transferase (GST)-NAIP fusion protein encoding amino acids 254 to 664 (exon 7 to exon 13) was utilised to obtain an affinity purified polyclonal antibody with binding specificity to NAIP. The ability of this antibody to bind NAIP was confirmed by two approaches: (1) immunofluoresence of COS-1 cells infected with the myc-tagged full length NAIP construct employing both the anti-NAIP and anti-Myc antibodies (Figure 4-1); and (2) Western blot analysis of protein extracts from these cells or cells infected with the adenovirus expressing NAIP (Figure 4-2). A protein of the expected molecular weight (147 kDa) was detected with both antibodies and their co-localisation demonstrated by immunofluouresence revealing a cytoplasmic distribution of NAIP.

Cell death assays

To analyse the effect of NAIP on apoptosis, expression plasmids alone (pcDNA3) or encoding a NAIP construct lacking exon 18 (SP 3.7) or Bcl-2 were transfected into CHO, Rat-1 and HeLa cells and stable pools were generated by selecting G418 resistant transformants after three weeks. Cell lines containing vector alone were utilised as a negative control and cell lines expressing the well documented inhibitor of apoptosis, bcl-2, were utilised as a positive control. In a second approach the effect of NAIP was investigated by infecting cells with adenovirus alone or adenovirus expressing NAIP. An antisense NAIP (*pian*) and LacZ virus were utilised as negative controls. NAIP and bcl-2 expressing pooled

Figure 4-1: Immunofluorescence of Cos-1 cells transfected with a myc-tagged NAIP expression construct. Cells were double labelled with the anti-NAIP (top panel) and anti-myc (bottom panel) antibodies.

Figure 4-2: Western blot analysis of NAIP expression detected by the anti-human NAIP (E1.0) antibody. Rat-1 cells were harvested for analysis 48 hr post infection with the adenovirus encoding NAIP with a myc tag or the antisense (*pian*) adenovirus. A prominent species of 147 kD is detected by both the NAIP antibody (left panel) and the myc antibody (right panel)

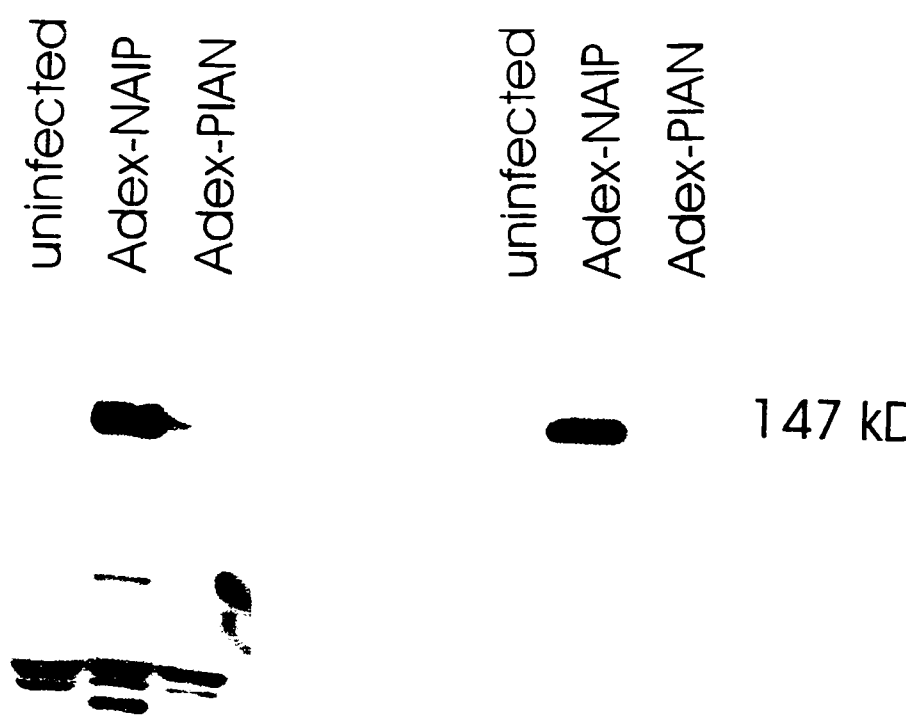
uninfected
Adex-NAIP
Adex-PIAN
uninfected
Adex-NAIP
Adex-PIAN
147 kD

Figure 4-3: Expression of NAIP in Rat-1, CHO and HeLa pooled stable lines and adenovirus infected cells analysed by Western blotting . (a-b) Cells infected with adenovirus encoding NAIP-myc detected by (a) mouse anti-myc monoclonal antibody or (b) a rabbit anti human NAIP polyclonal antibody. (c) Cells infected with adenovirus encoding NAIP detected by the NAIP polyclonal antibody. (d) Expression of myc-NAIP in representative pooled cell lines detected with antibodies against myc. (e-f) Rat-1 NAIP transfectants detected by e anti-myc and f anti-NAIP antibodies.

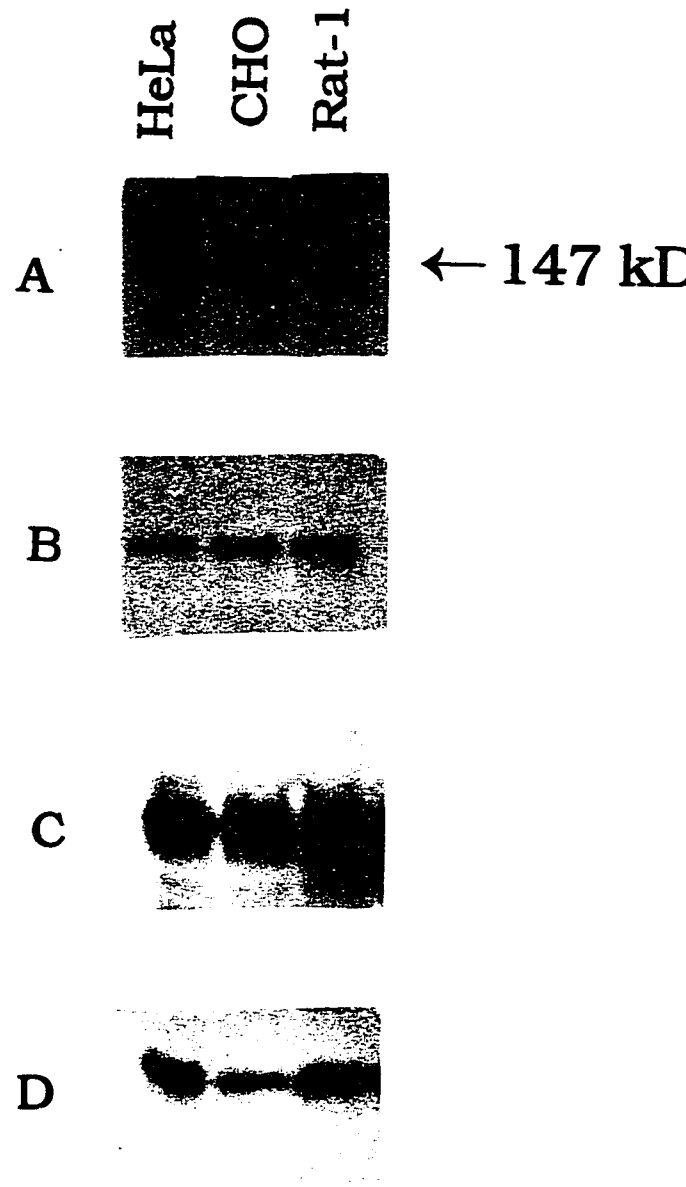
HeLa
CHO
Rat-1
A
← 147 kD
B
C
D

Figure 4-4: Expression of adenovirus expressing β-galactosidase and anti-sense NAIP. Rat-1 cells were infected with adenovirus expressing either β-galactosidase or anti-sense NAIP (*pian*) and expression determined 48 hr post-infection. Expression of β-galactosidase (top panel) was determined histochemically by addition of X-gal (see Materials and Methods). Expression of *pian* was determined by in situ hybridization with a DIG-labeled sense oligonucleotide.

clones and virally infected cells was confirmed by Western blotting and immunofluorescence using the affinity purified anti-NAIP polyclonal antibody (E1.0) or anti-Bcl-2 monoclonal antibody respectively (Figure 4-3). Cells infected with the adenovirus expressing *pian* were analysed by in situ and LacZ expressing cells were detected histochemically with X-gal (Figure 4-4).

Apoptosis was induced by serum deprivation in CHO cells and cell survival assayed at 24 and 48 hr. Cells infected with adenovirus alone, LacZ or antisense *naip* had survival rates of 48%, 50% and 45% respectively, observed at 48 hours (Fig. 4-5). In contrast, CHO cells infected with adenovirus expressing NAIP had a markedly enhanced resistance to serum deprivation induced apoptosis with a 30% increase in survival over the controls (78-83% survival). Cells expressing antisense NAIP had essentially no effect on the relative sensitivity of CHO cells to apoptosis. NAIP also induced survival in stably transfected CHO pools albeit slightly less then that seen in adenovirus infected cells; 44% of the vector transfectants and 65% of the NAIP transfectants survived at 48 hr (Fig. 4-5). Bcl-2 overexpressing cell lines provided protection from apoptosis that was slightly greater than that observed with the NAIP expressing cells.

We next sought to determine whether NAIP could rescue CHO and Rat-1 cells treated with the inducer of free radicals, menadione (Thor et al, 1983). Overexpression of NAIP in CHO cells treated with 20 μM menadione resulted in 20-30% increase in survival

Figure 4-5: Effect of NAIP on cell death induced by serum deprivation in CHO cells. Viability of CHO cells deprived of serum in adenovirus infected cells (top panel) and pooled transformants (bottom panel). Cell numbers were determined by trypan blue exclusion and calculated as a percentage of the starting number. All assays were performed in triplicate. Error bars represent the range of values obtained.

CHO-serum withdrawal

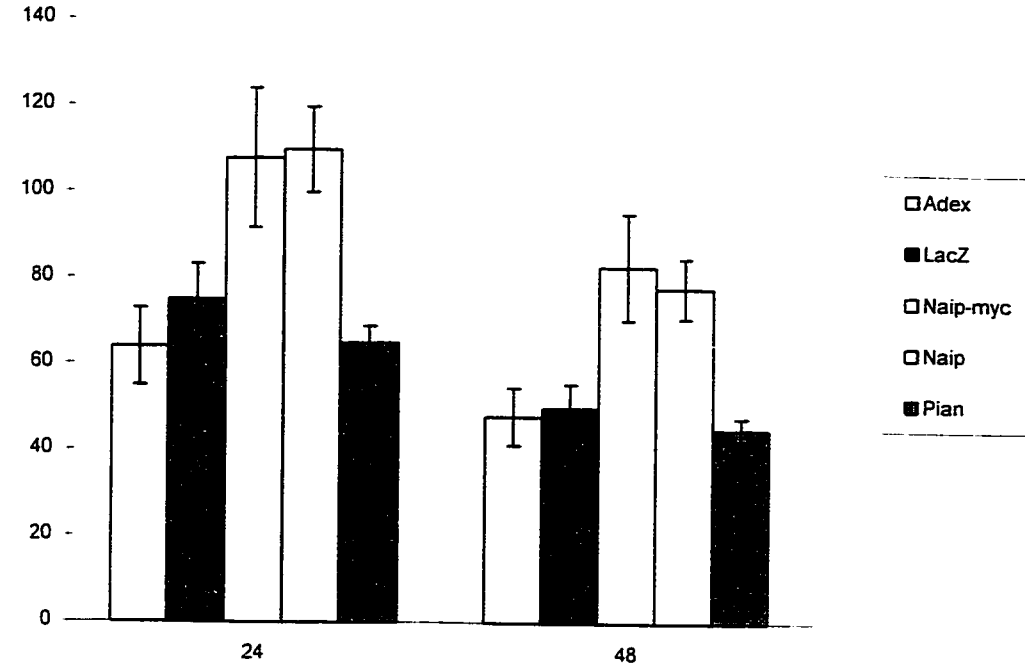

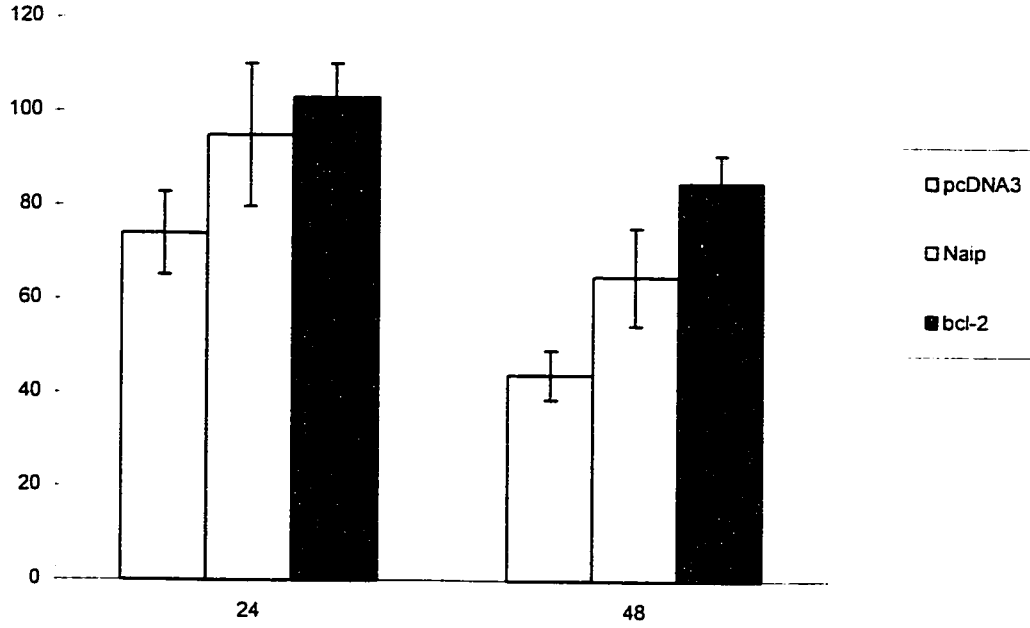

Figure 4-6: Effect of NAIP on cell death induced by treatment with menadione (20 μM) in CHO cells. Viability of CHO cells treated with menadione in adenovirus infected cells (top panel) and pooled transformants (bottom panel). Cell numbers were determined by trypan blue exclusion and calculated as a percentage of the starting number. All assays were performed in triplicate. Error bars represent the range of values obtained.

CHO -20uM menadione

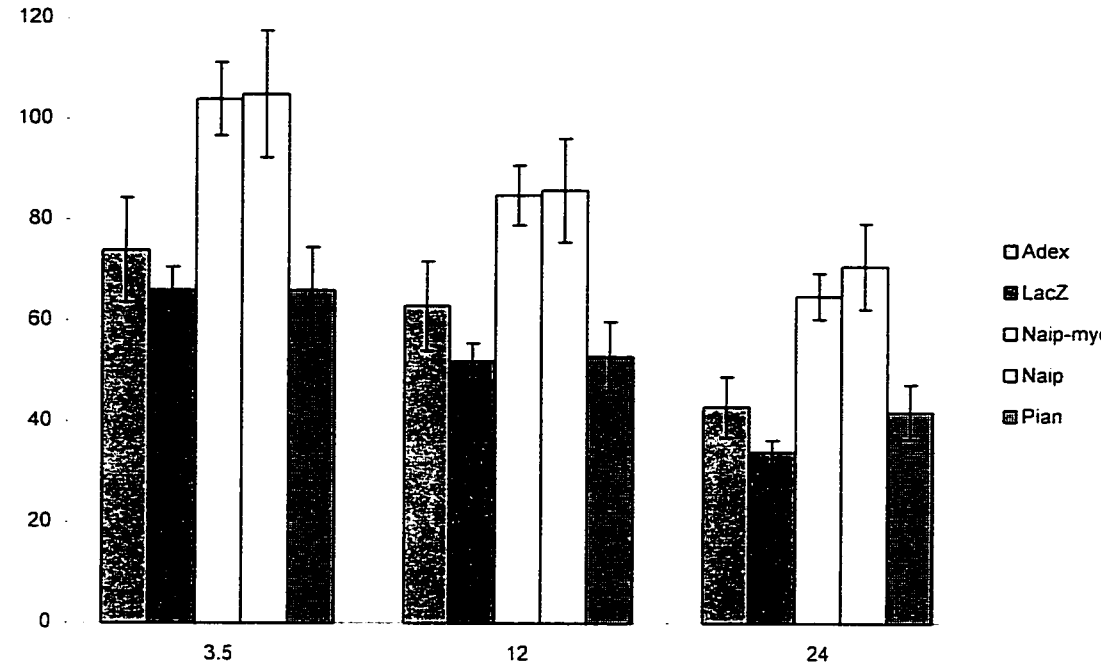

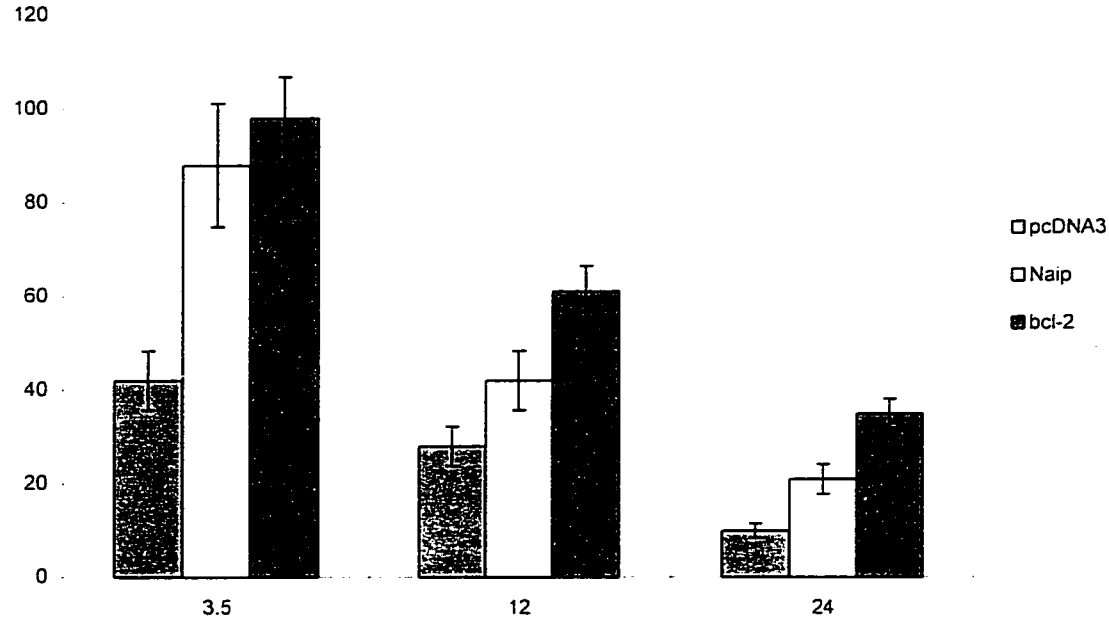

compared with controls after 24 hours in the adenovirus infected cells (Figure 4-6). In the pooled stable cell lines NAIP was partially protective with less than half of the cells surviving after 1 day and the increase in survival over controls reduced to 10%. Expression of Bcl-2 afforded greater protection from apoptosis compared with cells expressing NAIP however bcl-2 was also only partially protective. Overexpression of NAIP also protected menadione treated (10 μM) Rat-1 fibroblasts from undergoing cell death (Figure 4-7). Only 15% of cells infected with the LacZ expressing adenovirus were viable at 12 hours in contrast to 80% of NAIP infected cells. This increase in survival was also detected with the pooled Rat-1 NAIP transfectants. The protection form apoptosis appears to be dose dependent as greater cell survival was induced by NAIP overexpression at a lower menadione concentration (5 uM), with 98% of pooled NAIP transfectants and 33% of control transfectants viable at 24 hours (Figure 4-8). Consistent with the previous observations, the protection afforded by bcl-2 exceeded that afforded by NAIP. Furthermore Rat-1 cells were not rendered additionally sensitive to apoptosis by expression of PAIN.

We next assessed the protective effect of NAIP on cells exposed to the cytokine TNF-α. HeLa cells treated with TNF- and cyclohexamide were markedly protected from apoptosis upon infection of adenovirus expressing high levels of NAIP (139%) at 48 hours, an effect not observed with antisense NAIP (52%) (Figure 4-9). A similar effect was observed in pooled HeLa transformants. To confirm that cells surviving the

Figure 4-7: Effect of NAIP on cell death induced by treatment with menadione (10μM) in Rat-1 cells. Viability of Rat-1 cells treated with menadione in adenovirus infected cells (top panel) and pooled transformants (bottom panel). Cell numbers were determined by trypan blue exclusion and calculated as a percentage of the starting number. All assays were performed in triplicate. Error bars represent the range of values obtained.

Rat-1 -10uM Menadione

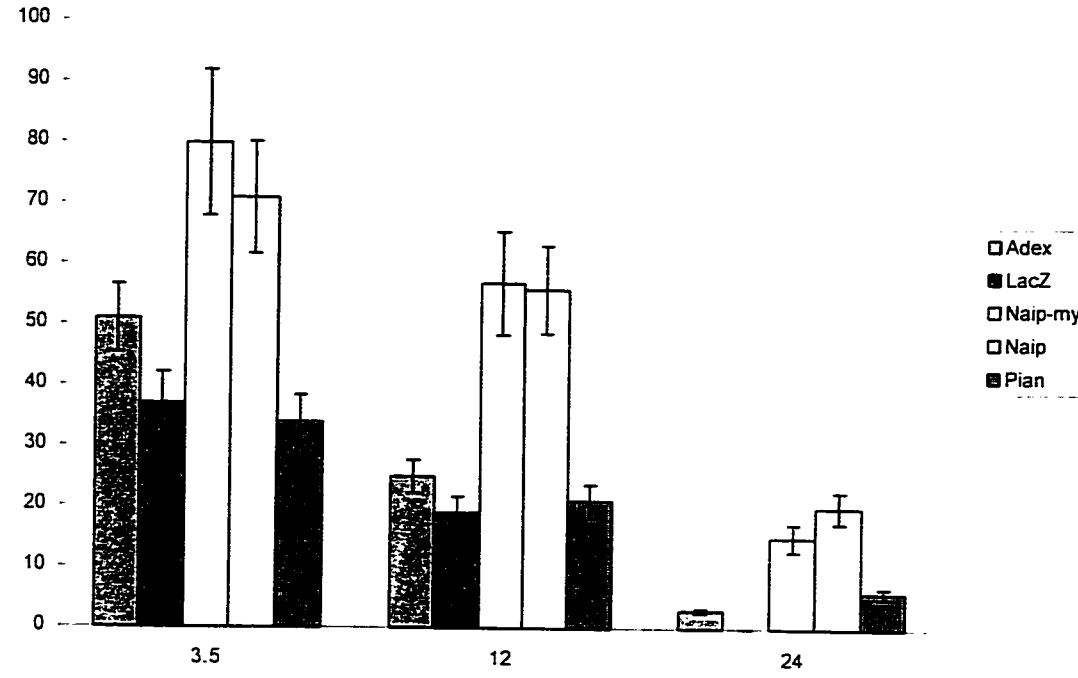

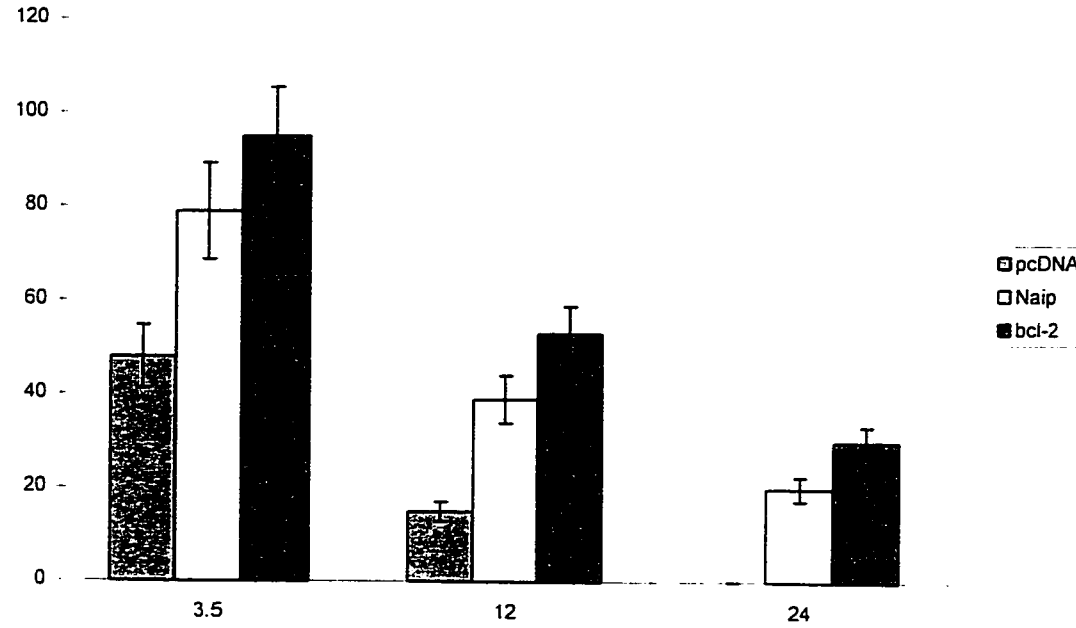

Figure 4-8: Effect of NAIP on cell death induced by treatment with menadione (5μM) in Rat-1 cells. Viability of Rat-1 cells treated with menadione in adenovirus infected cells (top panel) and pooled transformants (bottom panel). Cell numbers were determined by trypan blue exclusion and calculated as a percentage of the starting number. All assays were performed in triplicate. Error bars represent the range of values obtained.

Rat-1 - 5uM Menadione

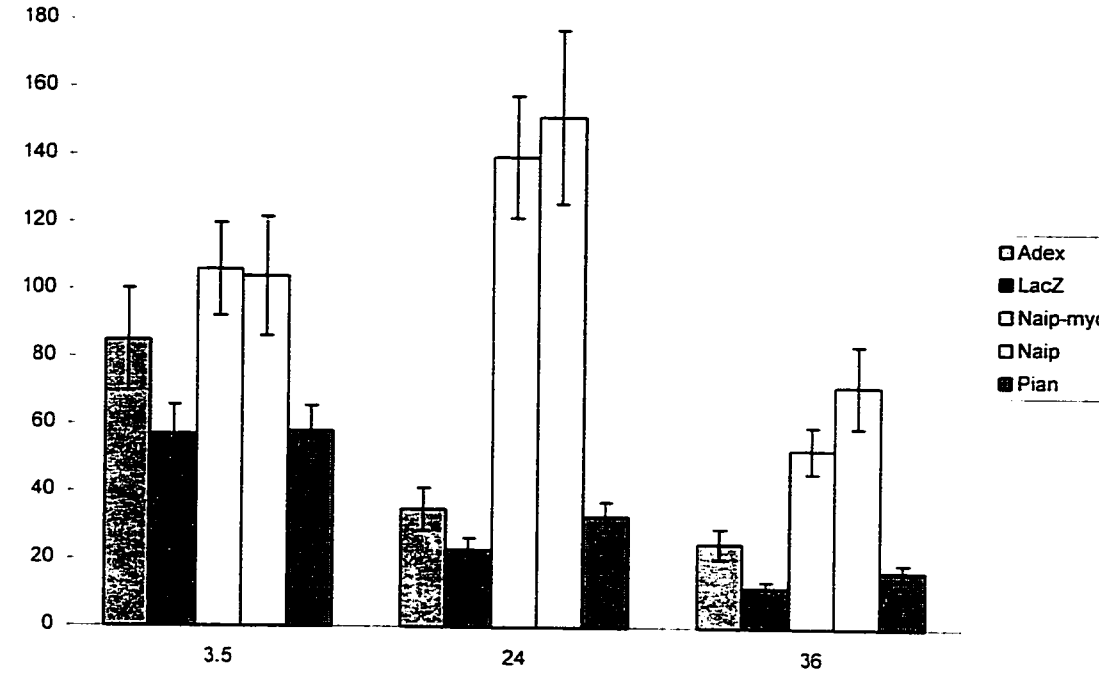

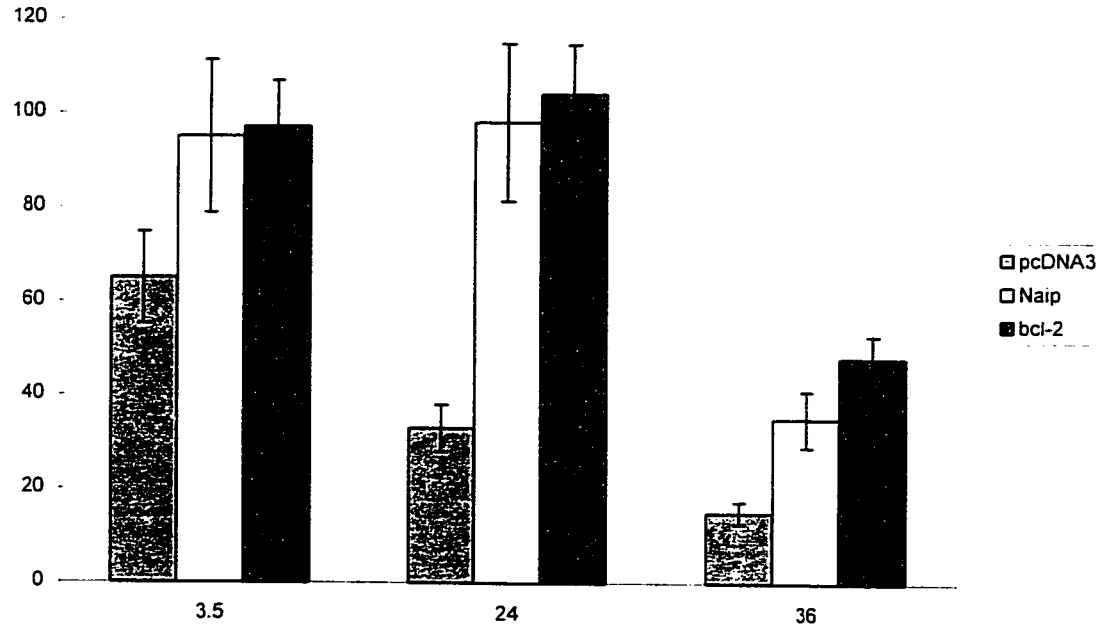

Figure 4-9: Effect of NAIP on cell death induced by treatment with TNF-α and cyclohexamide in HeLa cells. Viability of HeLa cells treated with TNFα in adenovirus infected cells (top panel) and pooled transformants (bottom panel). Cell numbers were determined by trypan blue exclusion and calculated as a percentage of the starting number. All assays were performed in triplicate. Error bars represent the range of values obtained.

HeLa -TNF-alpha/CHX

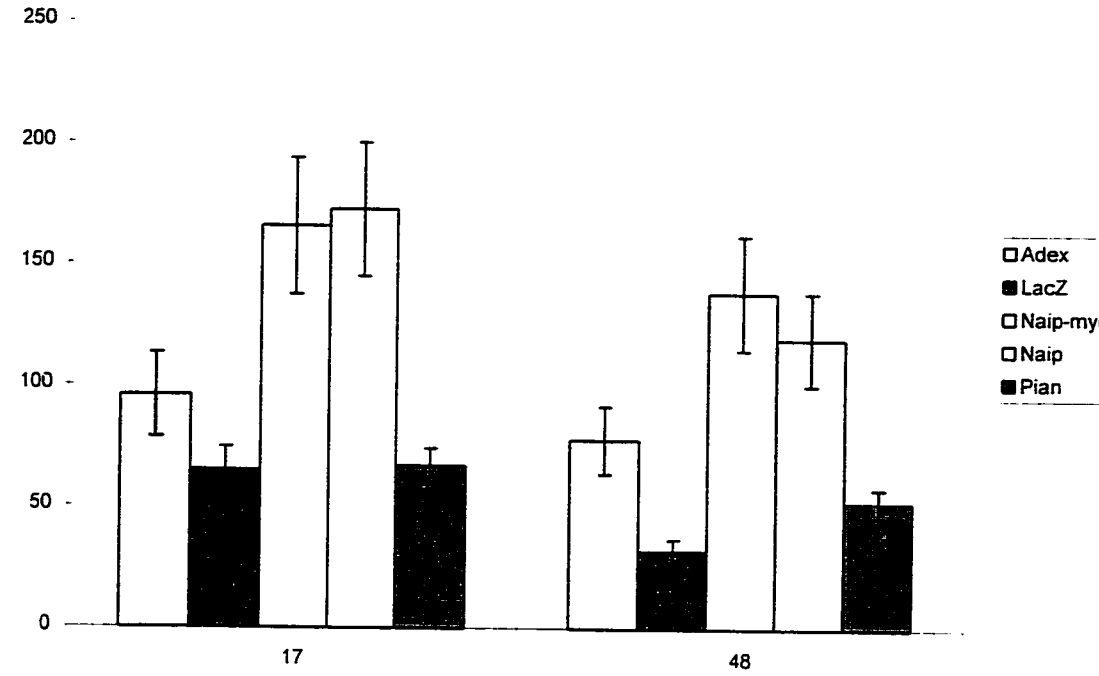

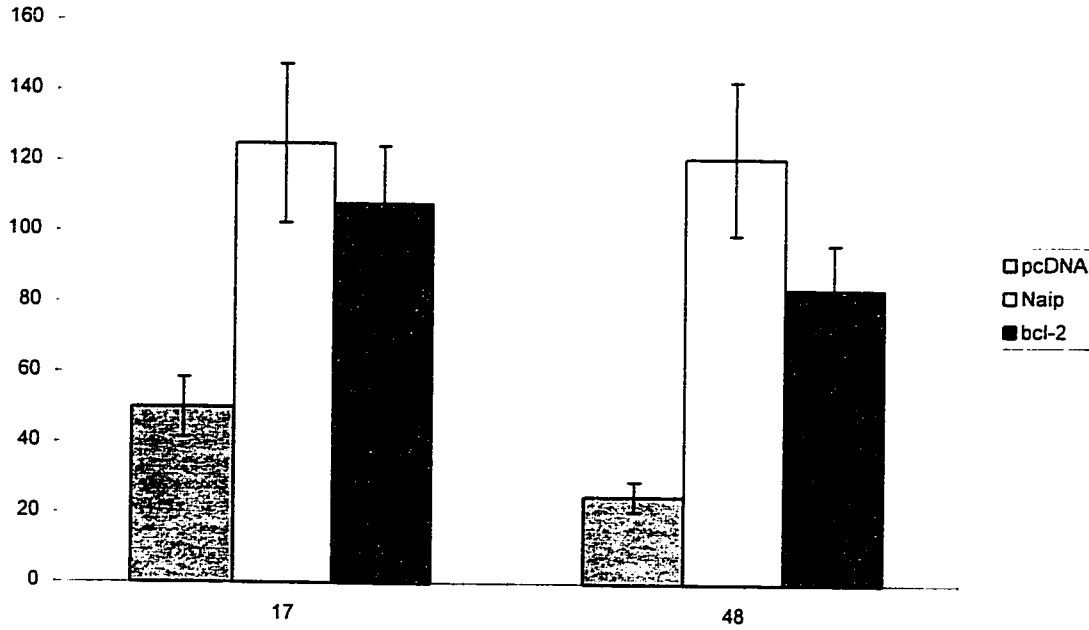

apoptotic agents expressed NAIP, immunofluorescence with anti-NAIP antisera was performed on a number of the cell death assays. An enrichment of NAIP expressing cells was observed, with no alteration of NAIP localisation noted . The NAIP conferred survival was consistently greater in infected cells than the effect documented in tranfectants for all assays, possibly reflecting a higher intracellular concentration of NAIP in the former case and/or the increased efficiency of infection compared with transfection. Furthermore the ability of bcl-2 to inhibit apoptosis induced by a variety of triggers is greater than that observed for NAIP.

Immunohistochemistry / Immunoblotting

We have previously demonstrated by reverse transcriptase PCR analysis that the *naip* transcript is present in human spinal cord . To more precisely define the cellular distribution of NAIP we utilised our anti-NAIP antisera which we had confirmed the ability of this antibody to detect NAIP. Sections of human spinal cord stained with anti-NAIP showed strong immunoreactivity in the cytoplasm of the anterior horn cells and intermediolateral neurons (Figure 4-10). These neurons were confirmed as cholinergic neurons by staining adjacent sections using acetlycholinesterase histochemistry. NAIP reactivity was also observed in dendrites and axons within these sections of the spinal cord. Anterior horn cells possess multiple dendrites and axons which exit via the ventral root while the intermediolateral neurons give rise to preganglionic sympathetic fibres that

Figure 4-10: Immunofluorescence analysis of human spinal cord tissue. *a* anterior horn cells *b*. intermediolateral neurons *c*. ventral roots. *d*. dorsal roots. NAIP immunoreactivity is observed in anterior horn cells , intermediolateral neurons and ventral roots. Immunoreactivity is not observed in the dorsal roots carrying the sensory axons.

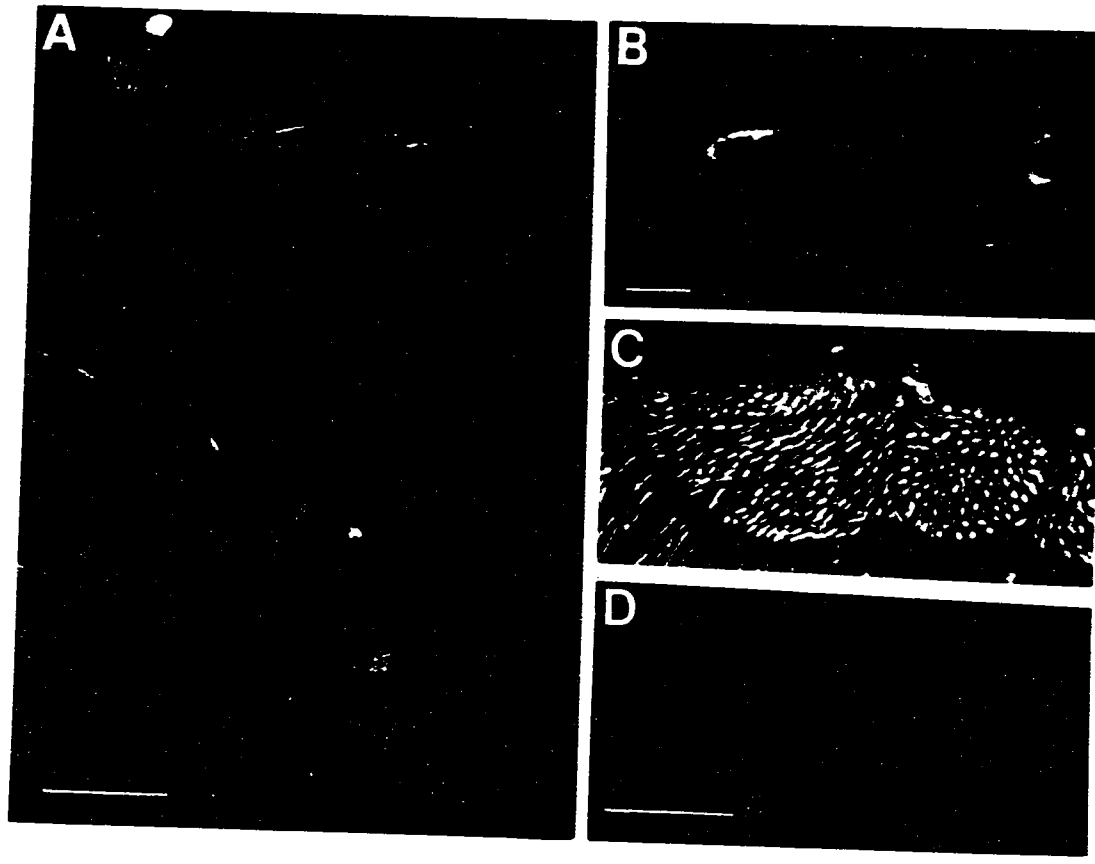
A
B
C
D

Figure 4-11: Western blot analysis of tissue protein extracts with anti-human NAIP antibody. A species of the predicted size (155 kD) is observed in spinal cord, sciatic nerve and muscle

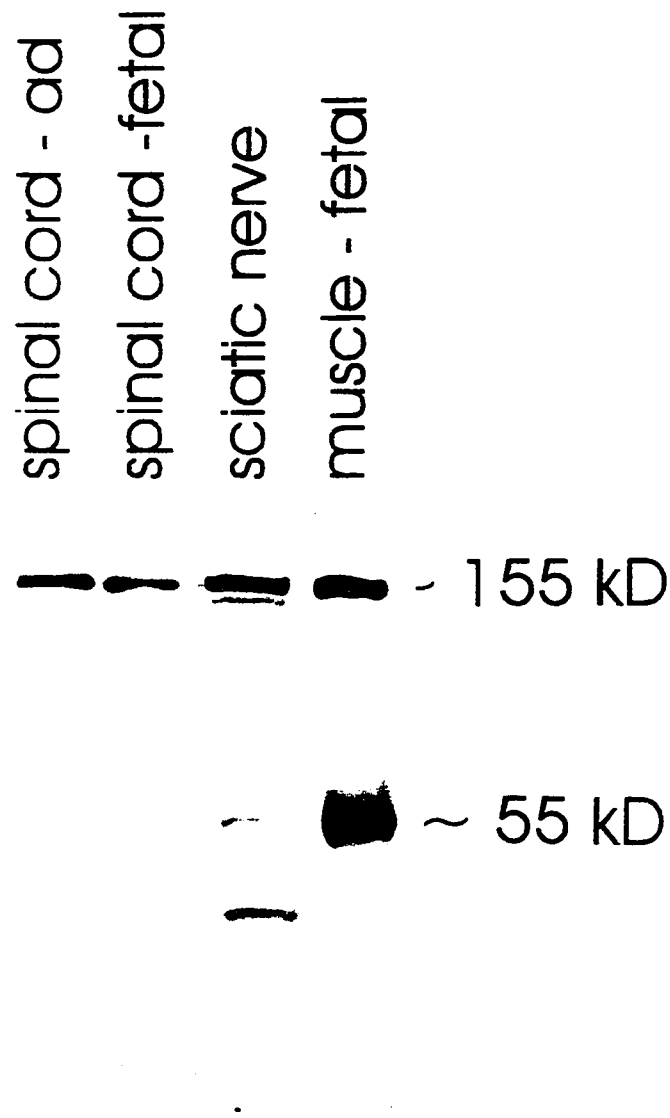
spinal cord - ad
spinal cord -fetal
sciatic nerve
muscle - fetal
155 kD
~ 55 kD

emerge as well via the ventral roots. Consistent with the motor neuron staining, NAIP reactivity was observed in the ventral roots which contain motor axons but not the dorsal roots comprised of sensory axons (Figure 4-10). Preabsorbtion of anti-NAIP with the NAIP-GST immunogen prior to tissue analysis abolished the immunoreactivity demonstrating the ability of the immunogen to compete with the tissue antigen recognised.

To confirm our immunohistochemical results, human spinal cord protein extracts were immunoblotted with anti-NAIP. A prominent species of 155 kDa was detected (Figure 4-11), in agreement with the predicted molecular weight, substantiating the immunoreactivity we observed in the spinal cord. The 155 kDa species was also observed in sciatic nerve and muscle tissue protein extracts. A predominant band of approximately 55 kd was also observed in muscle however wheather this band is an isoform of NAIP or a cross-reactive protein is not known at present.

The observation of NAIP motor neuron staining correlates well with the depletion of this cell type in individuals affected with SMA. However, the presence of NAIP in intermediolateral neurons which are not reported to be affected in SMA, implies heterogeneity in the apoptotic pathways between the two classes of neurons.

DISCUSSION

The depletion of spinal motor neurons observed in spinal muscular atrophy has been proposed to occur result from continuation or reactivation of the naturally occurring apoptosis of neurons that occurs during development (Sarnat, 1982, 1984). The isolation of *naip* as a candidate gene for SMA strongly supports this model. However , the identification of a second candidate gene, SMN that is deleted in a high proportion of individuals with SMA has left the contribution of the two genes to the SMA phenotype unclear. We confirm that NAIP functions to inhibit apoptosis induced by serum deprivation, menadione and TNF-α. The ability of NAIP to block cell death induced by a variety of stimuli suggests that NAIP may act at a common point to multiple cell death signalling pathways. Furthermore the recent demonstration that the baculovirus iaps can prevent apoptosis in mammalian cells suggests that these proteins act upon an evolutionarily conserved cell death pathway (Duckett et al, in press). We have also shown that NAIP is expressed in the cytoplasm of spinal cord motor neurons, those cells which degenerate in SMA. The intermediolateral neurons of the spinal cord also express NAIP however these cells have not been documented to die in SMA. The cell death cascade may differ between cell types which is supported by evidence that bcl-2 is capable of protecting sensory neurons from deprivation of nerve growth factor or brain derived

Figure 4-12: Domain structure of the IAP family. The position of the BIR motifs are shown by stipled boxes. The ring finger domain that is absent in NAIP is represented by black boxes. The proteins are drawn to scale except for the C-terminus of NAIP.

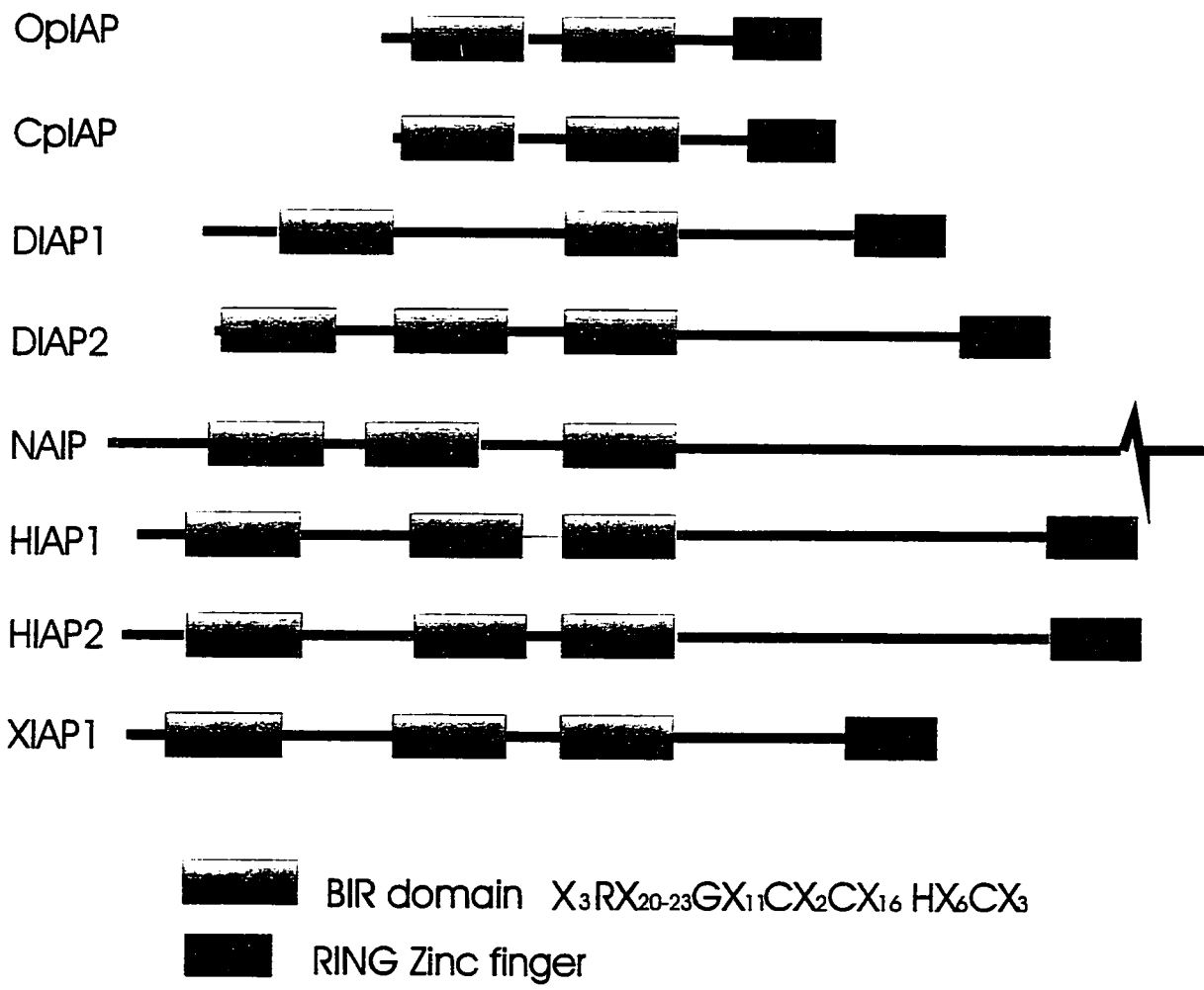
OpIAP
CpIAP
DIAP1
DIAP2
NAIP
HIAP1
HIAP2
XIAP1
BIR domain X3RX20-23GX11CX2CX16 HX6CX3
RING Zinc finger

nerve growth factor but not parasympathetic ciliary neurons from deprivation of ciliary neurotrophic factor (Allsop et al, 1993). Taken together, these data are in keeping with a possible role for *naip*, when mutated, in SMA pathogenesis.

Subsequent to the isolation of *naip* three additional human (*hiap-1/c-iap2*, *hiap-2/ciap-1*, *xiap*) and two *Drosophila* iaps (*diap-1*, *diap-2*) have been identified (Figure 4-12) (Liston et al, 1996; Rothe et al, 1995; Hay et al, 1995) . Liston and co-workers isolated these novel iaps based on their homology to the baculovirus iaps and have shown that all three are capable of inhibiting apoptosis induced by menadione and serum withdrawal. The *Drosophila* homologues DIAP-1 and DIAP-2 have also been shown to block apoptosis in the developing eye of *Drosophila* (Hay et al, 1995). HIAP-1, HIAP-2 and XIAP are similar to NAIP in that they contain three BIR domains however they also contain the RING finger which is present in the viral iaps but lacking in NAIP. DIAP-1 and DIAP-2 both contain the RING finger however interestingly DIAP-1 has two BIR domains while DIAP-2 contains three BIRs. Further the RING finger of diap-1 shows greater sequence similarity to the viral iaps than the human iaps while the converse is true for DIAP-2.

In *Drosophila* the genes reaper (rpr) and head involution defective (hid) control the programmed cell death which occurs normally during embryogenesis (White et al, 1994). Both gene products induce apoptosis hence transgenic flies which overexpress rpr

in the eye result in a small eyed phenotype. By crossing these flies with others containing chromosomal deletions , Hay and co-workers were able to screen for mutations which either enhance or suppress this phenotype thereby identifying genes which act as cell death inhibitors or activators respectively. One which enhanced rpr dependent death was found to result from lethal mutations in thread (th) which encodes a homolog of the iaps (diap-1). Diap-2 was identified in the database by virtue of its homology with DIAP-1.

There are two waves of programmed cell death which serve to rid of excess cells in the developing *Drosophilia* eye. The viral protein p35 can completely block this apoptosis while DIAP-1 and DIAP-2 were shown to partially inhibit this cell death. Additionally DIAP-1 and 2 may partially block apoptosis induced by overexpression of hid or completely block apoptosis induced by rpr in the eye. The fact that NAIP demonstrates anti-apoptotic activity despite lacking the RING zinc finger common to all other iaps, indicates that this domain is not essential for all IAP mediated mammalian apoptosis inhibition. Conversely, the fact that the BIR motif is common to the six baculoviral and human protein iaps which have been shown to inhibit cell death is consistent with a central role for this motif in mediating cellular protection. In support of this model, a diap-1 construct which lacks the RING finger is capable of suppressing apoptosis induced by expression of rpr, hid or X-ray irradiation and moreover shows an increase in survival compared to full length diap-1 (Hay et al, 1995). Moreover, extra cell death was observed by just the RING finger alone. Similar results were obtained when the ability of hiap2 (c-

iap1) with and without its RING finger to inhibit apoptosis in this system was examined (Hay et al, 1995). These data would support a role for the RING finger as a negative regulator of BIR induced inhibition of cell death. Due to the fact that NAIP lacks a RING finger it may have an increased ability to counter apoptosis. However, the role of the C-terminus of NAIP is not known and may act as a negative regulator itself. Death assays with deleted forms of NAIP will help elucidate these functions.

Hiap-1 and 2 were identified by one group based on their ability to associate with the tumor necrosis factor II receptor (TNFRII) via a TNF receptor associated factor 1 and 2 (TRAF1-TRAF2) heterocomplex (Rothe et al, 1995). Although the site and mechanism of NAIP's anti-apoptotic effect is unknown it is noteworthy that Hiap1 and hiap2 are implicated in the TNF signalling pathway and that NAIP is able to protect cells from TNFα induced cell death. The TRAFs were originally identified based on their interaction with a C-terminal region within the cytoplasmic domain of the tumor necrosis factor receptor II (TNFRII) responsible for signal transduction (Rothe et al, 1994). TNFRII is a member of the TNF/nerve growth factor (NGF) receptor superfamily which includes: p55 TNFRI, p75 TNFRII, CD27, CD30, CD40, OX40, FAS/APO-I and NFR. Binding of these receptors by their ligands induces receptor oligomerization that initiates a cascade of downstream signalling events (Tartaglia and Goeddel, 1992). Stimulation of TNFRII with agonist antibodies induces enhanced T-cell and human mononuclear cell proliferation, causes granulocyte-macrophage colony-stimulating factor (GM-CSF) secretion, has been

implicated in early haematopoiesis, and activates the transcription factor nucleur factor-κB (NF-κB) (Lenardo and Baltimore, 1989; Hohman et al, 1990; Tartaglia et al, 1991; Gehr et al, 1992; Vandenabeele et al, 1992; Tartaglia et al, 1993 and Jacobsen et al, 1994). TRAF1 and 2 interact with the signalling domain of TNFR2 in a heterodimeric complex via TRAF2. A third TRAF protein- TRAF3 (CD40 bp, CRAF1 or LAP-1) has been identified which interacts with the cytoplasmic domain of CD40 and the EBV protein, latent infection membrane protein (LMP-1) in a heterodimeric complex via TRAF2(Hu et al, 1994; Cheng et al, 1995; Mosialos et al, 1995; Sato et al, 1995; Rothe et al, 1995).. All three TRAFs contain a TRAF-N (putative coiled-coiled) domain which binds the iaps and a TRAF-C domain at their C-terminus which binds the receptor. Additionally, TRAF2 and TRAF3 contain a string of zinc fingers and a RING finger domain. CD40 and TNFRII activation of NF-κB has been shown to be induced by overexpressing TRAF2 but not TRAF1 or TRAF3 (Rothe et al, 1995). Hiap 1 and hiap2 (and possibly naip or xiap) may act as downstream regulators in these signalling pathways although activation of TNFRII is not usually associated with induction of the apoptotic pathway.

Transduction of apoptotic signals is associated with TNFRI activation. Additionally TNFRI plays a role in host defence and promotes antiviral activity, fibroblast proliferation and activation of the transcrition factor, NF-κB (Tartaglia et al, 1991; Espevik et al, 1989; Wong et al, 1992 and Pfeffer et al, 1993). A region of similarity found in the cytoplasmic domains of TNFRI and FAS termed the death domain is both necessary

and sufficient for transduction of cytotoxic signals, antiviral activity and activation of NF-κB (Tartaglia et al, 1993). This 80 amino acid region near the C-terminus of these receptors is involved in protein-protein interactions with other death domain containing proteins such as RIP (Seed et al, 1995), FADD (Chinnaiyan et al, 1995) and TRADD (Rothe et al, 1995). RIP and FADD associate with Fas while TRADD associates. While overexpression of RIP, FADD or TRADD results in apoptosis, overexpression of TRADD also leads to activation of NF-κB (Rothe et al, 1995). The two signalling pathways were shown to be distinct by the observation that apoptosis induced by TRADD could be suppressed by the protease inhibitor, crmA, while the activation of NF-κB was not. Surprisingly TRADD interacts with both FADD and TRAF2 (Hsu et al, 1996). Deletion analysis demonstrated that the TRADD-TRAF2 interaction occurred at the N-terminus of TRADD and the TRAF-C domain of TRAF2. TRADD and FADD interact via the death domain of TRADD, the same region which associates with TNFRI. Moreover the TRAF2 associates indirectly with TNFR1 via TRADD to activate NF-κB however TNFRII-TRADD-TRAF2 complexes have not been observed. This is thought to occur through TRADD and TNFRII interaction with and competition for the same site within TRAF. Although haip1 and hiap2 interact with TRAF2 they are unable to activate NF-κB hence their role in these signalling pathways is as yet unknown. The ability of NAIP to counter apoptosis induced by TNF-α suggests that it may inhibit transduction of the apoptotic signal in these pathways, yet its role remains to be elucidated.

The nerve growth factor receptor (NGF) p75, is a member of the TNF receptor superfamily. Analogous to tha case with TNFRI, binding of ligand (NGF) to p75 activates the sphingomylenase pathway (Dobrowsky et al, 1994; Tartaglia et al, 1993; Tartaglia and Goeddel, 1992). Both receptors activate cell death, however, in contrast to TNFRI, p75 activates rapid degeneration and apoptosis of neurons when unbound. Recently, the selective binding of NGF to p75 has been shown to activate NF-κB (Carter et al, 1996). Slight sequence homology has been detected between the cytoplasmic domain of p75 and TNFRI and it has been proposed that p75 has a death domain (Dale Bredesen, personal communication). At present , proteins which associate with this domain of p75 have not been identified however it is possible that like TNFRI, death domain proteins may be involved in p75 signalling. Just as the iaps have been shown to be a component of the TNF signalling cascade, one could postulate that NAIP may function downstream in the transduction pathway of NGF.

CrmA, the pox virus gene product, is a specific inhibitor of ICE, a cysteine protease involved in IL-1β processing (Thornberry et al, 1992; Ray et al, 1992). The observation that apoptosis induced by TNFRI or Fas antigen is blocked by CrmA supplied the first evidence of the involvement of ICE or an ICE-like protease in these apoptotic transduction pathways (Tewari and Dixit, 1995). Further evidence demonstrates that binding of TNFα to its receptor results in activation of the ICE family and that TRADD or FADD mediated cell death is inhibited by CrmA (Miura et al, 1993; Gargliardini et al,

1994). Given that naip inhibits cell death induced by TNFα , it may be that NAIP functions at this level of the apoptotic pathway, possibly by interacting with ICE or ICE like proteases. This is supported by the observation that p35, which can be functionally complemented by the viral iaps, inhibits death induced by TNFα by acting as a substrate for and consequently an inhibitor of the ICE proteases (Bump et al, 1995; Xue et al, 1995). In additional work, the RING zinc finger of the iaps was shown to act potentially as a negative regulator of apoptotic suppression suggesting that cleavage of the iaps might result in a protein lacking the RING finger with an increased ability to prevent apoptosis (Hay et al, 1995).

Several lines of evidence suggest that proteases may participate in neuronal death. Microinjection of CrmA into dorsal root ganglion neurons inhibits apoptosis resulting from nerve growth factor (NGF) deprivation (Gagliardini et al, 1994). In addition, in a chick tissue culture model system, the apoptosis of motoneurons which occurs as the result of trophic factor deprivation (Oppenheim et al, 1990; Milligan et al, 1994),can be partially blocked by peptide inhibitors of ICE (Milligan et al, 1995). Furthermore, treatment of chick embryos with these peptide inhibitors decreases the naturally occurring cell death reflected in the reduction of pyknotic cells in the lumbar region of the spinal cord. However, cervical spinal cord motoneuron death induced by limb bud removal could not be blocked. This could be explained if the components activated by target deprivation and naturally occurring cell death are distinct or diverge. Serine protease have

also been implicated in the fate of neuronal cells during development. The serine protease inhibitor, protease nexin I (PNI), rescues spinal motor neurons both during the naturally occurring cell death in the chick and after neonatal axotomy in the mouse (Houenou et al, 1995). Furthermore, the serine protease thrombin, induces death of neurons in vitro (Vaughan et al, 1994). The reduction of PNI in brains of patients with Alzheimer disease (Wagner et al, 1989) would be consistent with the hypothesis that serine proteases play a role in neurodegenerative disorders.

In conclusion, we have documented an anti-apoptotic effect of NAIP on mammalian cells and its distribution in the motor neuron. These findings are in keeping with the protein acting as a negative regulator of motor neuron apoptosis and, when deficient or absent ,contributing to the SMA phenotype. Such a model leaves open the question of *smn*'s involvement in SMA since any detectable anti-apoptotic effect with the SMN protein has not been demonstrated (Liston et al, 1996). Nonetheless, the genetic evidence for the gene's involvement in SMA is strong. SMN and NAIP may interact perhaps in a manner which is analogous to BAG-1 and bcl-2 where BAG-1 enhances the ability of bcl-2 to inhibit apoptosis (Sato et al, 1995).

CONCLUSIONS

The childhood onset SMAs are a group of autosomal recessive neurodegenerative disorders which manifest as symmetrical weakness and wasting of voluntary muscle. The pathological change that typifies the disorder is the loss of motor neurons at all levels of the spinal cord. The three forms of the disorder are classified by age of onset, severity of the disorder and lifespan (Dubowitz et al, 1978; 1991; Pearn, 1980). The onset of the most severe form, Type I is in the first six months and these children are never able to sit unaided with death normally ensuing within the first few years of life due to respiratory difficulties. Type II SMA is of intermediate severity and children are able to sit unsupported but are unable to walk unaided. The mildest form of SMA is Type III, with the age of onset in the late teens to adulthood and manifestations quite mild. The SMAs together affect 1 in 10000 live births with an overall carrier frequency of 1 in 80-100 (Emery, 1991).

The paucity of motor neurons observed in SMA, coupled with the morphological characteristics of these neurons, has led to suggestions that an apoptotic mechanism underlies the disorder (Sarnat, 1984). Cell death is a feature of the developing nervous system where approximately 50% of neurons, die during its maturation (Hamburger and Oppenheim, 1982; Oppenheim, 1991). An increasing amount of evidence supports a

model where neuronal cells, similar to other cell types, utilise the apoptotic pathway to die.

In 1990 the SMAs were genetically mapped to an approximate 10 Mb region of 5q11.2-q13.3 by linkage analysis (Brustowicz et al, 1990; Gilliam et al, 1990; Melki et al, 1990). The localisation of all three forms to 5q11.2-13.3 suggested the involvement of a single recessive gene or of several tightly linked genes. The identification of recombination events narrowed the SMA region to an interval defined centromerically by the marker D5S435 (Soares et al, 1993; Wirth et al, 1993) and telomerically by the marker D5S112 (Lien et al, 1991; MacKenzie et al, 1993; Wirth et al, 1994). More recently this region has been refined to the interval distal to CMS-1 (Yaraghi et al, 1995; van der Steege et al, 1995) and proximal to D5S557 (Francis et al, 1993). Although there are no obvious biochemical defects to aid in the elucidation of the gene, the localisation of SMA to a specific chromosomal region allowed the gene to be identified by positional cloning techniques.

We have assembled a physical map of contiguous YAC clones , spanning 3 Mb, encompassing the genetically defined SMA interval. The complex genomic structure of the 5q11.2-q13.3 region was revealed in the process. Repetitive sequences that include microsatellite markers and transcribed sequences are all represented multiple times in the 5q11.2-13.3 interval. In addition, chromosome 5 specific repetitive sequences that

additionally map outside of this region, to 5p and 5q33, have been identified (Francis et al, 1993; Kleyn et al, 1993, Theodoiou et al, 1994; Carpten et al, 1994). These structural features have greatly complicated the ordering of loci within the 5q11.2-q13.3 region and have led to discrepancies between groups in the estimate of the D5S435-SMA-D5S537 genetic interval. Estimates from 400 kb to 2.8 Mb have been proposed (Francis et al, 1993; Kleyn et al, 1993; Carpten et al, 1994). Based on our YAC contig, derived from three libraries, coupled with confirmation by long range restriction mapping, we estimate this genetic interval to be 1.4 Mb (Roy et al, 1995).

A higher resolution map was established by the assembly of a 500 kb PAC and a 210 kb cosmid contiguous array. These contigs aided in substantiating the order of loci at 5q13. The microsatellite marker, CATT-1, consisting of 5 subloci, was shown to have allelic association with Type I SMA in the American and Canadian populations (Burghes et al, 1994). More specifically the CATT-40G1 sublocus was shown to be in significant linkage disequilibrium with Type I SMA (Mclean et al, 1994). To define the region within the genetically defined SMA region most likely to contain the SMA gene, each sublocus was mapped to our PAC and cosmid contigs. All of the subloci were shown to map within a 140 kb interval, a region encompassed by both our PAC and cosmid contiguous arrays. A recombination event identified in one of our Canadian families defined the proximal boundary of the SMA region as a sublocus of the multicopy marker CMS-1 (Yaraghi et al, 1995; van der Steege et al, 1995). This sublocus was mapped to one of the

PAC clones in a region contiguous with the CATT loci which demonstrated significant allelic association with the disorder. Furthermore a second multicopy marker, Ag-1, also shown to be in linkage disequlibrium with Type I SMA (DiDonato et al, 1994)was shown to be contiguous with the CATT-1 loci based on our physical map. These data strongly suggested that the SMA gene was contained within, or in close proximity to our cosmid and PAC contiguous arrays.

An exon trapping system was then utilised to isolate coding sequences from the PAC contiguous array. An emphasis was placed on the PAC clone 125D9 based on its inclusion of the markers showing significant allelic association with the disorder and the inclusion of the genetically defined proximal SMA boundary. This approach, in addition to the screening of cDNA libraries with this PAC clone, culminated in the identification of the SMA candidate gene, the neuronal apoptosis inhibitory protein (NAIP).

Analysis of the *naip* genomic organisation in our PAC clones revealed multiple *naip* loci, characteristic of other loci mapping to the 5q11.2-q13.3 region. These loci include in addition to full length forms, internally deleted and truncated forms that are found in a polymorphic number in the general population. The first two coding exons of *naip* were shown to be homozygously deleted in 45 % of individuals with Type I SMA and 18% of Type II and II SMA individuals. Although the multiple loci have confounded mutational analysis, it appears that a reduction of *naip* loci including the internally deleted, truncated

and full length loci contributes to the SMA phenotype. The multiple copies of NAIP and the repetitive nature of the 5q13 region, suggests that unequal crossing over between the various copies may result in deletion or addition of *naip* loci. This phenomenon would contribute to the instability of the region.

NAIP has homology to two baculoviral inhibitor of apoptosis proteins, Cp-iap and Op-iap. These proteins function to suppress cell death of the host cell allowing the virus to replicate to a high titre (Clem et al, 1991; Clem and Miller, 1994). These viral proteins prevent apoptosis upon induction with other apoptotic stimuli suggesting that they block cell death at a step which is conserved in the apoptotic cascade (Clem and Miller, 1994). The mechanism of action of the iaps is however, unknown at present. The common structural domain of the IAPs is the BIR motif, suggesting that it may be the domain that functions to suppress apoptosis. Although two such motifs are found in the viral IAPs, three are found in NAIP. Cp-iap and Op-iap have a RING zinc finger at their carboxy terminus that is absent in NAIP. However, the homology of NAIP with these viral iaps strongly suggests that it also functions in the apoptotic pathway to inhibit cell death. This function would be in keeping with the model of SMA that proposes that the motor neuron death characteristic of SMA results from the inappropriate continuation or reactivation of motor neuron apoptosis.

Concurrent with the isolation of *naip* a second candidate gene, the survival motor neuron gene (SMN) was identified that also maps to 5q13 and is mutated in a significant majority of individuals with SMA (Lefevbre et al, 1995). *Smn* was reported to be present in two copies at 5q13 and one of these copies (the telomeric form) is deleted in 97 % of individuals with SMA (Lefevbre et al, 1995). SMN does not shown any homology to any known proteins therefore no indication to its function can be deduced. *Smn* is contiguous with *naip* at 5q13 and analogous to the situation with *naip*, is found in a polymorphic number between individuals.

The high proportion of individuals with SMA that are deleted for *smn*, supports a model in which *smn* is necessary for the SMA phenotype. There is however no correlation between *smn* genotype and SMA phenotype. Although the homozygous deletion of *naip* exons 5 and 6 is less frequent in individuals with SMA than that observed for *smn*, mutations in *naip* are observed predominantly in individuals with Type I SMA. This data suggests that deletions of *smn* are necessary for SMA with *naip* possibly acting as a modifier gene such that deletions of *naip* determine the severity of the disorder. This model is supported by the observation that in SMA, homozygous deletion of *naip* exons 5 and 6 always coexists with a homozygous deletion of SMNtel exon 7 however, deletions of *naip* exon 5 and 6 alone are not observed in SMA.

However, it should be noted that *smn* telomeric deletions (or mutation) while apparently necessary for SMA, are not always sufficient. Deletions of*smn* have been identified in three unaffected siblings of SMA individuals respectively (Cobben et al, 1995). In such a case an epistatic effect of by the centromeric copy of SMN, NAIP and or other genes may be involved. In keeping with this hypothesis, it has been reported that SMA Type II and Type III individuals have an increased number of the centromeric form of *smn.*

The homology of NAIP to viral proteins that function to block apoptosis strongly suggested that NAIP may have a similar anti-apoptotic function. To help elucidate the role of NAIP in SMA pathogenesis, the ability of NAIP to inhibit apoptosis was examined in CHO, Rat-1 and HeLa cells upon serum deprivation, treatment with menadione and TNF-α respectively. NAIP prevented apoptosis induced by these stimuli confirming its function as an apototic suppressor and suggesting that it may act at a common point in the apoptotic cascade. NAIP lacks the RING finger present in the viral iaps suggesting that the BIR motifs, which are the common structural feature of the IAPs, confer the apoptotic suppression. Furthermore we have demonstrated that NAIP is expressed in motor neurons of the spinal cord, the cells that degenerate in SMA. These results support a model in which NAIP acts to suppress apoptosis in neurons possibly during development and when defective results in the continuation of cell death which in combination with SMN mutations, manifests as the SMA phenotype.

The function of SMN , which appears to be unable to inhibit apoptosis, remains to be elucidated (Liston et al, 1996). It may be that SMN and NAIP interact, with SMN increasing the ability of NAIP to counter apoptosis analogous to the role of BAG-1 with respect to bcl-2 (Sat et al, 1995). The fact that this would suggest that *smn* would act as a modifying gene, which is not supported by the genetic data, suggests that other factors are involved.

Since the isolation of *naip*, three novel human and two *Drosophila* IAPS have been identified (Rothe et al, 1995; Liston et al, 1996). Structurally these novel human IAPs are similar to NAIP in that they contain three BIR motifs however they also contain the RING finger motif present in the viral IAPs. The *Drosophila* IAPS both have a RING zinc finger but they differ in that one has two BIR motifs while the other has three. All of these iap family members have been shown to suppress apoptosis upon induction with various apoptotic stimuli (Liston et al, 1996; Hay et al, 1995). In support of our data, suggesting that the BIR motifs confer the anti-apoptotic ability , Diap constructs lacking the RING finger had a greater survival effect than a full length construct (Hay et al, 1995). Consistent with this data, apoptosis was increased by just the RING finger alone. This suggests that the RING finger acts as a negative regulator of apoptotic suppression.

Hiap1 and *hiap2* were isolated by Rothe and co-workers (1995) based on their ability to interact with the cytokine receptor TNFRII via a TRAF2/TRAF1 heterocomplex. TNFRII is implicated in cellular proliferation and activation of NF-kB (Tartaglia et al, 1993). Transduction of the apoptotic signal is attributed to signalling through TNFRI. Although the IAPs have been observed to associate with the TRAF proteins their role in these signalling pathways is as yet unknown. It remains to be determined if NAIP interacts with any of the TRAF proteins or whether it is also a component of these signal transduction pathways. The ability of NAIP to inhibit apoptosis induced by TNF-α suggests that it may function in these pathways.

Several lines of evidence suggest that the IAPs may act at the level of the ICE proteases in the apoptotic cascade. The involvement of ICE or an ICE-like protease in TNF cytotoxicity has been demonstrated (Enari et al, 1995). In addition the viral protein, p35, that can be functionally complemented by the viral iaps, acts as an inhibitory substrate of these proteases blocking cell death (Bump et al, 1995; Xue and Horvitz, 1995). Moreover , the viral iaps have recently been shown to inhibit apoptosis induced by ICE (Duckett et al, 1996). The ability of the iap family to act directly as a substrate for the ICE proteases or upstream in the apoptotic cascade inhibiting their activation remains to be determined.

Finally, although we have shown that NAIP suppresses apoptosis and is expressed in the cells that degenerate in SMA, its exact role in SMA pathogenesis remains elusive. The genetic evidence supports a model in which NAIP acts as a modifying gene, determining the severity of SMA. Mouse models which lack NAIP or SMN will help clarify the contribution of the two genes to the SMA phenotype. It may be that additional genes that reside at 5q13 play a role. Nonetheless we have isolated the first human member of a family of proteins which suppress apoptosis. The level at which NAIP acts in the apoptotic cascade is unknown however its elucidation shall lead to a better understanding of programmed cell death in general and of the contribution of NAIP to SMA.

REFERENCES

Albertson, H.M., Abderrahim, H., Cann, H.M., Dausset, J., le Paslier, D. and Cohen, D. (1990). Construction and characterization of a yeast artificial chromosome library containing seven haploid genome equivalents. *Proc. Natl. Acad. Sci. USA.* **87:** 4256-4260.

Allsopp, T.E., Wyatt, S., Paterson, H.F., Davis, A.M. (1993) The proto-oncogene bcl-2 can selectively rescue neurotrophic factor dependent neurons from apoptosis. *Cell* **73:** 295-307.

Altschul, S.F., Warren, G., Miller, W., Myers, E.W., and Lipman, D.J. (1990) Basic alignment search tool *J. Mol. Biol.* **215:** 403-410.

Arends, M.J., and Wyllie, A.H. (1991) Apoptosis: mechanisms and roles in pathology. *Int. Rev. Exp. Pathol.* **32:** 223-254.

Armitage, R.J., Tough, T.W., Macduff, B.M., Fanslow, W.C., Spriggs, M.K., Ramsdell, F., Alderson, M.R. (1993) CD40 ligand is a T cell growth factor. *Eur. J. Immunol.* **23:** 2326-2331.

Bakshi, A., Jensen, J.P., Goldman, P., Wright, J.J., McBride, O.W., Epstein, A.L., and Korsmeyer, S.J. (1985) Cloning the chromosomal breakpoint of t(14:18) human lymphomas: clustering around J_H on chromosome 14 and near a transcriptionally active unit of 18. *Cell* **41:** 899-906.

Batistou, A., Merry, D.E., Korsmeyer, S.J., Greene, L.A. (1993) Bcl-2 affects survival but not neuronal differentiation of PC12 cells*J. Neurosci* **13:** 4422-4428.

Benardy, S.G. (1978) Spinal muscular atrophy in childhood: Review of 50 cases. *Dev. Med Child Neurol* **20:** 746-757.

Birnbaum, M.J., Clem, R.J., and Miller, L.K. (1994) An apoptosis inhibiting gene from a nucleur polyhedrosis virus incoding a peptide with cys/his motifs. *J. Virol.* **68:** 2521-2528.

Birnboim, H.C.,and Doly, J. (1979). A rapid alkaline extraction procedure for screening recombinanat plasmid DNA. *Nucleic Acids. Res.* **7:** 1513-1523.

Boise, L.H., Gonzalez-Garcia, M., Postema, C.E., Ding, L., Lindsten, T., Turka, L.A., Mao, X., Nunez, G., and Thompson,C.B. (1993) Bcl-x, a Bcl-2 related gene that functions as a dominant regulator of apoptotic cell death. *Cell* **74:** 597-608.

Boldin, M.P., Varfolomeev, E.E., Pancer, Z., Mett, I.L, Camonis, J.H., and Walllah, D. (1995) A novel protein that interacts with the death homain of Fas/APO1 contains a sequence motif related to the death domain. *J. Biol. Chem.* **270:** 7795-7798.

Brahe, C., Velona, U., van der Steege, G., Zappata, S., van de Veen, A.Y., Osinga, J., Tops, C.M., Fodde, R., Khan, M., Ruys, C.H. and Neri, G. (1994) Mapping of two new markers within the smallest interval harboriing the spinal muscular atrophy locus by family and radiation hybrid analysis. *Hum. Genet.* **93:**494-501.

Brooke, M. *A Clinicians view of Neuromuscular Disorders* (Baltimore: Williams and Williams) (1986).

Brzustowitcz, L.M., Lehner, T., Castilla, L.H., Penchaszadeh, G.K., Wilhelmsen, K.C., Daniels, R., Davies, K.E., Leppert, M., Ziter, F., Wood, D., Dubowitz, V., Zerres, K., Hausmanowa-Petrusewicz, I., Ott, J., Munsat, T.L. and Gilliam, T.C. (1990). Genetic mapping of chronic childhood-onset spinal muscular atrophy to chromosome 5q11.2-13.3. *Nature* **344:** 540-541.

Brustowicz, L.M., Klyen, P.W., Boyce, F.M., Lien, L.L., Monaco, A.P., Penchaszadeh, G.K., Das, K., Wang, C.H., Munsat, T.L., Ott, J., Kunkel, L.M., and Gilliam, T.C. (1992) Fine-mapping of the spinal muscular atrophy locus to a region flanked by MAP-1B and D5S6. *Genomics* **13:** 991-998.

Buchthal, F., and Olsen, P.Z. (1970) Electromyography and muscle biopsy in infantile spinal muscular atrophy. *Brain* **93:** 15-30.

Buckler, A.J., Chang, D.D., Graw, S.L., Brook, J.D., Haber, D.A., Sharp, P.A., and Housman, D.E. (1991) Exon amplification: A new strategy to isolate mammalian gnes based on RNA splicing. *Proc. Natl. Acad. Sci. U.S.A.* **88:** 4005-4009.

Bump, N.J., Hackett, Hugunin, M., Seshagiri, S., Brady, P., Chen, P., Ferenz, C., Franklin, S., Ghayur, T., Li, P., Licari, P., Mankovich, J., Shi, L., Greenberg, A., Miller, L.K., and Wong, W. (1994) Inhibition of ICE family proteases by baculovirus anti-apoptotic protein p35. *Science* **269:** 1885-1888.

Burghes, A.H.M., Ingraham, S.E>, Kote-Jarai, Z., Rosenfield, S., Herta, N., Nadkarni, N., DiDonato, C.J., Carpten, J., Hurko, O., Florence, J. (1994) Linkage mapping of the spinal muscular atrophy gene. *Hum. Genet.* **93:** 305-312.

Burghes, A.H.M., Ingraham, S.E., McLean, M., Thompson, T.G., McPherson, J.D., Kote-Jarai, Z., Carpten, J.D., DiDonato, C.J., Ikeda, J-E., Surh, L., Wirth, B., Sargent, C.A., Ferguson-Smith, M.A., Fuerst, P., Moysis, R.K., Grady, D.L., Zerres, K., Korneluk, R., MacKenzie, A. and Wasmuth, J.J. (1994). A multicopy dinucleotide marker that maps close to the spinal muscular atrophy gene. *Genomics* **21:** 394-402.

Burke, D.T., Carle, G.F., and Olson, M.N. (1987) Cloning of large segments of exogenous DNA into yeast by means of artifical chromosome vectors. *Science* **236:** 806-812.

Busciglio, J., and Yanker, B.A. (1995) Apoptosis and increased generation of reactive oxygen species in Down's syndrome neurons in vitro. *Nature 378:* 776-779.

Carpten, J.D., DiDonato, C.J., Ingraham, S.E., Wagner-McPherson, C., Nieuwenhuijsen, B.W., Wasmuth, J.J. and Burghes, A.H.M. (1994) A YAC contig of the region containing the spinal muscular atrophy gene (SMA): Identification of an unstable region. *Genomics.* **24:** 351-356.

Carter, B.D., Kaltschmidt, C., Kaltschmidt, B., Offenhauser, N., Bohm-Matthaei, R., Baeuerle, P.A., and Barde, Y-A. (1996) Selective activation of NF-κB by nerve growth factor through the neurotrophin receptor p75. *Science* **272:** 542-545.

Cheng, E.H.L., Levine, B., Boise, L.H., Thompson, C.B., and Hardwick, M. (1996) Bax-independent inhibition of apoptosis by Bcl-xl. *Nature* **370:** 554-556

Cheng, J., Zhou, T., Liu, C., Shapeiro, J.P., Brauer, M.J., Kiefer, M.C., Barr, P.J., Mountz, J.D. (1994) Protection from Fas mediated apoptosis by a soluble form of the Fas molecule. *Science* **263:** 1749-1751.

Cheng, G., Cleary, A.M., Ye, Z.-S, Hong, D.I., Lederman, S., and Baltimore, D. (1995) Involvement of CRAF1, a relative of TRAF in CD40 signaling. Science 267: 1494-1498.

Chinnaiyan, A.M., O'Rourke, K., Tewari, M., and Dixit, V.M. (1995) FADD, a novel death domain-containing protein, interacts with the death somain of Fas and initiates apoptosis. *Cell* **81:** 505-512.

Chittenden, T., O'Connor, R., Flemington, C., Lutz, R.J., Evan, G.I., and Guild, B.C. (1995) Induction of apoptosis by the Bcl-2 homolog Bak. *Nature* **374:** 733-736.

Chou, S.M. and Faradey, V.A. (1971) Ultrastructure of chromatolytic motoneurons and anterior spinal roots in a case of Werdnig-Hoffmann disease. *J. Neuropathol. Exp. Neurol.* **30:** 368-379.

Chu, K., Niu, X., and Williams, L.T. (1996) A novel protein FAF-1, potentiates Fas mediated apoptosis. *Proc. Natl. Acad. Sci.* (in press).

Church, D.M., Stotler, C.J., Rutter, J.L., Murrell, R.J., Trofatter, J.A., and Buckler, A.J. (1994) Isolation of genes from complex sources of mammalian genomic DNA using exon amplification. *Nature Genet.* **6:** 98-105.

Clem, R.J., Fechheimer, M. And Miller, L.K. (1991) Prevention of apoptosis by a Baculovirus gene during infection of insect cells. *Science* **254,** 1388-1390

Clem, R.J., and Miller, L.K. (1993) Apoptosis reduces both the in vitro replication and the in vivo infectivity of a baculovirus. *J. Virol.* **67:** 3730-3738.

Clem, R.J and Miller, L.K. (1994) Control of programmed cell death by the baculovirus genes p35 and iap. *Mol. Cell Biol.* **14,** 5212-5222

Clermont, O., Burlet, P., Burglen, L., Lefebvre, S., Pascal, F., McPherson, J., Wasmuth, J., Cohen, D., Le Paslier, D., Weissenbach, J., Lathrop, M., Munnich, A., and Melki, J. (1994). Use of genetic and physical mapping to locate the spinal muscular atrophy locus between two new highly polymorphic DNA markers. *Am. J. Hum. Genet.* **54:** 687-694.

Cohen, P.L., and Eisenberg, R.A. (1991) *Lpr* and *gld*: Signal gene models of systemic autoimmunity and lymphoproliferative disease. *Annu. Rev. Immunol.* **9:** 243.

Collier, S., Mayada, T. and Strachan, T. (1993) A de novo pathological point mutation at the 21-hydroxylase locus: implications for gene conversion in the human genome. *Nature Genet.* **3:** 260-264.

Cowan, W.M., Fawcett, J.W., O'Leary, D.D., and Stanfield, B.B. (1984) Regressive events in neurogenesis. *Science* **225:** 1258-1265.

Crook, N.E., Clem, R.J. and Miller, L.K. An apoptosis inhibiting baculovirus gene with a zinc finger like motif *J. Virol.* **67,** 2168-2174 (1993).

Cunningham, T. J. (1982) Naturally occuring death and its regulation by developing neural pathways. *Intl. Rev. Cytol.* **74:** 163-186.

Dana, S., and Wasmuth, J.J. (1982). Linkage of the leuS, emtB, and chr genes on chromosome 5 in humans and expression of human genes encoding protein synthesis components in human-Chinese hamster hybrids. *Somatic Cell Genet.* **8:** 245.

Davis, L.G., Dibner, M.D. and Battey, J.F. (1986). Basic Methods in Molecular Biology. Elsevier, New York.

Debbas, M., and White, E. (1993) Wild-type p53 mediates apoptosis by E1A which is inhibited by E1B. *Genes. Dev.* **7:** 546-554.

DiDonato, C.J., Morgan, K., Carpten, J.D., Fuerst, P., Ingraham, S.E., Prescott,, G., McPherson, J.D., Wirth, B., Zerres, K., Hurko, O., Wasmuth, J.J., Mendell, J.R., Burghes, A.H.M., and Simard, L.R. (1994) Association between Ag-1ca alleles and severity of autosomal recessive proximal spinal muscular atrophy.*Am. J. Hum. Genet.* **55:** 1218-1229.

Dragunow, M., Faull, R.L., Lawlor, P., Beilharz, E.J., Singleton, K., Walker, E.B., and Mee, E. (1995) In situ evidence for DNA fragmentation in Huntington's disease striatum and Alzheimer's disease temporal lobes. *Neuroreport* **6:** 1053-1057.

Duan, H., Chinnaiyan, A.M., Hudson, P.L., Wing, J.P., He, W-W., Dixit, V.M. (1996) ICE-LAP3, a novel mammalian homologue of the*Caenorhabditis elegans* cell death protein ced-3 is activated during Fas- and tumor necrosis factor induced apoptosis. *J. Cell. Biol.* **271:** 1621-1625.

Dubowitz, V. (1978). Muscle Disorders in Childhood, W.B. Saunders Co. Ltd., East Sussex, pp. 146-190.

Dubowitz, V. (1991). Chaos in classification of the spinal muscular atrophies of childhood. *Neuromusc. Disord.* **1:** 47-53.

Duckett, C.S., Nava, V.E., Gedrich, R.W., Clem, R.J., Dongen, J.L., Gilfilan, M., Sheil, H., Hardwick, J.M., and Thompson, C.B. (1996) A conserved family of cellular genes related to the baculovirus iap gene and encoding apoptosis inhibitors. *EMBO* (in the press).

Ellis, H.M., and Horvitz, H.R. (1986) Genetic control of programmed cell death in the nematode C.elegans. *Cell* **44:** 817-829.

Ellis, H.M., Jacobsen, D.M., and Horvitz. (1991) Genes required for the engulfment of cell corpses during programmed cell death in*Caenorhabditis elegans.Genetics* **129:** 79.

Ellison, K.S., Gworzd, T., Prendergast, J.A., Paterson, M.C., and Ellison, M.J (1991) A site-directed approach for constructing temperature-sensitive ubiquitin-conjugating enzymes reveals a cell cycle function and growth function for RAD6.*J. Biol. Chem.* **266:** 24116-24120.

Emery, A.E.H., Daie, A.M., Holloway, S., and Skinner, R. (1976) International collaborative study of the spinal muscular atrophies. Analysis of genetic data.*J. Neurol. Sci.* **30:** 375 - 384.

Emery, A.E.H. (1991) Population frequencies of inherited neuromuscular diseases: a world survey. *Neuromusc. Disord.* **1:** 19-29.

Enari, M., Hug, H., and Nagata, S., (1995) Involvement of an ICE-like protease in Fas mediated apoptosis. *Nature* **375:** 78-81.

Espivik, T., Brockhaus, M., Loetscher, N., and Shalaby, R. (1990) Characterixation of binding and biological effects of monoclonal antibodies against a human tumor necrosis factor receptor. *J. Exp. Med.* **171:** 415-426.

Farrow, S.N., White, J.H.M., Martinou, I., Raven, T., Pun, K.T., Grinham C.J., Martinou, J.C., and Brown. (1995) Cloning of a bcl-2 homologue by interaction with the adenovirus E1B 19K *Nature* **374:** 731-733.

Faucheu, C., Diu, A., Chan, A.W.E., Blanchet, A.M., Miossec, C., Herve, F., Collard-Dutilleul, V., Gu, Y., Aldape, R.A., Lippke, J.A., Rocher, C., Su, M.S.-S., Livingston, D.J., Hercend, T., and Lalanne, J.-L. (1995) A novel human protease similar to the interleukin-1β converting enzyme induces apoptosis in transfected cells. *EMBO* **14:** 1914-1922.

Feinberg, A.P. and Vogelstein, B. (1983). A technique for radiolabeling DNA restriction endonuclease fragments to high specific activity. *Anal. Biochem.* **132:** 6-13.

Fernandes-Alnemri, T., Litwack, G., and Alnemri. (1994) CPP32, a novel human apoptotic protein with homology to *Caenorhabditis elegans* cell death protein Ced-3 and mammalian interleukin-1β-converting enzyme. *J.Biol. Chem.* **269:** 30761-30764.

Fidzanska, A. and Rafalowska, J. (1983) Human ontogenesis. III. Ultrastructural differences between two types of fetal motoneurons.

Fidzianska-Dolot, A. and Hausmanowa-Petrusewicz, I. (1984) Morphology of the lower motor neuron ans muscle. in Progressive spinal muscular atrophies. editorsGamstrop, I; Sarnat, H.B. New York, Raven Press.

Forloni, G., Chiesa, R., Smiroldo, S., Verga, L., Salmona, M., Tagliavini, F., Angeretti, N. (1993) Apoptosis mediated neurotoxicity induced by chronic application of β amyloid fragment. *Neuroreport.* **4:** 523-526.

Francis, M.J., Morrison, K.E., Campbell, L., Grewal, P.K., Christodoulo, Z., Daniels, R.J., Monaco, A.P., Frichauf, A.M., McPherson, J., Wasmuth, J. and Davies, K.E. (1993). A contig of non-chimeric YACs containing the spinal muscular atrophy gene in 5q13. *Hum. Mol. Genet.* **2:** 1161-1167.

Fried, K., and Emery, A.E.H. (1971) Spinal muscular atrophy type II.*Clin. Genet.* **2:** 203-209.

Fried, K., and Emery, A.E>H. (1977) Spinal muscular atrophy type II. A separate genetic and clinical entitiy from Type I (Werdnigg-Hoffmann disease) and type III (Kugelberg-Welander disease). *Clin. Genet.***2:** 203-211.

Furuse, M., Hirase, T., Itoh, M., and Nagafuchi, A. (1993) Occludin: a novel integral membrane protein localizing at tight junctions. *J. Cell Biol.* **123:** 1777-1788.

Gagliardini, V., Fernandez, P-A., Lee, R.K.K., Drexler, H.C.A., Rotello, R.J., Fishman, M.C., Yuan, J. (1994) Prevention of vertebrate neuronal death by the crmA gene. *Science* **263:** 826-828.

Garcia, I., Martinou, I., Tsujimoto, Y. and Martinou, J.C. (1992) Prevention of Programmed cell death of sympathetic neurons by the Bcl-2 proto-oncogene. *Science* **258:** 302-304.

Garvie, J.M., and Woolf, A.L. (1966). Kugelberg-Welander syndrome (hereditary proximal spinal muscular atrophy). *Brit. Med. J.* **1:** 1958-1967.

Gruss, H-J., and Dower, S.K. (1995) Tumor necrosis factor ligand superfamily: involvment in the pathology of malignant lymphomas. Blood 85: 1178-3402.

Gennarelli, M., Lucarelli, M., Capon, F., Pizzuti, A., Merlini, L., Angelini, C., Novelli, G., and Dallapiccola, B. (1995) Survival motoor neuron gene transcript analysis in muscles form spinal muscular atrophy patients. *Bio. Bio. Res. Comm.* **213(1)** 342-348.

Gilliam, T.C., Freimer, N.B., Kaufmann, C.A., Powhik, P.P., Bassett, A.S., Bengtsson, U., and Wasmuth, J.J. (1989). Deletion mapping of DNA markers to a region of chromosome 5 that cosegregates with schizophrenia. *Genomics* **5:** 940-944.

Gilliam, T.C., Brzustowitcz, L.M., Castillo, L.H., Lehner, T., Penchaszadeh, G.K., Daniels, R.J., Byth, B.C., Knowles, J., Hislop, J.E., Shapira, Y., Dubowitz, V., Munsat, T.L., Ott, J. and Davies, K.E. (1990). Genetic homogeneity between acute and chronic forms of spinal muscular atrophy. *Nature* **345:** 823-825.

Gamstrop, I (1967) Progressive spinal muscular atrophy with onset in infancy or early childhood. *Acta. Paediatr. Scand. 56: 408-414.*

Graham, F.L., and Eb AJ, V.A.N. (1973) A new technique for the assay of infectivity of human adenovirus 5 DNA. *Virology* **52:** 456-467.

Greenfield, J.G. and Stern, R.O. (1927) The anatomical identity of the infantile muscular atrophy. *Brain* **50:** 652-686.

Gruss, H-J., and Dower, S.K. (1995) Tumor necrosis factor ligand superfamily: involvment in the pathology of malignant lymphomas. Blood 85: 1178-3402.

Hamburger, V., and Oppenheim, R.W. (1982) Naturally occuring neuronal death in vertebrates. *Neurosci. Comm.* **1:** 39-55.

Hausmanowa-Petrusewicz, I., and Fidzianska, A. (1974) Spinal muscular atrophy-fetal like histopathological pattern in Werdnig-Hoffmann disease. *N.Y. Acad. Med.* **50:** 1157-1168.

Hausmanowa-Petrusewicz, I., Fidzianska, A., Niebroj-Dobosz, I., and Strugalska, M.H. (1980) Is Kugelberg-Welander spinal muscular atrophy a fetal defect ?*Muscle Nerve* **3:** 389-402.

Hay, B.A, Wolff, T., and Rubin, G.M. (1994) Expression of aculovirus p35 prevents cell death in *Drosophila. Development* **120:** 2121-2129.

Henderson, S., Huen, D., Rowe, M., Dawson, C., Johnson, G., and Rickinson, A. (1993) Epstein-Barr virus-coded BHRF1 protein, a viral homologue of Bcl-2, protects human B cells from programmed cell death. *Proc. Natl. Acad. Sci. U.S.A.* **90:** 8479-8483.

Henderson, S., Rowe, M., Gregory, C., Croom-Carter, D., Wang, F., Longnecker, R., Kieff, E., and Rickson, A. (1991) Induction of bcl-2 expression by Epstein-Barr virus latent membrane protein 1 protects infected B cells from programmed cell death. *Cell* **65:** 1107-1115.

Hengartner, M.O., Ellis, R,E. and Horvitz, R.H. (1994) *Caenorhabditis elegans* gene *ced-9* protects cells from programmed cell death. *Nature* **356**: 494-499.

Hengartner, M.O. and Horvitz, R.H. (1994) C. elegans cell survival gene *ced-9* encodes a functional homolog of the mammalian proto-oncogene *Bcl-2. Cell* **76:** 665-676.

Hersberger, P.A., LaCount, D.J., and Freisen, P.D. (1994) The apoptotic suppressor p35 is required early during baculobirus replication and is targeted to the cytosol of infected cells. *J. Virol.* **68:** 3467-3477.

Hershberger, S., Dickson, J.A., and Friesen, P.D. (1992) Site specific mutagenesis if the 35-kilodalton protein gene encoded by *Autographa californica* nuclear polyhedrosis virus: Cell line-specific effects on virus replication. *J. Virol.* **66:** 5525.

Hirose, K., Longo, D.L., Oppenheim, J.J., Matsushima, K. (1993) Overexpression of mitochondrial mangenese superoxide dismutase promotes the survival of tumor cells exposed to interleukin-1, tumor necrosis factor, selected anticancer drugs and ionzing radiation. *FASEB* **7:** 361-368.

Hockenberry, D.M., Zutter, M., Hickey, W.,, Naham, M., and Korsmeyer, S.J. (1991) Bcl-2 protein is an inner mitochondrial membrane protein that blocks cell death. *Nature* **348:** 334-336.

Houenou, L.J., Turner, P.L., Li, L., Oppenheim, R.W., and Festoff, B.W. (1995) A serine protease inhibitor, protease nexin I, rescues motoneurons from naturally occuring and axotomy-induced cell death. *Proc. Natl. Acad. Sci. USA.* **92:** 895-899.

Hudson, T.J., Englestein, M., Lee, M.K., Ho, E.C., Rubenfield, M.J., Adams, C.P., Housman, D.E., and Dracopoli, N.C. (1992). Isolation and chromosomal assignement of 100 highly informative human simple sequence repeat polymorphisms. *Genomics* **13:** 622-629.

Hsu, H., Xiong, J., and Goeddel, D.V. (1995) The TNF receptor 1 associated protein TRADD signals cell death and NF-κB activation. *Cell* **81:** 495-504.

Jacobson, M.D., Burne, J.F., Raff, M.C. (1994) Programmed cell death and bcl-2 protection in the absence of a nucleus. *EMBO J.* **13:** 1899-1910.

Ju, S.T., Panka, D.J., Cui, H., Ettinger, R., El-Khatib, M., Sherr, D.H., Stanger, B.Z., and Marshak-Rothstein, A. (1995) Fas(CD95)/FasL interactions required for programmed cell death after T-cell activation. *Nature* **373:** 444-448.

Kamada, S., Shinto, A.A., Tsujimura, Y., Takahshi, T., Noda, T., Kitamura, Y., Kondoh, H., and Tsujimoto, Y. (1995) Bcl-2 defiency in mice leads to pleiotrophic abnormalities: accelerated lymphoid cell death in the thymus and speen, polycystic kidney, hair hypopigmentation and distorted small intestine. *Cancer Res.* **55:** 354-359.

Kamens. J., Paskind, M., Huguinin, M., Talanian, R.V., Allen, H., Banach, D., Bump, N., Hackett, M., Johnston, C.G., Li, P., Mankovitch, J.A., Terranova, M., and Ghayur, T.

(1995) Identification and characterization of Ich-2, a novel member of the interleukin-1β converting enzyme family of cysteine proteases. *J. Biol. Chem.* **270:** 15250-15256.

Kerr, J.R.F., Wyllie, A.H., and Currie, A.R. (1972) Apoptosis: A basic biological phenomenon with wide ranging implications in tissue kinetics. *Br. J. Cancer.* **26:** 239.

Kleyn, P.W., Wang, C.H., Lien, L.L., Vitale, E., Pan, J., Ross, B.M., Grunn, A., Palmer, D.A., Warburton, D., Brzustowicz, L.M., Kunkel, L.M. and Gilliam, T.C. (1993). Construction of a yeast artificial chromosome contig spanning the spinal muscular atrophy disease gene region. *Proc. Natl. Acad. Sci. USA* **90:** 6801-6805.

Krajewski, S., Mai, J.K., Krajewska, M., Sikorska, M.J., Mossakowski, M.J. and Reed, J.C. (1995) Upregulation of bax protein levels in neurons following cerebral ischemia. *J. Neurosci.* **15:** 6364-6376.

Kuida, K., Lippke, J.A., Ku, G., Harding, M.W., Livingston, D.J., Su, M.S.-S., and Flavell, R.A. (1995) Alteredcytokine export and apoptosis in mice deficient in interleukin-1β converting enzyme. *Science* **267:** 2000-2003.

Kouprina, N., Eldarov, M., Moyzis, R., Resnick, M. and Larionov, V. (1994). A model system to assess the integrity of mammalian YACs during transformation and propagation in yeast. *Genomics* **21:** 7-17.

Kumar, S., Kinshita, M., Noda, M., Copeland, N.G., and Jenkins, N.A. (1994) Induction of apoptosis by the mouse Nedd2 gene, which encodes a protein similar to the product of *Caenorhabiditis elegans* cell death gene ced-3 and mammalian IL-1β converting enzyme. *Genes & Dev.* **8:** 1613-1626.

LaFlerla, F.M., Tinkle, B.T., Brieberich, C.J., Haudenschild, C.C., and Jay, G. (1995) The Alzheimers A beta peptide induces neurodegeneration and apoptotic cell death in transgenic mice. *Nat. Genet* **9:** 21-30.

Larin, Z., Monaco, A.P. and Lehrach, H. (1991). Yeast artificial chromosome libraries containing large inserts from mouse and human DNA. *Proc. Natl. Acad. Sci USA* **87:** 4123-4127.

Lefebvre, S., Bürglen, L., Reboullet, S., Clermont, O., Burlet, P., Viollet, L., Benichou, B., Cruad, C., Millasseau, P., Zeviani, M., LePasleir, D., Frézal, J., Cohen, D., Weissenbauch, J., Munninch, A., and Melki, J. (1995). Identification and characterization of a spinal muscular atrophy-determining gene. *Cell* **80.** 155-165.

Lien, L.L., Boyce, F.M., Kleyn, P., Brzustowicz, L.M., Menninger, J., Ward, D.C., Gilliam, T.C., and Kunkel, L.M. (1991). Mapping of human microtubule associated protein 1B in proximity to the spinal muscular atrophy locus at 5q13.1. *Proc. Natl. Acad. Sci.* **88:** 7873-7876.

Linnik, MD., Zobrist, R.H., and Hatfield, M.D. (1993) Evidence supporting a role for programmed cell death in focal cerebral ischema in rats. *Stroke* **24:** 2002-2009.

Liston, P. *et al.* Suppression of apoptosis in mammalian cells by NAIP and a related family of IAP genes. *Nature* **379,** 349-353 (1996).

Loo, D.T., Copari, A., Pike, C.J., Whittemore, E.R., Walencewicz, A.J., and Cotman, C.W. (1993) Apoptosis is induced by β-amyloid in cultured central nervous system neurons. *Proc. Natl. Acad. Sci. USA.* **90:** 7951-7955.

MacKenzie, A., Roy, N., Besner, A., Mettler, G., Jacob, P., Korneluk, R. and Surh, L. (1993). Genetic linkage analysis of Canadian spinal muscular atrophy kindreds using flanking microsatellite 5q13 polymorphisms. *Hum. Gen.* **90:** 501-504.

MacManus, J.P., Buchan, A.M., Hill, I.E., Rasquinha, I., and Preston, E. (1993) Global ischemia can cause DNA fragmentation indicative of apoptosis in rat brain. *Neurosci. Lett.* **164:** 89-92.

MacManus, J.P., Hill, I.E., Huang, Z.G., Rasquinha, Xue, D., and Buchan, A.M. (1994) DNA damage consisent with apoptosis in transient ischemia in neocortex. *NeuroReport.* **5:** 493-496.

Mah, S.P., Zhong, L.T., Liu, Y., Roghani, A., Edwards, R.H., Bredesen, D.E. (1993) The protooncogene bcl-2 inhibits apoptosis in PC12 cells. *J. Neurochem* **60:** 1183-1186.

Mankoo, B.S., Sherrington, R., De La Concha, A., Kalsi, G., Curtis, D., Melmer, G. and Gurling, H.M.D. (1991). Two microsatellite polymorphisms at the D5S39 locus. *Nucleic Acids Res.* **19:** 1963.

McDonnell, T.J., Deane, N., Platt, F.M., Nunez, G., Jaeger, U., McKearn, J.P., and Korsmeyer, S.J. (1989) Bcl-2 immunoglobulin transgenic mice demonstrate extended B cell survival and follicular lymphoproliferation. *Cell*c**57:** 79-88.

McLean, M.D., Roy, N., MacKenzie, A.E., Salih, M., Burghes, A., Simard, L., Korneluk, R.G., Ikeda, J-E, and Surh, L. Two 5q13 simple tandem repeat loci are in linkage disequilibrium with type I spinal muscular atrophy. *Hum Mol. Genet.* In Press.

Melki, J., Abdelhak, S., Sheth, P., Bachelot, M.F., Burlet, P., Marcadet, A., Aicardi, J., Barois, A., Carriere, J.P., Fardeau, M., Fontan, D., Ponsot, G., Billsette, T., Angelini, C., Barbosa, C., Ferriere, G., Lanzi, G., Ottolini, A., Babron, M.C., Cohen, D., Hanauer, A., Colerget-Darpox, F., Lathrop, M., Munnich, A. and Frezal, J. (1990). Gene for chronic proximal spinal muscular atrophies maps to chromosome 5q. *Nature* **344:** 767-768.

Melki, J., Burlet, P., Clermont, O., Pascal, F., Paul, B., Abdelhak, S., Sherrington, (1993) Refined linkage map of chromosome 5 in the region of the spinal muscular atrophy gene. *Genomics* **15:** 521-524.

Melki, J., Lefebvre, S., Burglen, L., Burlet, P., Clermont, O., Millasseau, P., Reboullet, S., Benichou, B., Zevianai, M., LePaslier, D., Cohen, D., Weissenbach, J. and Munnich, A. (1994). *De novo* and inherited deletions of the 5q13 region in spinal muscular atrophies. *Science* **264:** 1474-1477

Miesfeld, R., Keystal, M., and Arnheim, N. (1981) A member of a new repeated sequence family which is conserved throughout eukaryotic evolution is found between the humanγ and β globin genes. *Nucleic Acids Res.* **9:** 5931-5947.

Milligan, C.E., Prevette, D., Yaginuma, H., Homma, S.A., Cardwell, C., Fritz, L.C., Tomaselli, K.J., Oppenheim, R.W., and Schwartz (1995). Peptide inhibitors of hte ICE protease family arrest programmed cell death of motoneurons in vivo and in vitro. *Neuron* **15:** 385-393.

Miura, M., Zhu, H., Rotello, R., Hartwieg, E.A., and Yuan, J. (1993) Induction of apoptosis in fibroblasts by IL-1β converting enzyme, a mammalian homolog of the C. elegans cell death gene *ced-3. Cell* **75:** 653-660.

Moosa, A., and Dubowitz, V. (1973) Spinal muscular atrophy in childhood; two clues to clinical diagnosis. *Arch. Dis. Child.* **48:** 386-388.

Moosa, A., and Dubowitz, V. (1976) Motor nerve conduction velocity in spinal muscular atrophy of childhood. *Archives of Disease in Childhood.* **51:** 974-977.

Morrison, K.E., Daniels, R.J., Suthers, G.K., Flynn, G.A., Francis, M.J., Buckle, V.J., and Davies, K.E. (1992) High-resolution genetic map around the spinal muscular atrophy (SMA) locus on chromosome 5. *Am. J. Hum. Genet.* **50:** 520-527.

Mosialos, G., Birkenbach, M., Yalamanchili, VanArsdale, T., Ware, C., and Kieff, E. (1995) The epstein-barr virus transforming protei LMP-1 engages signaling proteins for the tumor necrosis factor receptor family. Cell 80: 389-399.

Munday, N.A., Vaillancourt, J.P., Ali, A., Casano, F.J., Miller, D.K., Molineaux, S.M., Yamin, T. -T., Yu, V.L., Nicholson, D.W. (1995) Molecular cloning and pro-apoptotic activity of ICErel-II and ICErelIII, members of the ICE/CED-3 family of cysteine proteases. *J.Biol. Chem.* **270:** 15870-15876.

Neamati, N., Fernandez, A., Wright, S., Kiefer, J., and McConkey, D.J. (1994) Degredation of lamin B1 precedes oligonucleosomal DNA fragmentation in apoptotic thymocytes and isolated thymocyte nuclei.*J. Immunol.* **154:** 1693-1700.

Neil, D.L., Villasante, A., Fisher, R.B., Vetrie, D., Cox, B. and Tyler-Smith, Chris. (1990). Structural instability of human tandemly repeated DNA sequnces cloned in yeast artificial chromosome vectors. *Nucleic Acid Res.* **18:** 1421-1428.

Nelson, D.L., Brownstein, B.H. (eds) (1993). YAC libraries: A users guide. W.H. Freeman and Company, New York pp. 86-89.

Nicholson, D.W., Ali, A., Thornberry, N.A., Vaillancourt, J.P., Ding, C.K., Gaillant, M., Garreau, Y., Griffen, P.R., Labelle, M., Lazebnik, Y.A., Munday, N.A., Raju, S.M., Smulson, M.E., Yamin, T.T, Yu, V.L., and Miller, D.K. (1995) Identification and inhibition of the ICE/CED-3 protease necessary for mammalian apoptosis. *Nature* **376:** 37-43.

Nunez, G., London, L., Hockenberry, D., Alexander, M., and McKearn, J.P. (1990) Deregulated bcl-2 gene expression selectivly prolongs survival of growth factor-deprived heopoietic cell lines. *J. Immunol.* **144:** 3602-3610.

Olivai, Z.N., Milliman, C.L. and Korsmeyer. (1993) Bcl-2 heterodinmerizes in vivo with a conserved homolog, Bax, that accelerates cell death. *Cell* **74:** 609-619.

Oppenheim, R.W. (1991) Cell death during development of the nervous system. *Ann. Rev. Neurosci.* **14:** 253-501.

Oppenheim, R.W., Prevette, D., Tytell, M., and Homma, S. (1990) Naturally occuring and induced neuronal death in the chichk embryo in vivo requires protein and RNA synthesis: evidence for the role of cell death genes. *Dev. Biol.* **138:** 104-113.

Oshima, A., Kyle, J.W., Miller, R.D., Hoffmann, Powell, P.P., Grubb, J.H., Sly, W.S., Tropak, M., Guise, K.S., and Gravel, R.A. (1987). Cloning, sequencing and expression of cDNA for human beta-glucuronidase. *Proc. Natl. Acad. Sci. USA.* **84:** 685-689.

Oshima, A., Kyle, J.W., Miller, R.D., Hoffmann, Powell, P.P., Grubb, J.H., Sly, W.S., Tropak, M., Guise, K.S., and Gravel, R.A. (1987). Cloning, sequencing and expression of cDNA for human beta-glucuronidase. *Proc. Natl. Acad. Sci. USA.* **84:** 685-689.

Pearn, J. (1980) Classification of the spinal muscular atrophies. *Lancet* **1:** 919-922.

Pearn, J.H., Carter, C.O., Wilson, J. (1973) The genetic identity of acute infantile spinal muscular atrophy. *Brain* **96:** 463-470.

Pfeffer, K., Matsuyama, T., Kundig, T.M., Wakeman, A., Kishihara, K., Shanhinian, A., Wiegmann, K., Ohashi, P.S., Kronke, M., Mak, T.W. (1993) Mice resistant for the 55 kd Tumor Necrosis Factor receptor are resistant to endotoxic shock yet succumb to L. monocytogenes infection. *Cell* **73:** 457-467.

Rabizadeh, S., LaCount, D.J., Freisen, P.D., and Bredesen, D.E. (1993) Expression of the baculovirus p35 gene inhibits mammalian neuronal cell death. *J. Neurochem.* **61:** 2318-2321.

Rao, L., Dwbbas, M., Sabbatini, P., Hockenberry, D., Korsmeyer, S., and White, E. (1992) The adenovirus E1A proteins induce apoptosis which is inhibited by the E1B 19K and Bcl-2 proteins. *Proc. Natl. Acad. Sci.* **89:** 7742-7746.

Ray, C.A., Black, R.A., Kronheim, S.R., Greenstreet, T.A., Sleath, P.R., Salvesen, G.S., and Pickup, D.J. (1992) Viral inhibition of inflammation: Cowpox virus encodes an inhibitor of the interleukin -1β cor. erting enzyme. *Cell* **69:** 597-604.

Rodrigues, N.R., Owen, N., Talbot, K., Ignatius, J., Dubowitz, V., and Davies, K.E. (1995) Deletions in the survival motor neruon gene on 5q13 in autosomal recessive spinal muscular atrophy. *Hum. Mol. Genet.* **4(4):** 631-634.

Rothe, M., Wong, S.C., Henzel, W.J., and Goeddel, D.V. (1994) A novel family of putative signal transducers associated with the cytoplasmic domain of the 75 kD tumor necrosis factor receptor. Cell 78: 681-692.

Rothe, M., Pan., M-G., Henzel, W.J., Ayers, T.M., and Goeddel, D.V. (1995) The TNFR2-TRAF signaling complex contains two novel proteins related to baculoviral inhibitor of apoptosis proteins. Cell 83: 1243-1252.

Rosenfield, M.A., Yoshimura, K., Trapnell, B.C., Yoneyama, K., Rosenthal, E.R., Dalemans, W., Fukayama, M., Bargon, J., Steir, L.E., Stratford-Perricaudet, L. (1992) In vivo transfer of the human cystic fibrosis transmembrane conductance regulator gene tot he airway epithelium. *Cell* **68:** 143-155.

Roy, N., Mahadevan, M.S., McLean, M., Shutler, G., Yaraghi, Z., Farahani, R., Baird, S., Besner-Johnston, A., Lefebrve, C., Kang, X., Salih, M., Aubry, H., Tamai, K., Guan, X., Ioannou, P., Crawford, T., de Jong., P.J., Surh, L., Ikeda, J-E., Korneluk, R.G. and

MacKenzie, A. (1995). The gene for neuronal apoptosis inhibitory protein is partially deleted in individuals with spinal muscular atrophy. *Cell.* **80.** 167-178.

Sambrook, J., Fritsch, E.F., and Maniatis, T. (1989). Molecular Cloning: A Laboratory Manual," 2nd ed., Cold Spring Harbor Laboratory Press, Cold Spring Harbor

Sarnet, H.B. (1984) Commentary: Pathology of Spinal muscular atrophy. In*Progressive Spinal Muscular Atrophy*. Gamstorp, I. and Sarnat, H.B. eds. (New York: Raven), pp91-110.

Sarnat, H.B. (1984) Histopathology of SMA. In *Progressive Spinal Muscular Atrophy.* Gamstorp, I. and Sarnat, H.B. eds. (New York: Raven), pp91-110.

Sarnat, H.B. (1992) *Cerbral Dysgenesis: Embryology and Clinical Expression* (Oxford, Oxford University Press)

Sato, T., Irie, S., Kitade, S., and Reed, J.C. (1995) FAP-1: A protein tyrosine phosphatase that associates with Fas. *Science*. **268:** 411-415.

Sentman, C.L., Shutter, J.R., Hockenberry, D., Kanagawa, O., and Korsmeyer, S.J. (1991) Bcl-2 inhibits multiple forms of apoptosis but not negative selection in thymocytes. *Cell* **67:** 879-888.

Seto, M., Jaeger, U., Hockkett, R.D., Graninger, W., Bennett, S., Goldman, P., and Korsmeyer, S.J. (1988) Alternate promoters and exons, somatic mutation and transcriptional deregulation of the Bcl-2-Ig fusion gene in lymphoma. *EMBO* **7:** 123-131.

Scherer, S. and Tsui, L.-C. (1991). Adolph, K.W., ed Cloning and analysis of large DNA molecules. Advanced Techniques in Chromosome Research. Dekker, New York. pp.33-72.

Soares, V.M.,, L.M., Kleyn, P.W., Knowles, J.A., Palmer, D.A., Asokan, S., Penchaszadeh, G.K., Munsat, T.L. and Gilliam, T.C. (1993). Refinement of the spinal muscular atrophy locus to the interval between D5S435 and MAP1B. *Genomics* **15:** 365-371.

Shen, L., Wu, L.C., Sanlioglu, S., Chen, R., Mendoza, A.R., Dangel, A.W., Carroll, M.C., Zipf, W.B., and Yu, C.Y. (1994) Structure and genetics of the partially duplicated gene RP located immediately upstream of the complement C4A and the C4B genes in the HLA class III region. Molecular cloning, exon-intron structure, composite retroposon and breakpoint of gene duplication. *J. Biol. Chem.* **269:** 8466-8476.

Sherrington, R., Melmer, G., Dixon, M., Curtis, D., Mankoo, B., Kalsi, G. and Gurling, H. (1991). Linkage disequilibrium between two highly polymorphic microsatellites. *Am. J. Hum. Genet.* **49:** 966-971.

Shizuya, H., Birren, B., Kim, U-J., Mancino, V., Slepak, T., Tachiri, Y., and Simon, M. (1992) Cloning and stable maintenance of 300-kilobase pair fragments of human DNA in *Esherichia coli* using an F-factor-based vector. *Proc. Natl. Acad. Sci. U.S.A.* **89:** 8794-8797.

Shutler, G., Korneluk, R.G., Tsilfidis, C., Mahadaven, M., Bailly, J., Smeets, H., Jansen, G., Wieringa, B., Lohman, F., Asanidis, C., and de Jong, P.J. (1992). Physical mapping and cloning of the proximal

Sinnott, P., Collier, S., Costigan, C., Dyer, P.A., Harris, R., and Strachan, T. (1990) Genesis by meiotic unequal crossover of a de novo deletion that contributes to steroid 21-hydroxylase defiency. *Proc. Natl. Acad. Sci. USA* **87:** 2107-2111.

Smith, C.A., Davis, T., Anderson, D., Solam, L., Beckmann, M.P., Jerzy, R., Dower, S.K., Cosman, D., and Goodwin, R.G. (1990) A receptor for tumor necrosis facotr defines an unusual family of cellular and vial proteins. *Science* 248: 1019-1023.

Smith, C.A., Farrah., and Goodwin, R.G. (1994) The TNF receptor family of cellular and viral proteins: activation, costimulation and death. Cell 76: 959-962.

Stanger, B.Z., Leder, P., Lee, T.H., Kim., and Seed, B. (1995) RIP: A novel protein contaning a death domain that interacts with Fas/Apo-1 (CD95) in yeat and causes cell death. *Cell* **81:** 513-523.

Sternberg, N. (1990) A bacteriophage P1 cloning systm for the isolation, amplification and recovery of DNA fragments as large as 100 kb. *Proc. Natl. Acad. Sci. U.S.A.* **87:** 103-107.

Sugimoto, A.P., Freisen, P.D., and Rothman, J.H. (1994) Baculovirus p35 prevents developmentally programmed cell death and rescues a ced-9 mutant in the nematode caenorabditis elegans. *EMBO J.* **13:** 2023-2028.

Tagle, D.A., Collins, F.S. (1992). An optimized *Alu*-PCR primer pair for human-specific amplification of YACs and somatic cell hybrids. *Hum. molec. Genet.* **1:** 121-122.

Takayama, S., Sao, T., Krajewski, S., Kochel, K., Irie, S., Millan, J.A., and Reed, J.C. (1995) Clonong and functional analysis of BAG-1: a novel bcl-2 binding protein with anti-cell death activity. *Cell* **80:** 279-284.

Talley, A.K., Dewhurst, S., Perry, S.W., Dollard, S.C., Gummuluru, S., Fine, S.M., New, D., Epstein, L.G., Gendelman, H.E., and Gelbard, H.A. (1995) Tumor necrosis factor alpha-induced apoptosis in human neuronal cells: protection by the antioxidant N-acetylcysteine and the genes bcl-2 and crmA. *Mol. Cell Biol.* **15:** 2359-2366.

Tartaglia, L.A., Weber, R.F., Figari, I.S., Reynolds, C., Palladino, M.A., and Goeddel, D.V. (1991) The two different receptors for tumor necrosis factor mediate distinct cellular responses. *Proc. Natl. Acad. Sci. USA.* **88:** 9292-9296.

Tartaglia, L.A., and Goedell, D.V. (1992). Two TNF receptors. *Immunology Today* **13:** 151-153.

Tartaglia, L.A., Ayres, T.M., Wong, G.H.W., and Goeddel, D.V. (1993) A novel domain within the 55 kd TNF receptor signals cell death. Cell 74, 845-853.

Tewari, M., and Dixit, V.M. (1995) Fas- and TNF-induced apoptsis is inhibited by the poxvirus *crmA* gene product. *J. Biol. Chem.* **270:** 3255-3260.

Tewari, M., Quan, L.T., O'Rourke, K., Desnoyers, S., Zeng, Z., Beidler, D.R., Poirer, G., Salvasen, G.S., and Dixit, V.M. (1995) Yama/CPP32, a mammalian homolog of CED-3, is a CrmA-inhibitable protease that cleaves the death substrate poly(ADP-ribose) polymerase. *Cell* **81:** 801-809.

Theodosiou, A.M., Morrison, K.E., Nesbit, A.M., Daniels, R.J., Campbell, L., Francis, M.J., Christodoulou, Z., and Davies, K.E. (1994) Complex repetitive arrangements of gene sequence in the candidate region of the spinal muscular atrophy gene in 5q13. *Am. J. Hum. Genet.* **55:** 1209-1217.

Thompson, C. (1995) Apoptosis in the pathogenesis and treatment of disease. *Science* **267:** 1456-1462.

Thompson, T.G., Morrison, K.E., Kleyn, P., Bengtsson, U., Gilliam, T.C., Davies, K.E., Wasmuth, J.J. and McPherson, J.D. (1993). High resolution physical map of the region surrounding the spinal muscular atrophy gene. *Hum. Mol. Genet.* **2:** 1169-1176.

Thor, H., Smith, M.T., Hartzell, P., Bellomo, G., Jewell, A., and Orrenius, S. (1982) The metabolism of menadione (2-methy-1,4-naphthoquinone) by isolated hepatocytes. A study of implications of oxidative stress in intact cells. *J. Biol. Chem.* **257:** 12419-12425.

Thornberry, N.A., Bull, H.G., Calaycay, J.R., Chapman, K.T., Howard, A.D., Kostura, M.J., Miller, D.K., Molineaux, S.M., Weidner, J.R., and Aunins,J. (1992) A novel heterodimeric cysteine protease is required for interleukin-1β processing in monocytes. *Nature* **356:** 768-774.

Trauth, B.C., Klas, C., Peters, A.M. J., Matzku, S., Moller, P., Falk, W., Debatin, K.M., and Krammer, P.H. (1989) Monoclonal antibody-mediated tumor regression by induction of apoptosis. *Science* **245:** 301-305.

van der Steege, G., Cobben, J-M., Osinga, J., Scheffer, H., van Ommen, G-J.B., and Buys, C.H.C.M. A sublocus of the multicopy microsatellite marker CMS1 maps proximal to SMA as shown by recombinant analysis. *Hum. Genet.* **96:** 589-591.

Vaux, D.L., Cory, S., and Adams, J.M. (1988) Bcl-2 promotes the survival of haemopoietic cells and cooperates with c-myc to immortilize pre-B cells. *Nature* **335:** 40-442.

Veis, D.J., Sorenson, C.M., Shutter, J.R., and Korsmeyer, S.J. (1993) Bcl-2 deficient mice demonstrate fulminant lymphoid apoptosis, polycystic kidneys and hypopigmented hair. *Cell* **75:** 229-240.

Wang, L., Miura, M, Bergeron, L., Zhu, H., and Yuan, J. (1994) *Ich*, an *ice/ced-3* related gene, encodes both positive and negative regulators of programmed cell death. *Cell* **78:** 739-750.

Watanabe-Fukunaga, R., Brannan, C., Copeland, N., Jenkins, N.A., and Nagata, S. (1992) Lymphopfoliferation disorder in mice explained by defects in Fas antigen that mediates apoptosis. *Nature* **356:** 314-317.

Weber, J.L., and May, P.E. (1988) An abundant new class of human DNA polymorphisms. *Am. J. Hum. Genet. (Suppl)* **43:**A161.

Weddel, A., and Luthman, H., (1993) Steroid 21-hydroxylase (P450c21): a new allele and spread of mutations through the pseudogen. *Hum. Genet.* **91:** 236-240.

White, K., Grether, M.E., Abrams, J.M., Young, L., Farrell, K. and Steller, H. (1994) Genetic control of programmed cell death in *Drosophila. Science* **264:** 677-683.

White, E., Sabbatini, P. Debbas, M., Wold, W.S.M., Kusher, D.I., and Gooding, L. (1992) The 19-kilodalton adenovirus E1B transforming protein inhibits programmed cell death and prevents cytolysis by tumor necrosis factor. *Mol. Cell. Biol.* **12:** 2570-2580.

Wirth, B., Voosen, B., Röhrig, D., Knapp, M., Piechaczek, B., Rudnik-Schöneborn. and Zerres, K. (1993). Fine mapping and narrowing of the genetic interval of the spinal muscular atrophy region by linkage studies. *Genomics* **15:** 113-118.

Wirth, B., Pick, E., Leuter, A., Dadze, A., Voosen, B., Knapp, M., Piechaczak-Wappenschmidt, B., Rudnik-Schoneborn, S., Schonling, J., Cox, S., Spurr, N.K. and Zerres, K. (1994). Large linkage analysis in 100 families with autosomal recessive spinal muscular atropy (SMA) and 11 CEPH families using 13 polymorphic loci in the region 5q11.2-q13.3. *Genomics* **20:** 84-93.

Wirth, B., Hanen, E., Morgan, K., DiDonato, C.J., Dadze, A., Rudnik-Schoneborn, S., Simard, L.R., Zerres, K., and Burghes, A.H.M. (1995). Alleleic association and deletions in autosomal recessive proximal spinal muscular atrophy: association of marker genotype with disease sevrity and candidate cDNAs. *Hum. Mol. Genet.* **4(8):** 1273-1284.

Wong, G.H., Tartaglia, L.A., and Goeddel, D.V. (1992) Antiviral activity of tumor necrosis factor is signaled through the 55-kDa type 1 TNF receptor. *J. Immunol.* **149:** 3550-3553.

Xue, D., and Horvitz, H.R. (1995) Inhibition of the Caenorhabditis elegans cell death protese CED-3 by a CED-3 cleavage site in baculovirus p35 protein. *Nature* **377:** 248-251.

Yang, E., Zha, J., Jockel, J., Boise, L.H., Thompson, C.B., and Korsmeyer, S. (1995) Bad, a heterodimeric partner for Bcl-x_l and Bcl-2, displaces Bax and promotes cell death. *Cell* **80:** 285-291.

Yin, X-M, Oltvai, Z.N. and Korsmeyer, S.J. (1994) BH1 and BH2 domains of Bcl-2 are required for inhibition of apoptosis and heterodimerization with Bax. *Nature* **360**:

Yuan, J., Shaman, S., Ledoux, S., Ellis, H.M., and Horvitz, H.R. (1993) The C. elegans cell death gene *ced-3* encodes a protein similar to mammalian interleukin-1β-converting enzyme. *Cell* **75:** 641-652.

Yaraghi, Z., Kang, X, Ikeda, J-E. and MacKenzie, A. *Hum.Mol. Genet.* **24:** 117. .

Yaraghi, Z., McLean, M., Roy, N., Surh, L., Ikeda, J-E., and MacKenzie, A.E. (1995) A recombination event occuring within the two complex 5q13.1 simple tandem repeat polymorphisms suggests a telomeric mapping of spinal muscular atrophy. *Hum Genet.* **96:** 330-334.

Yonehara, S., Ishii, A., and Yonehara, M. (1989) A cell killing monoclonal antibody (anti-Fas) to a cell surface antigen co-downregulated with the receptor of tumor necrosis factor. *J. Exp. Med.* **169:** 1747-1753.

IMAGE EVALUATION TEST TARGET (QA-3)

150mm

6"